Selectivity study on thermochemical conversion of fruit residues (Plums) to platform chemicals (HMF)

In partial fulfilment of the requirements for the degree of European Master's in Quality in Analytical Laboratories

By

Dawit Firemichael Bebizuh

Supervisors : Camilla Løhre (PhD, Associate Professor)

: Tanja Barth (Professor)

University of Bergen

Department of Chemistry

September 2023

Bergen, Norway

Acknowledgement

My foremost gratitude is to Almighty God and his mother Saint Merry for His Mercies and Grace, to have spared my life in good health and sound mind to undertake this research. I want to thank Dr. Camilla Løhre and Professor Tanja Barth for giving me the opportunity to work on such a challenging yet fantastic research topic. I am grateful for their compassionateness, guidance, and wealth of experience. I appreciate the invaluable suggestions, guidance, and well-seasoned technical comments provided by both of my supervisors.

I acknowledge the technical assistance provided by the staff members of the University of Bergen. Especially, I appreciated and benefited immensely from the expertise of Dr. Bjarte Holmelid. I would like to extend my special thanks to Prof. Bjørn Grung and EMQAL Program Management Teams for giving me the opportunity to enroll in EMQAL program and for their support and guidance throughout the program. In addition, I am grateful to all the professors of the modules that I took, from each one I picked up a piece of knowledge and experience. I do not want to miss this opportunity to acknowledge the European Education and culture executive agency (EACEA) for providing the Erasmus Mundus scholarships.

Special thanks also go to my colleagues for their friendship and selfless assistance in and out of the laboratory. I would also like to acknowledge the unwavering support from my EMQAL friends. Most importantly, I wish to express my heartfelt appreciation to my family for their unalloyed contributions through thick and thin of my academic sojourn. I would not have been able to achieve this feat without your mentorship, love, and care.

Abstract

5-hydroxymethylfurfural (HMF) is one of the versatile platform compounds derived from the dehydration of carbohydrates originating from biomass. However, the non-selective production of HMF from carbohydrates and its subsequent separation from the solvents remains challenging. Hence, the present thesis takes a systematic approach to understanding the conversion of Plum biomass to HMF and leverages this knowledge to propose strategies for improving conversion selectivity and HMF yield. The focus lies on optimizing the effect of conversion variables and developing an analytical strategy to characterize the feedstock (Plum) and product fraction. A rapid and robust selective ion monitoring (SIM) based LC-ESI-MS/MS method using analytical quality by design (AQbD) principles was developed for the simultaneous analysis of sugars and HMF. The developed method has been successfully applied to quantify sugar and HMF in Plum biomass before and after thermochemical conversion. The technique demonstrated high sensitivity, selectivity, throughput, and accuracy, with recovery (91% to 103%), limits of detection (0.11 to 1.72 μg/mL), and coefficients of variation (1.2 to 2.0%). Calibration curves for all analytes were linear with R2 values greater than 0.991. Plum biomass has a high moisture content (78 ± 4%), and 84% of its dry weight is covered by sugar. Glucose and fructose were found to be the dominant monosaccharide, 47% and 19% based on the dry weight basis, respectively. A simple, fast, and efficient process for HMF production from Plum's samples was developed, where sulfamic acid and MIBK were used as a catalyst and solvents under conventional heating. The critical reaction parameters, including substrate load, temperature, and aqueous phase percentage were optimized using definitive screen design (DSD) followed by central composite design (CCD). A higher HMF yield (32%), selectivity (~51%), and sugar conversion (~93%) were achieved at optimal reaction conditions (temperature (210 0C), aqueous phase (30 %V), time (120 min), sulfamic acid load (0.01 g), and substrate load (0.1 g)). The relative error between the experimental and predicted response for HMF selectivity and product (HMF) yield was found to be in the acceptable range (< 2%). In conclusion, the low-cost catalyst and solvent system, the practical and environmentally friendly reaction conditions, and the simple procedure provided in this study confirmed that the proposed strategy and feedstock are very efficient for HMF production. However, further study on the isolation and purification of the produced HMF from the reaction solutions is essential in the future.

Table of Contents

List of figures

List of tables

Acronyms

ACN	Acetonitrile
APCI	Atmospheric Pressure Chemical Ionization
AQbD	Analytical quality by design
ATP	Analytical Target Profile
BHMF	2,5- bis(hydroxymethyl) furan
CCD	Central Composite Design
CMAs	Critical Method Attributes
CMPs	Critical Method Parameters
DFA	Difructose dianhydrides
DMA	Dimethylacetamide
DMSO	Dimethylsulfoxide
DoE	Design of Experiment
DSD	Definitive Screen Design
ESI	Electrospray Ionization
FA	Formic acid
FDCA	2,5 Furandicarboxylic acid
HILIC	Hydrophilic Interaction Liquid Chromatography
HMF	5-Hydroxymethylfurfural
ICH	International Conference on Harmonization
ILs	Ionic Liquids
KS	Knowledge Space
LA	Levulinic acid
LBP	Low Boiling Point
LC-MS	Liquid Chromatography-Mass Spectrometry
LOD	Limit of Detection
LOD	Limit of Quantification
MIBK	Methyl-Isobutyl-Ketone

MODR	Method Operable Design Region
MP	Mobile Phase
MS/MS	Tandem mass spectrometry
NaAc	Sodium Acetate
NMR	Nuclear Magnetic Resonance
NREL	National Renewable Energy Laboratory
OFAT	One Factor at a Time
PR	Peak Resolution
QbD	Quality-by-Design
QRA	Quality Risk Analysis
QRM	Quality Risk Management
RPN	Risk Priority Number
RSM	Response Surface Methodology
RTLP	Retention Time of the Last Peak
SIM	Selective Ion Monitoring
THF	Tetrahydrofuran
TPA	Total Peak Area

1. Introduction

1.1.Backgrounds of the study

Biomass-derived furans have received attention as promising renewable intermediate chemicals because they can be converted into an array of valuable fuels and chemicals.[1] Despite the fact that furans can be produced directly from biomass with relatively quite good yields, their production typically involves a liquid-phase pretreatment followed by biological conversion to release C_5 and C_6 sugars, such as xylose and glucose, and then their selective conversion into intermediates and chemicals with added value.[2-4]

5-Hydroxymethylfurfural (HMF) is a chemical that has gained a lot of attention from the scientific community, since it is an intermediate to fuel components like furans.[5] HMF can also be oxidized to form the possible biopolymer precursors 2,5-furandicarboxylic acid (FDCA) and 2,5-bis(hydroxymethyl)furan (BHMF).[6] Currently, HMF production from fructose has attracted attention because of the fructose yields are higher than those from other sugar precursors. Brønsted acids commonly catalyze the three consecutive dehydration processes required to convert fructose to HMF. Acids can catalyze several undesirable side reactions in addition to the pathway for HMF synthesis from fructose, which lowers HMF yields. For instance, acid- or base-catalyzed degradation can transform fructose and HMF into polycondensation products and humins. HMF can also be rehydrated to produce formic acid (FA) and levulinic acid (LA).[7]

Previous studies in our research group and elsewhere have suggested that reaction temperature, time, catalyst load and choice, and solvent composition may all influence yields in biomass conversion to HMF. However, no comprehensive study has been applied to determine how reaction selectivity relates to the process parameters through mechanistic insights. Therefore, in this MSc project, we have tried to address this issue with a systematic approach.

1.2.Objective of the study

The major objective of this MSc project (thesis) is to study the selectivity of a biphasic thermochemical conversion system that can be employed for the effective conversion of fruit wastes to HMF. The following specific goals are established to accomplish the primary objective:

I. Characterization of the feedstocks (substrate). Both free and total sugar content will be identified and quantified. To achieve this, we develop a LC-ESI-MS/MS analysis procedure for both the identification and quantification of sugar.

II. Identify and optimize the primary factor that controls the selectivity of the thermochemical biomass conversion system. To achieve this, systematic conversion analyses with appropriate design of experiment (DoE) are used. Both screening and optimization of primary factors are done using definitive screening and central composite design.

III. Quantification of product fraction. To achieve this, experiments are conducted by applying optimum conditions identified from the experimental design (screen design and central composite design).

1.3. Scope of Research

The first part of this work is to develop an LC-ESI-MS/MS method for identification and quantification of sugar in fruit biomass (Plums). The method development covers all steps according to the AQbD (analytical quality by design) approach including method design development & understanding, method performance qualification, and life-cycle management. Once available sugar in the fruit sample is identified and quantified using the developed LC-MS/MS method, the fruit biomass is subjected to a biphasic thermochemical conversion process to study the effect of variables (time, temperature, substrate load, catalyst concentration, and water content) on the selectivity of the conversion system to convert the sugars into HMF. The conversion gives information about critical parameters that correlate with the HMF selectivity and improve the HMF yield. This research opens new possibilities for improving the biomass to HMF conversion process and facilitates the commercialization process.

2. Literature Reviews

2.1. Synthesis of Furans and their derivatives

Exploiting renewable resources will be of utmost importance in both the scientific and industrial communities to minimize the dependence on fossil resources. In this perspective, Furfural and HMF (5-hydroxymethylfurfural) represent fundamental building blocks for the biorefinery, seeing as their production is environmentally sustainable and economically feasible. Lignocellulosic residues from agriculture and/or sawmills can be used to produce furfural and HMF. HMF is considered as a flexible important platform-chemical that might be produced from biomasses rich in carbohydrates[8]. The HMF chemical structure consists of a furanic ring, an aldehyde, and an alcohol group (Figure 1), making it a particularly reactive molecule that can be used to synthesize a variety of added-value products, such as monomers, biofuels, food additives, and medicines[9].

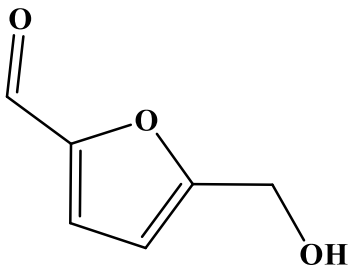

Figure 1: Chemical structure of HMF

Hexoses, such as fructose and glucose, are well-known to be efficient feedstocks for the manufacture of HMF. Surprisingly, Fructose is a direct precursor of HMF, making it usable as the initial feedstock possible to obtain better selectivity than glucose (Figure 2)[8].

The depolymerization of polysaccharides, which typically takes place under basic catalysis, and the dehydration of the C6-sugar with the loss of three molecules of water are the fundamental processes in the synthesis of HMF. Due to HMF's strong affinity for water, extracting and purifying it from an aqueous media is a significant challenge. To carry out the extraction process, several organic solvents like dichloromethane, ethyl acetate, and tetrahydrofuran have been utilized[10]. The primary issues with this process, which increase the ultimate cost of the product, are the employment of two distinct catalysts and the inclusion of co-solvent to extract the final product. In comparison to glucose, fructose is more likely to be in the acyclic conformation, which results in increased reactivity. This favors the dehydration process[11].

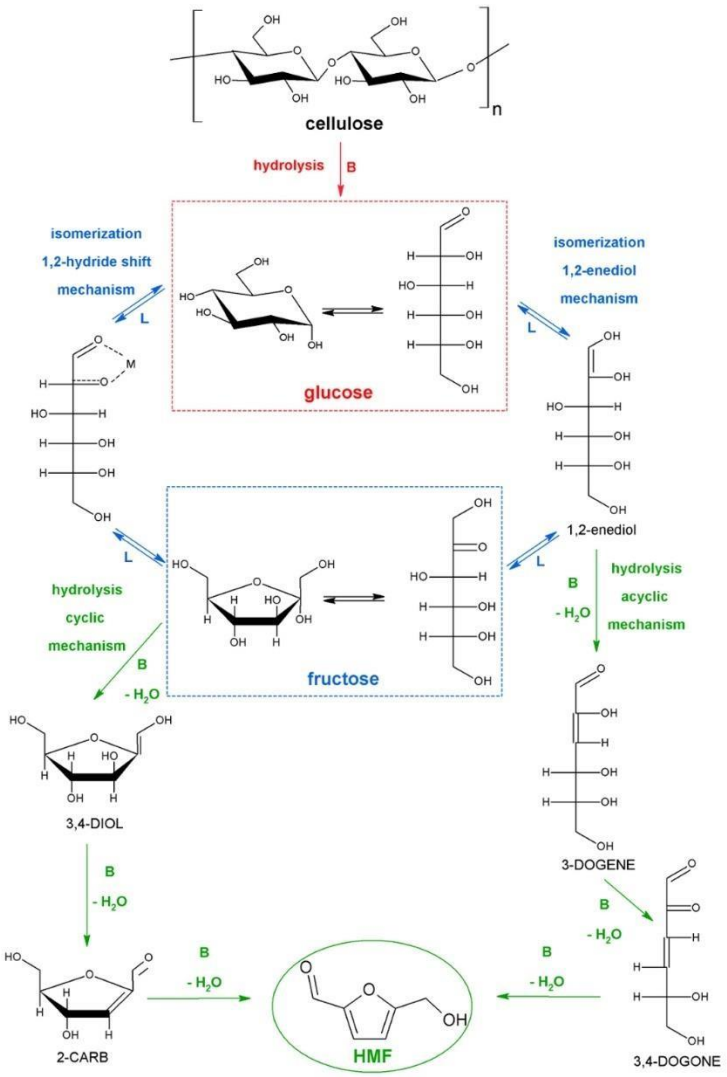

Figure 2: Mechanism of HMF synthesis from cellulose, carried out in the presence of both Brønsted (B) and Lewis (L) acids. "M" stands for "metal center"(adopted from Fulignati et al., 2022 without modification)[8]

Glucose is not very active also because its limiting step is the process of enolization of the aldehydic group, giving low conversion and low selectivity (Figure 2). This indicates that the isomerization of glucose to fructose is one of the most significant processes present in A furan/HMF-based biorefineries. The dehydration of hexoses using different acid catalysts such as organic acid (oxalic and maleic)[12], inorganic acid (HCl and H_2SO_4)[13, 14], ion exchange resins[15], zeolite[16], organic and inorganic salts[17] and $VOPO_4$[18] are reported in recent publication.

Unfortunately, the dehydration process has relatively low selectivity and conversion because so many byproducts are produced. Furan ring cleavage and HMF oligomerization/polymerization are

the two subsequent reactions to the synthesis of HMF that cause the majority of the process' side reactions[19]. The furan ring opens by the addition of two molecules of water to HMF, followed by the dehydration of the hydroxyl group at position 5, and the furan cleaves with the production of one molecule of formic acid and one molecule of levulinic acid as the final step. The auto condensation that results in high molecular weight polymers is another parallel reaction that might take place during the synthesis of HMF. The best HMF selectivity (80%) can be achieved even with a low fructose conversion (25–50%) using a niobium-based catalyst and water-soluble vanadium phosphate[20].

High-boiling organic solvents include DMSO (dimethylsulfoxide) and N-methyl pyrrolidone have also been employed, with good results (conversion of 70–90%) when an acid resin serves as the catalyst. The great selectivity is a result of by-products like humic acids and levulinic acid not forming when using an organic solvent like DMSO. The inability to easily separate HMF and the production of hazardous byproducts based on sulfur are the drawbacks. The synthesis of HMF in aqueous solution under supercritical conditions at 240°C with zirconium phosphate is one of the new catalytic systems that has been created recently. The catalyst was stable, and the only side products obtained were soluble polymers[21, 22].

Technical-economic studies have been carried out in the industrial sector to investigate the feasibility of scaling up the HMF production process and to estimate potential production costs. The cost of raw materials and the cost of fructose have a direct bearing on the price of HMF production. The cost of HMF should be about $1/Kg to use it as a platform chemical in the future biorefinery and then make the chemicals competitive on the market[23]. The development of catalytic processes utilizing heterogeneous catalysts has led to numerous designs for pilot plants. Even today, comprehensive information about the optimum catalyst for producing HMF, such as its lifetime, regeneration after deactivation, and the solvent required for the final product's extraction and purification, is virtually not found in the literature[24].

2.1.1. Solvent system for biomass conversion to HMF

The three main categories of employed solvents are ionic liquid, organic-ionic liquid, and biphasic systems (organic-ionic liquid or organic-water). Single phase systems include aqueous and organic solvents (Table 1). In terms of green chemistry principles, water-based techniques for dehydrating

carbohydrates are preferable. In high quantities, water also dissolves most carbohydrate substrates. The non-selective nature of HMF production in aqueous media, however, frequently leads to low yields because of subsequent reactions with levulinic acid and insoluble polymeric molecules (humins)[25]. HMF may be either: a) stabilized with some solvents or b) continually removed from the reaction mixture to increase its selectivity and stop subsequent degradation processes.

By slowing down the rate of HMF degradation, rehydration, or condensation, organic solvents, particularly the polar aprotic ones (dimethylsulfoxide (DMSO), N,N-dimethylformide (N,N-DMF), and dimethylacetamide (DMA), typically produce higher HMF yields. Except for polar coordinating solvents like DMSO and DMF, which are relatively soluble in organic solvents, carbohydrates are very poorly soluble in these substances. Due to its high solubility for carbohydrates and good stability for HMF, DMSO is the most widely used solvent for the synthesis of HMF. However, due to their high boiling points and the high solubility of HMF in these solvents, it is difficult to separate HMF, necessitating energy-intensive methods for product recovery. Furthermore, product separation is more difficult and expensive due to the formation of hazardous sulfur compounds during the high temperature distillation of DMSO[26].

Another intriguing class of solvents is alcohol, which can be produced from biomass, dissolves sugars more effectively, and has a range of boiling points. Alcohol is a cost-effective, simple to use, and ecologically friendly reaction medium. Under acidic conditions, HMF could react with alcohols to generate HMF-ether, which might stop HMF from further deterioration or oligomerization. It might, however, provide issues when converting HMF to other downstream compounds[27].

Ionic liquids (ILs) are a different category of solvent systems and have purportedly been employed to produce HMF from carbohydrates due to their relatively higher catalytic activity and tunable composition. Furthermore, ILs have a remarkable ability to dissolve polymeric carbohydrates, making them potentially useful for pretreating lignocellulosic biomass[28, 29].

Some of the disadvantages that limit the use of ILs in industrial processes include their toxicity, expense, corrosiveness, and limited recyclability. ILs' high cost necessitates effective recycling, yet due to their low volatility, little progress has been made in this area. A further difficulty that restricts the amount of feedstock concentration that may be transformed into HMF is the relatively poor solubility of carbohydrates due to the viscosity of ILs[30-32].

A reactive phase and an extractive phase make up the biphasic system. An additional benefit of a biphasic system that uses organic solvent as the extractive phase (THF) and imidazolium-based IL as the reactive phase is that it requires less energy to run. The poor mixing of the reactive and organic phases, which impedes HMF extraction and frequently results in decreased HMF yield in addition to the system's intrinsic issue with product isolation, poses a significant obstacle. In terms of solubility and reaction effectiveness, a water-organic biphasic system seems to be considerably more appropriate[33].

By employing this method, the organic phase of the biphasic system allows for in situ extraction and accumulation of HMF right after its production while the aqueous phase serves as the reactive phase. As a result, this approach makes it simple to separate and reuse the reactive aqueous phase. Additionally, the continuous extraction method's low concentration of HMF in the aqueous phase reduces the rate of side reactions, increasing HMF yield. Despite the appeal of the water-organic biphasic system, isolating HMF may require a significant volume of extracting solvent[34].

Table 1: Strength/weakness analysis of various processes for HMF production

Processes		**Selec.**	**Isolation**	**Efficiency**	**Environ. Impact**	**Cost**	**Processability**
Single phase	Aqueous	-	-	-	+	++	-
	DMSO	+++	-	++	-	+	-
	Ionic liquid	+++	-	++	-	-	-
	[a]LBP solvent	++	++	++	++	++	++
Biphasic	Organic/aqueous	+	+	+	+	+	+
	Organic/ionic Liquid	++	+	+	-	-	-

[a]Low boiling point green solvents

2.1.2. Selectivity of biomass conversion to HMF

The use of renewable raw resources is necessary for the chemical industry to have a sustainable future. Carbohydrates make up almost two thirds of renewable biomass, and their catalytic upgrading is a very real issue. Hexose carbohydrates are frequently processed by converting them to 5-hydroxymetylfurfural (HMF) in a water medium under the influence of an acid catalysts[35].

For biomass conversion to HMF , a variety of catalysts including solid catalysts and mineral acids have been used. The principal drawback of solid catalysts is their deactivation by tar and humic

substances, which, depending on the desired products, are produced in quantities of at least 5–10 weight percent during the process. The strongest mineral acids in water have the highest acidity and catalytic activity at moderate temperatures (~100^{o}C)[36]. To produce HMF different organic solvents including ionic liquids are applied.

Maintaining excellent selectivity of the conversion process while increasing the substrate load is the key challenge in the carbohydrate acid-catalyzed conversion to HMF. The main cause of the low selectivity at high carbohydrate concentration was associated with the instability of 5-HMF and its condensation to humic substances[37]. According to Buttersack *et al.*,2021[38], the earlier kinetic models for fructose conversion in the presence of strong proton acids consider the stage of yields (80–95 mol%), which are only attained in very low carbohydrate concentrations and drop off sharply at higher concentrations. Therefore, from both a theoretical and practical standpoint the effect of the conversion reaction parameter on selectivity of the process is very crucial.

In an effort to pinpoint the selectivity-controlling parameters, a number of mechanistic pathway for acid-catalyzed dehydration of fructose to HMF in aqueous and aprotic environments have been reported[7]. Figure 3 presents a detailed flow chart of the acid-catalyzed conversion of fructose to HMF. It has been suggested that fructose's initial dehydration is followed by the formation of DFA (Di-fructose dianhydrides). In this mechanism, fructose is first dehydrated to a fructosyl cation intermediate, which can then interact with another fructose molecule via a parallel and reversible pathway and resulted strong six-membered ring between the two-fructose tautomers[39]. Fructose can produce the two major DFA-tautomer's, fructofuranose-fructofuranose anhydride and fructofuranose-fructopyranose anhydride[40]. Because DFAs have a stable six-membered ring structure, their hydrolysis back to fructose is often slower than the conversion of fructose to HMF. Therefore, the synthesis of HMF from biomass is protected by the presence of DFAs. Using high temperature or changing the solvent to dipolar aprotic solvents, a fast equilibrium between the fructose tautomer in solution can be moved toward the furanose form of fructose. While fructofuranose results in the synthesis of HMF upon dehydration, fructopyranose produces humins[41].

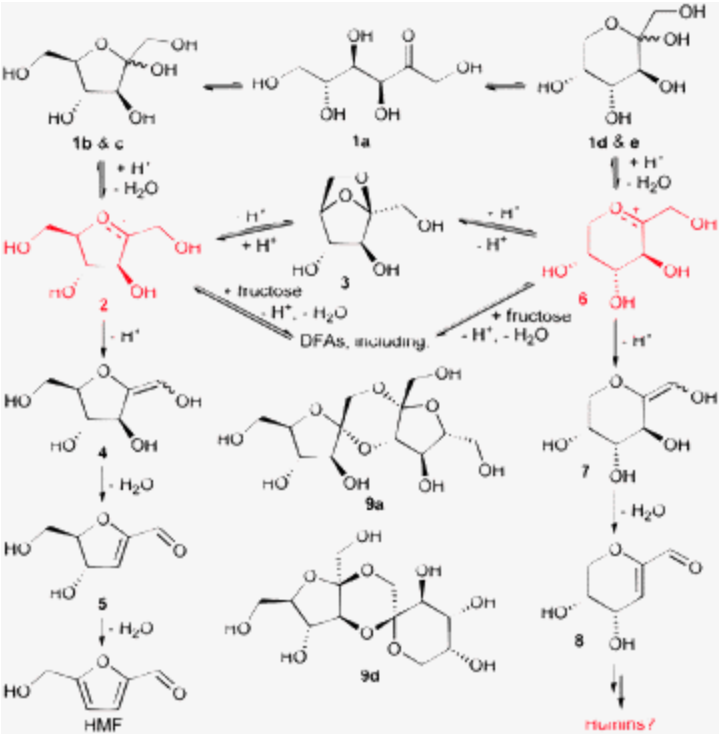

Figure 3: Molecular isomers of fructose (1a–e) and their acid catalyzed dehydration to HMF and side products (copy from Akien et al.,2012)[39]

The mechanism unequivocally demonstrates that the main controller of HMF selectivity are the ratios between the furanose and pyranose forms. This is most likely caused by the acyclic and cyclic tautomer's tautomerization being a quicker pathway than any acyclic conversion pathway[42]. Additionally, the formation of DFAs, which behave as protective intermediates, is a second pathway to synthesize HMF. DFAs enhance selectivity to HMF at longer reaction times, while it is unclear whether they directly convert to HMF or hydrolyze back to fructose[7].

Furthermore, the HMF selectivity and yield strongly depends on the substrate used, with fructose giving far better yields than glucose. The techno-economic analysis shows that glucose is a more desirable feedstock due to its greater abundance and significantly lower cost when compared to fructose. An appealing idea to increase the overall HMF yield from glucose or glucose-rich cellulosic biomass is a two-step process that integrates the (equilibrium) isomerization of glucose to fructose and the subsequent selective fructose dehydration to HMF, with glucose remaining (largely) unconverted and recycled (Figure 4)[43].

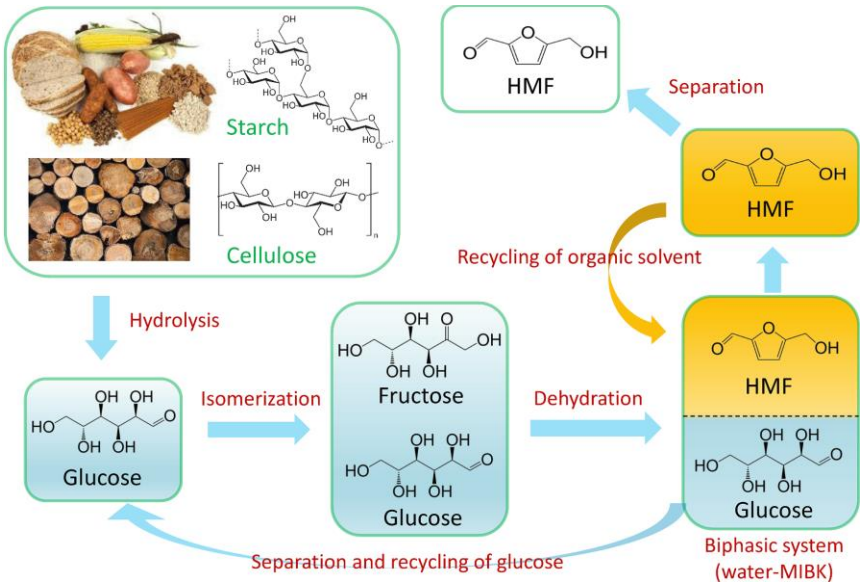

Figure 4: Concept of the integrated process for HMF production from glucose or glucose-rich cellulosic biomass (copy from Guo et al., 2021)[43]

Several past studies have demonstrated the effect of thermochemical conversion parameters on the selective formation of HMF using a model substrate like fructose, however no comprehensive study has been made to determine how reaction selectivity relates to the process parameters through mechanistic insights on real biomass sample. Therefore, the selectivity of thermochemical conversion of fruit biomass to HMF was the major objective of this study.

2.2. Experimental design and its application on thermochemical biomass conversion

Biomass conversion via the thermochemical process depends on several complex chemical reactions. The different variables that are involved in the synthesis of HMF and other chemicals from biomass required an efficient empirical laboratory screening toward an optimized conversion process and use, i.e., to obtain maximum yield and selectivity with low cost and minimum environmental impact.

The traditional one factor at a time (OFAT) approach applied on HMF production involves getting optimized synthesis and processing routes by choosing an experimental setup with the highest probability of resulting in a particular performance (high yield and selectivity). OFAT becomes feasible when the conversion product property and the effect of each variable is well explored, i.e., when all experimental conditions necessary for the conversion process and its production yield are sufficiently correlated[44]. The main challenges that prevent the concrete use of OFAT approaches

by a single research group are time and laboratory costs. The statistical concept of design of experiments (DOE) has been demonstrated to be a powerful tool for identifying important parameters to optimize chemical processes, whether in the industrial or academic fields[45].

Using the Design of Experiments (DOE) mathematical technique, experiments are planned, carried out, and their findings are analyzed and interpreted. It is a subfield of applied statistics that is employed for carrying out research studies on a system, procedure, or product in which input variables (Xs) were changed to examine their impacts on the measured response variable (Y). The design of experiments is a versatile strategy that may be used to identify significant input elements (input variables) and how they connect to the outcomes in a variety of circumstances (response variable)[46]. Additionally, DoE can be applied in a variety of circumstances and is basically regression analysis. Commonly used class of experimental design are the following[47]:

1 Comparison– this is one factor among multiple comparisons to select the best option that uses t–test, Z–test, or F–test.
2 Variable screening– these are usually two-level factorial designs intended to select important factors (variables) among many that affect performances of a system, process, or product.
3 Transfer function identification– if important input variables are identified, the relationship between the input variables and output variable can be used for further performance exploration of the system, process, or product via transfer function.
4 System Optimization: the transfer function can be used for optimization by moving the experiment to optimum setting of the variables. On this way performances of the system, process or product can be improved.
5 Robust design deals with reduction of variation in the system, process, or product without elimination of its causes. Robust design was pioneered by Genichi Taguchi, who made the system robust against noise (environmental and uncontrollable factors are considered as noise). Generally, factors that cause product variation can be categorized in three main groups:
    - external/environmental (such as temperature, humidity, and dust)
    - internal (wear of a machine and aging of materials)
    - Unit to unit variation (variations in material, processes, and equipment)

There are three principles of DOE , i.e., randomization, replication, and blocking. There are generally two categories of DOE: classical and modern designs. Classical designs are mostly used to introduce DOE concepts, whereas modern designs are mostly used by industry practitioners in carrying out experiments. Full factorial designs, fractional factorial designs (Screening designs), response surface designs, mixture designs, Taguchi array designs, and split plot designs are categorized under classical (Textbook) design. On the other hand, Definitive screening design (DSD), and custom designs are categorized as modern design.

2.2.1. Definitive screening design (DSD)

In a comparatively small-scale experimental campaign, statistical screening designs are intriguing for determining the relative influence of various factors on an interesting result. Most screening designs only allow for two levels of each factor, focusing instead on estimating the primary effects and preventing the measurement of the curvature between the factor and the response. As a result, adding middle levels during the second experimental set is necessary to capture the curvature[48]. It was recently suggested to use the definitive screening design (DSD), a new and better class of three-level designs, to get accurate main effect estimates that are unaffected by any quadratic effects and two-factor interactions[49]. Unlike traditional screening by two-level fractional factorial designs, DSD may render follow-up experiments unnecessary in many situations, and further, it avoids the confounding of effects, and it can identify factors having a nonlinear or curvilinear effect on the response[50].

Additionally, experimenters can fit a response surface model using DSD without running extra experiments. Once inconsequential components have been excluded, a second-order model with quadratic effects can be estimated in the remaining factors because the first set of runs contains enough of each factor. They are an excellent alternative to factorial experiments when expected response variable curvature is present and the experimenter wants to avoid performing additional experimental runs[51]. However, DSD can handle a few categorical factors at two levels, but if most of the factors are categorical, using a DSD is inefficient[52].

2.3. Analytical techniques and Instrumentation

Advanced analytical techniques can contribute significantly to the biomass supply chains, be they of plant or animal origin. However, given the chemical diversity of plant-derived biomass such as

cellulose, hemicellulose and lignin, it presents both the greatest challenges and the greatest opportunity for technical and scientific advancement. It is important to note that chemical analysis is used to characterize physical and chemical properties, investigate composition, and determine the concentration of desired chemical species[53]. Components of an economic chain derived from biomass and the use of analytical methods are depicted in a simplified manner in Figure 5.

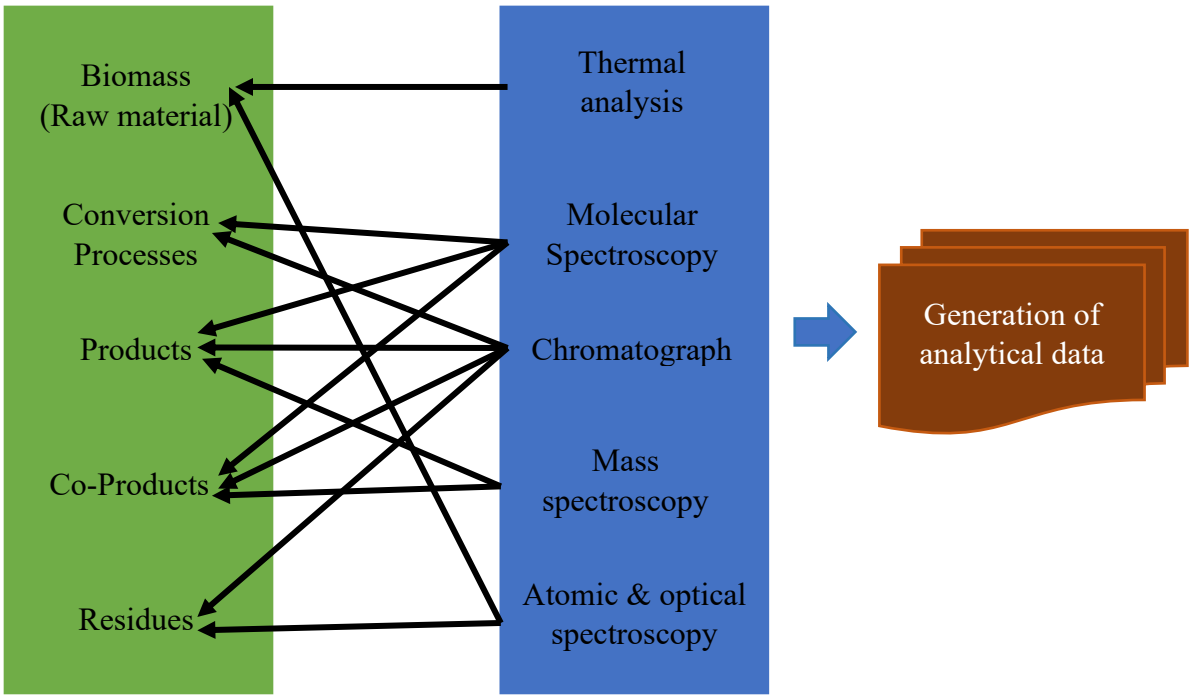

Figure 5: A flowchart of the relationship between components of a biomass chain and chemical analyses to generate analytical data

In general, all analytical methodology that is applicable for biomass characterization and conversion are critical tools for researchers, students and professors who work on biomass conversion to fuels, chemicals, and products. Advanced analytical chemistry methods and techniques can now provide detailed compositional and chemical measurements of biomass, biomass conversion process streams, intermediates, and products.

The analysis of the chemical composition of raw materials from biomass usually requires analytical techniques that provide a rapid response (the shortest period between the beginning of the measurement and the result) because the results of the analysis will determine whether the biomass material is accepted for a production process.

At present, NMR has an important role in the study of biomass components, particularly the lignin structure. For instance, two-dimensional heteronuclear single-quantum coherence NMR with ^{1}H and ^{13}C heteronuclear couplings can be applied to identify the monomeric and dimeric structures present in lignin[54]. Furthermore, Løhre *et al*., 2021[55] reported the application of quantitative nuclear magnetic resonance (qNMR) spectroscopy for rapid identification and quantification of organic molecules in aqueous product that generated from thermochemical conversion of plant biomass.

2.3.1. HPLC-MS/MS

The LC-MS technology involves use of an HPLC, wherein the individual components (Figure 6) in a mixture are first separated followed by ionization and separation of the ions based on their mass/charge ratio. After being separated, the ions are sent to a photo or electron multiplier tube detector, where each ion is identified and measured. The ion source is a crucial part of any MS analysis since it essentially facilitates the effective creation of ions for analysis. Ion sources for ionizing intact molecules include ESI (Electrospray Ionization), APCI (Atmospheric Pressure Chemical Ionization), and others. The choice of ion source also depends on whether the target analyte is polar or non-polar chemically[56]. Different affinities of the constituents for a stationary phase packed into a column and a mobile liquid phase that travels through it are utilized by liquid chromatography system. A suitable sample detector can be used to monitor the column effluent, and an elution chromatogram, which typically relates the concentration of the components in the mobile phase with time from the application of the mixture to the column, can be used to determine whether the separation was successful[57].

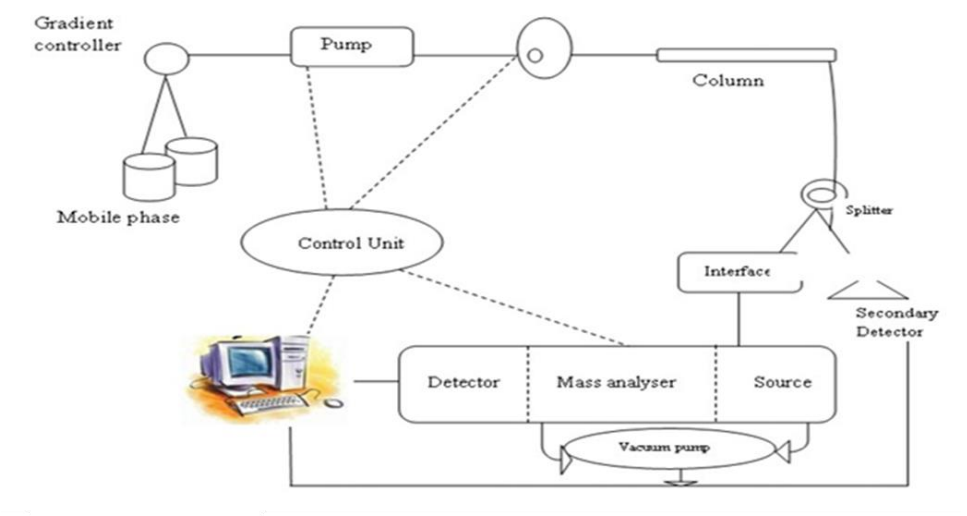

Figure 6: Basic instrumentation of HPLC-MS (copy from Parasuraman et al.,2014)[57]

Mass spectrometry (MS) has been described as the smallest scale in the world, this is not only because of its size of what it weighs a molecule, but mostly it related to the microanalytical technique that can be used selectively to detect and determine the amount of a given analyte. MS can also be used to ascertain an analyte's molecular structure and elemental content. The power of MS to directly determine the nominal mass of an analyte as well as its ability to create and identify fragments of the molecule that correspond to distinct groups of atoms of various elements that disclose structural details are its unique properties.

The tools of MS are mass spectrometers, and the data they produce are known as mass spectra. These spectra can be displayed in a variety of ways, making it possible to readily extract the desired analyte information. A MS is a device that creates a beam of gaseous ions from a sample, separates the resulting mixture of ions based on mass-to-charge ratios, and gives output signals that represent measurements of the relative abundance of each ionic species present. However, all MS can be characterized as ion optical devices that separate ions based on their mass-to-charge (m/z) ratios by applying electric and/or magnetic force fields[58]. MS are often categorized based on how the mass separation is performed (Figure. 7).

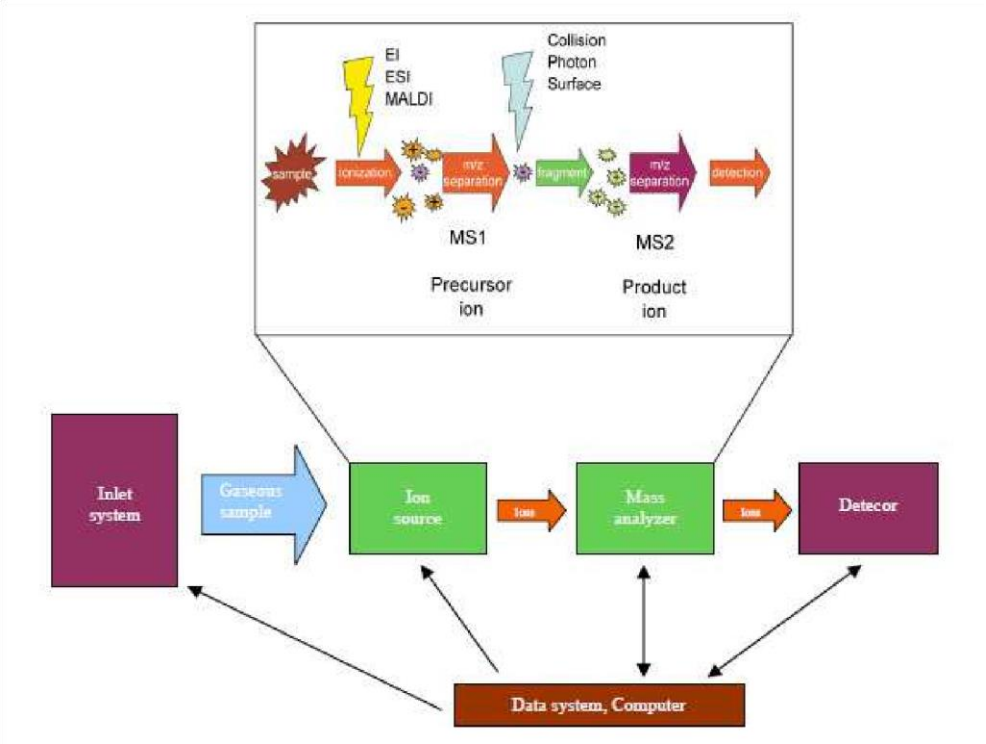

Figure 7: Basic principle of mass separation in MS (adopted from Kang, 2012 without modification) [58]

The concept behind MS is to create ions from a sample, separate the ions according on their m/z ratio (which can be the same as the mass as the ion typically only has a single charge), and then calculate the ion abundance. All the operations (ionization separation of the ions, rate of data capture, detection of the ions, and storage of the data) in modern MS instruments used for environmental investigations are computer controlled (Figure 8). In the ion source, gaseous molecules are ionized to generate molecular ions, some of which will fragment. Ions with varied m/z values travel to the detector one at a time through the mass analyzer through a variety of methods. When the ions strike the detector, they are converted into an electrical signal which, in turn, is converted into a digital response that can be stored by the computer[59].

Instead of determining mass directly, a mass spectrometer measures the m/z of an ion to estimate the mass of a molecule. One may ascertain what is present by knowing the m/z value of the ions, and one can ascertain how much is present by measuring the ion intensities. Additionally, a thorough understanding of the ionization process may be obtained from the mass spectra by systematic interpretation, which can then be applied to the elucidation of molecular structures. This explanation of the term "m/z" is crucial to comprehending MS. The m/z value is a

dimensionless number that is always used in mass spectrometry. Instead of the physical scale that is typically thought of as mass, the mass component that makes up the dimensionless m/z unit is based on an atomic scale. The mass spectrometer only detects ions, and any nonionic particles without a charge are driven out of the mass spectrometer by the continual pumping that keeps the vacuum in place. Ions must first be produced in the gas phase by the MS[58].

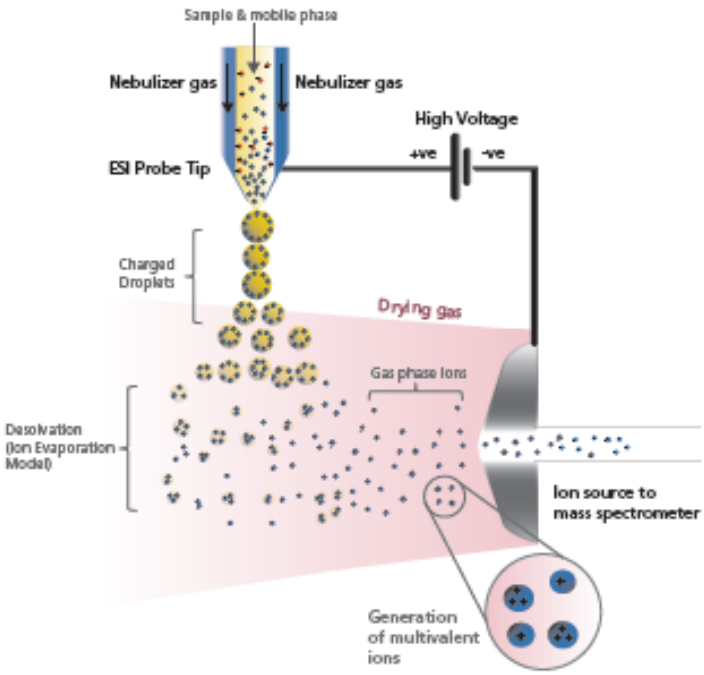

Figure 8: Ionization process in MS (adopted from Shimadzu Fundamental Guide to LCMS)[60]

These ions are separated based on their m/z values in a vacuum where they are unable to collide with any other kind of matter (Figure 9). The mass spectrum is obtained by separating and detecting ions with different m/z values under evacuated environment (high vacuum). The direction of an ion's flight may be changed if it collides with neutrals in an elastic collision during the ion separation process, and the ion may not reach the detector. If the collision between ion and neutral is inelastic, enough energy transfer may cause it to breakdown, rendering the original ion undetectable. Ions with the same charge can have their paths deflected by close contact. Direct contact between ions of opposite charge signs will result in neutralization. Ions are molecules, clusters of atoms, or positively or negatively charged atoms. Ionization is the process by which an electrically neutral atom or molecule acquires or loses one or more of its extra nuclear electrons, causing it to become electrically charged. Although positive and negative ions can both be studied

by MS, positive ions are typically the focus of investigation because they are typically produced in greater quantities than negative ions in most ion sources. For ion formation to take place, a certain amount of energy known as the "ionization potential" must be present. The energy input necessary to remove (to an infinite distance) a valence electron from the highest occupied atomic or molecular orbital of the neutral particle to form the corresponding atomic or molecular ion, also in its ground state, is known as the first ionization potential of an atom or molecule. An ion is referred to as an atomic or molecular ion when only one electron is taken out; the term "parent ion" is frequently used. It is possible to think of the formation of parent ions as ionization without cleavage[61].

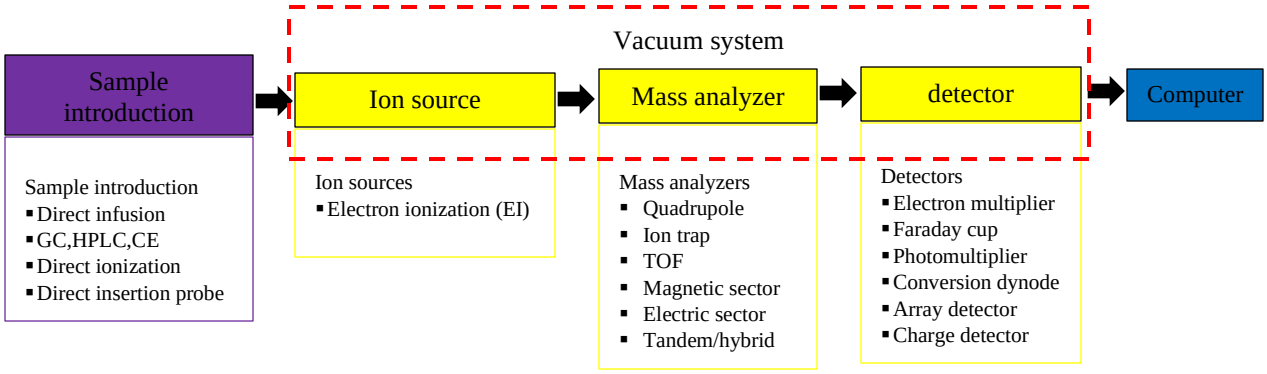

Figure 9: Basic instrumentation of MS

The basic mass spectrometry of instrumentation are consisted of (1) introduction of sample; a sample which can be a solid, liquid, or vapor is loaded onto a mass spectrometry device and is vaporized, (2) ionization; sample components are ionized by one of several available methods to create ions, (3) mass analyzer; the ions are sorted in an analyzer according to their m/z ratios through the use of electromagnetic fields, (4) detector; the ions then pass through a detector where the ion flux is converted into a proportional electrical current and (5) date conversion; the magnitude of the ion/electrical signals is converted into a mass spectrum (Figure 10).

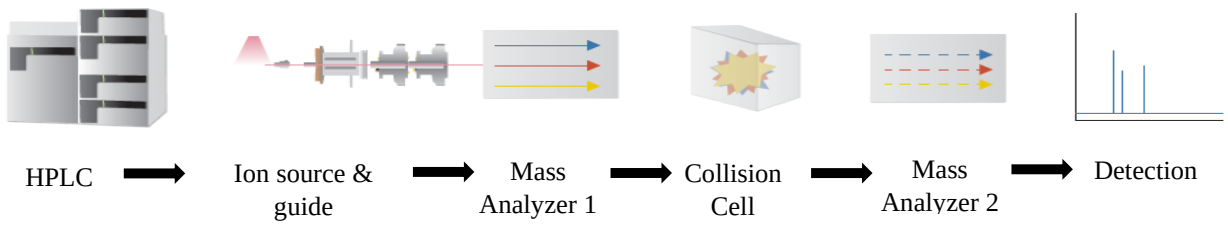

Figure 10 : Basic instrumentation of a LC-MS/MS

The basic components in an MS/MS system are illustrated in Figure 10. Like LCMS, MS/MS system can be coupled to a LC prior to MS analysis. The main difference between a LCMS and a LC-MS/MS is the addition of a collision cell and a MS2. The single mass analyzers described earlier can be integrated into an MS/MS system.

2.3.2. Analytical Quality by Design (AQbD) approach to develop a LC-MS/MS method

Joseph M. Juran, a quality specialist, coined the phrase "quality-by-design" (QbD) in the 1970s, and it gained popularity in the 1990s[62]. In the pharmaceutical field, the International Conference on Harmonization (ICH) Q8(R2) defines QbD as a systematic approach to development that begins with predefined objectives and emphasizes product and process understanding and process control based on sound science and quality risk management[63].

The quality by design concept has been well adapted by analytical chemists and termed “analytical quality by design”(AQbD). Analytical quality by design (AQbD) is defined as a science and risk-based paradigm for analytical method development, endeavoring for understanding the predefined objectives to control the critical method variables affecting the critical method attributes to achieve enhanced method performance, high robustness, ruggedness, and flexibility for continual improvement[64, 65].

The process flow in AQbD approach is like QbD for drug development as shown in Figure 11. The analytical target profile (ATP) of the method and its intended use are first defined in AQbD. In analytical methods development, the processes that the technique must include such as sample preparation, sample introduction, sample analysis, and data analysis are referred to as method attributes. The method parameters are the specific stages of a method attribute, just as the process parameters. The plan for method quality control is then developed based on an understanding of how important each method parameter is for each method attribute[66].

Generally, the main goals of AQbD have been to define meaningful system suitability criteria, develop robust method operable design regions or design spaces, and promote ongoing life cycle management. The development of strong, well-understood analytical procedures to reliably deliver the intended performance across the product lifecycle has typically used analytical quality by design (AQbD) paradigms[67].

With its focus on two fundamental components, Quality Risk Management (QRM) and Design of Experiments (DoE), AQbD sets out to prioritize the "possible so many" input variables that are high-risk and influential. It then moves on to define an "optimal" analytical solution in the form of a design space[68]. Application of novel techniques such as Monte Carlo simulations and the variance inflation factor (VIF), respectively, can be used to validate the developed design space against the probabilistic design space and to rule out the likelihood that multicollinearity among the selected input factors is prevalent[69].

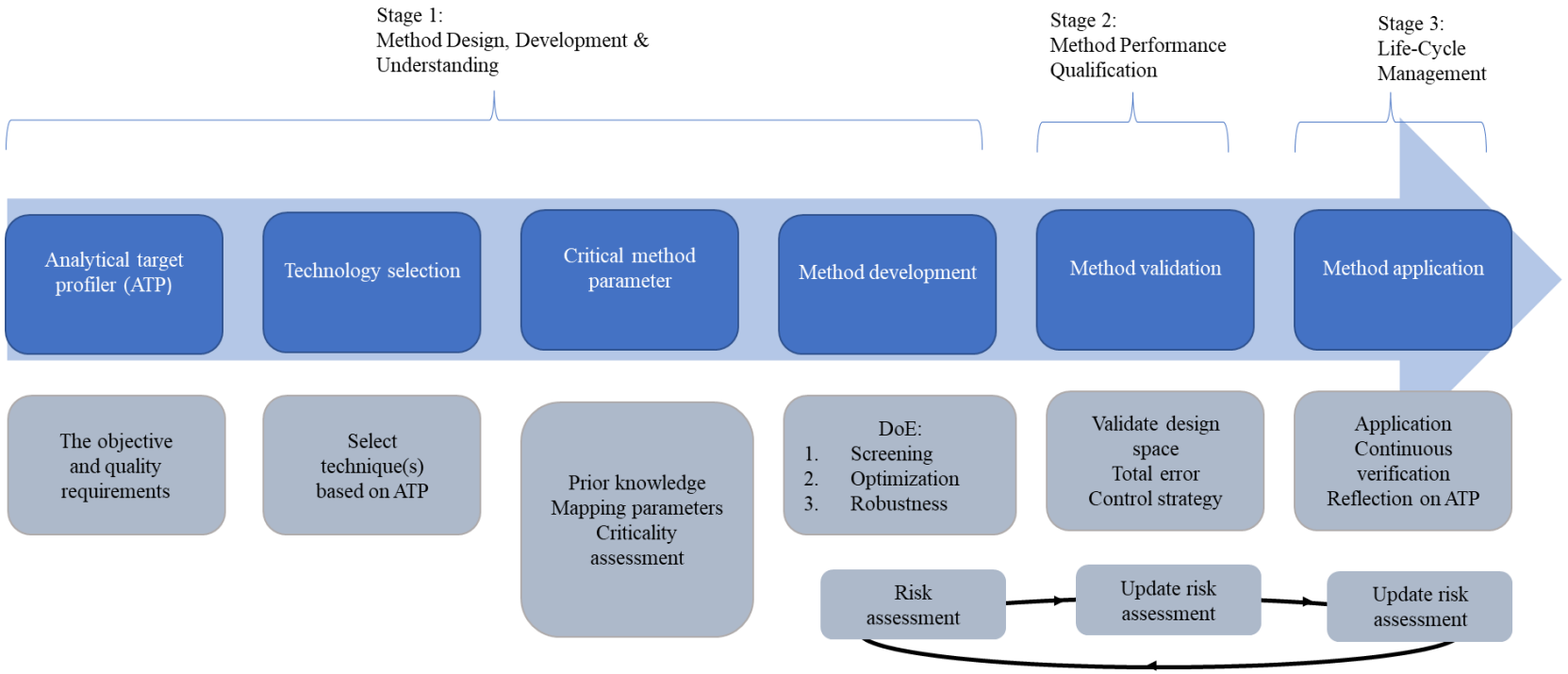

Figure 11: Schematic representation of the steps of the AQbD process: Analytical targe profile (ATP), risk assessment, screening design, optimization, method operable design region (MODR), analytical procedure validation, and control strategy

3. Experimental

This work describes the development of LC-ESI-MS/MS method for sugar analysis in biomass sample and conversion selectivity study on thermochemical biphasic transformation of fruit biomass to HMF. The LC-ESI-MS/MS method has been developed based on AQbD approach for characterization of the raw biomass, and the effect of variables in the selectivity of the thermochemical conversion were screened and optimized using definitive screen experimental design. The sugar content of raw feedstock and the product fraction of the thermochemical conversion were analyzed using the developed LC-ESI-MS/MS method.

3.1. Chemicals and materials

The following reagents were used for this work: 5-hydroxymethyl-2furfural, sugar standard (D-glucose, D-fructose, D-galactose, mannose, xylose , ribose, arabinose , maltose , sucrose , and lactose), Acetonitrile , Methanol, Formic acid, Sodium Acetate , Methyl-isobutyl-ketone (MIBK) Sulfuric acid and Sulfamic acid obtained from Sigma-Aldrich. Fruit biomass (plums) was obtained from Hardanger Fjordfrukt BA. The thermochemical conversion processes were conducted in a 22mL Series 4700, 316 Stainless steel batch Parr reactor.

3.2. Standards and reagents

Individual standard stock solution and internal standard stock solution were prepared in methanol/water (1:1, v/v), and stored at −4 °C. Working standard mixture solutions and internal standard mixture solutions were prepared in water and stored at −4 °C. Standard solutions for the calibration curve were prepared in water before each analytical run.

3.3. Characterization of Fruit biomass (Plum & cherry)

The sugar content of the fruit biomass was analyzed by the newly developed LC-MS/MS method. We followed analytical quality by design approach (AQbD) for developing new LC-MS/MS method for sugar analysis in fruit biomass (Appendix 1).

3.3.1. Experimental design

In accordance with the experimental design, critical method factors were investigated, this including the flow rate of the mobile phase (X1), concentration of NaAc (X2), column temperature

(X3), gas flow rate (X4), gas temperature (X5), nebulizer pressure (X6), and capillary voltage (X7). The coded and uncoded values of each parameter are shown in Table 1. and then the effects of these seven parameters on the analytical responses were performed by a definitive screening experimental design, as shown in Table 2.

Table 2: The factors and levels of definitive screening design

Factor	Term	Unit	Code	
			-1	1
Flow rate of the mobile phase	X_1	mL/min	0.2	0.4
Concentration of NaAc	X_2	mM	0.1	0.5
Column temperature	X_3	^{0}C	25	50
Gas flow rate	X_4	L/min	3	8
Gas temperature	X_5	^{0}C	200	300
Nebulizer pressure	X_6	Psi	25	45
Capillary voltage	X_7	KV	2.5	4.5

3.3.2. Fruit sample preparation

Samples examined in this study included two types of fruits i.e., plums sold in the Norwegian market. The fruits biomass sample were prepared according to NREL Laboratory Analytical Procedures "Preparation of sample for compositional analysis"[70] and "Determination of structural carbohydrates and lignin from biomass"[71]. The fruit sample was deseeded, dried in an oven at 45 ^{0}C, weighed and stored in desiccator. To prepare the hydrolysate 0.3 gm (± 0.01 gm) previously dried samples were loaded into autoclave pressure tubes (600mL). The samples were then mixed with 3 mL of 72% H_2SO_4 and placed in a 30 ^{0}C water bath for 1 hour. After the samples were removed from the water bath, 84 mL of water was added to each tube and the tubes were autoclaved at 121 °C for 1 hour. The samples were allowed to cool to room temperature and the liquid hydrolysate fraction was then decanted into 250 mL conical tubes and neutralized with $CaCO_3$ to a pH of 7. The neutralized samples were centrifuge at 5000 rpm for 10 minutes; the liquid hydrolysate fraction was filtered at 2 microns to ensure all solids were removed from the solution. Filtered hydrolysates were stored in 100 mL microfuge tubes until further preparation for quantitative LC-MS/MS analysis.

3.3.3. Instrumentation

The sugar separation was performed on an Agilent 1260 Infinity Quaternary liquid chromatography (LC) system (Agilent Technology Inc., Wilmington, DE), using an XBridge Premier BEH Amide VanGuard FIT Column (2.5 μm particle size, 2.1 mm I.D. × 100 mm, Waters Inc., Milford, MA). Acetonitrile (ACN)/Methanol (98:2, v/v) (solvent A) and 0.5mM NaAc with 30% Methanol (solvent B) were used as mobile phases. The following analyses were carried out using the best chromatographic settings for LC operation. The flow rate of the mobile phase was 0.4 mL/min. The gradient elution was 0–10 min, 85–40% solvent A; 10–10.1min, 40–85% solvent A; 10.1–15 min, 85% solvent A. The column was maintained at 40 °C. The sample volume injected was 2 μL. During the first 0.8 min and the last 5 min of the gradient, the mobile phase was redirected to waste and not to the mass spectrometer. Between each sample, the autosampler's injection needle was washed for 10 seconds. The LC sample compartment was kept constant at 4 °C. The LC system was coupled with an Agilent 6420 Triple Quad mass spectrometer (Agilent Technology Inc., Wilmington, DE) with an electrospray interface. All analytes were ionized in positive mode as $[M+Na]^+$. The mass spectrometer was operated under single ion monitoring (SIM) mode. The fragmentation voltage for each analyte and analog were optimized separately by direct infusion of individual standard solution. Agilent Mass hunter® Software Version 6.1 (Applied Biosystems, Foster City, CA) was used for data acquisition.

3.3.4. Method validation

In accordance with our method validation plan, the linearity, sensitivity, analytical precision, accuracy, and robustness experiments of the developed method were carried out. The limit of detection (LOD) and the limit of quantification (LOQ) were assessed based on an S/N at 3:1 and 10:1, respectively. The same standard solution was injected six times continuously to evaluate injection precision. For evaluation of intra-day precision, six sample solutions were prepared in parallel and analyzed during a single day. For evaluation of inter-day precision, replicate samples were analyzed for six consecutive days, respectively.

For evaluation of method accuracy, recovery experiments conducted in triplicate at low and high concentration level. Recoveries for all analytes were assessed by spiking known amounts of analytes at low and high levels into the sample. The spiking solution was prepared by adding and mixing analytes in water. The calculated volume of spiking solution for low- or high-level recovery

experiment was aspirated with pipette and dispensed on the sample. Control blank samples without spiking analytes were prepared as regular unknown samples. Five replicates were prepared and analyzed for each set of recovery experiment samples (control blank, low level spiked, and high level spiked). Replicate concentrations for each analyte were averaged, and the analyte concentration in control blank was subtracted from the measured analyte concentration in prepared low- or high-level spiked samples. The recovery was calculated as the percentage ratio of calculated spiked concentration to the theoretically spiked concentration.

3.3.5. Quantitation

JMP Version 16.2 (SAS Campus Drive, Cary, NC), Agilent Mass hunter® Software Version 6.1 (Applied Biosystems, Foster City, CA) and MestReNova (Mestrelab Research, Santiago de Compostela, SPAIN) Software was used for experimental design (DOE) data analysis, peak integration, calibration, and quantitation. Each peak was manually inspected to confirm correct integration. Relative response factor was calculated based on the ratio of the peak area of the analyte quantitation to that of the internal standard. The peak area ratio of the analyte quantitation to the internal standard was used to quantify the unknowns through comparison with the calibration curve. Sample results are reported as % (w/w).

3.4.Thermochemical conversion fruit biomass to HMF

The selectivity study of the thermochemical conversion of fruit biomass to HMF was investigated using a systematic experimental design approach.

3.4.1. Experimental design

Screening and optimization of the primary factor that controls the selectivity of the thermochemical conversion system was examined. In this section, a unifying mechanism will be developed to explain how the experimentally observed rate, yield, and selectivity of biomass conversion to HMF are controlled. First, the primary factors were screened using DoE that controls the selectivity of the conversion system. For this purpose, the conversion reactions Were carried out in a Series 4700, 316 Stainless steel batch Parr reactor of size 22 mL by considering the following factors as the main variable that influence the conversion process. The minimum and

maximum values are set based on our group previous work by Molnes (2021)[72], Mayhew (2022)[73] and recently published literature by another group[7].

Table 3: Maximum and minimum value of each continuous factor

Factors	Minimum value	Maximum value
Substrate load (g)	0.1	0.4
Sulfamic acid concentration (g)	0.01	0.04
Temperature (^{0}C)	150	210
Aqueous phase (V %)	30	80
Time (min)	30	120

For screening and optimization study of the main factors, definitive screening design (DSD) was used. A total of 17 experimental run were performed to screen and optimize the main thermochemical factors (Table 3).

Table 3: DSD experimental run for screening and optimization of thermochemical conversion of plums biomass

Run No.	**Substrate load (g)**	**Catalyst load (g)**	**Temp. (^{0}C)**	**Aqueous phase (V%)**	**Time (min)**
1	0.4	0.01	210	30	30
2	0.25	0.04	210	80	120
3	0.25	0.01	150	30	30
4	0.4	0.025	210	80	30
5	0.1	0.025	150	30	120
6	0.25	0.025	180	55	75
7	0.1	0.01	150	80	30
8	0.4	0.04	210	30	120
9	0.4	0.01	150	55	120
10	0.4	0.01	180	80	120
11	0.4	0.04	150	80	30
12	0.1	0.04	150	80	120
13	0.1	0.04	180	30	30
14	0.4	0.04	150	30	75
15	0.1	0.04	210	55	30
16	0.1	0.01	210	30	120
17	0.1	0.01	210	80	75

3.4.2. Thermochemical conversion reaction

The conversion processes were conducted in a 22mL Series 4700, 316 Stainless steel batch Parr reactor. Pre-prepared (according to section 3.3.3) fruit sample was used for the biphasic reaction system as shown Figure 12. We used biphasic reaction system developed by Molnes (2021)[72] with appropriate modification.

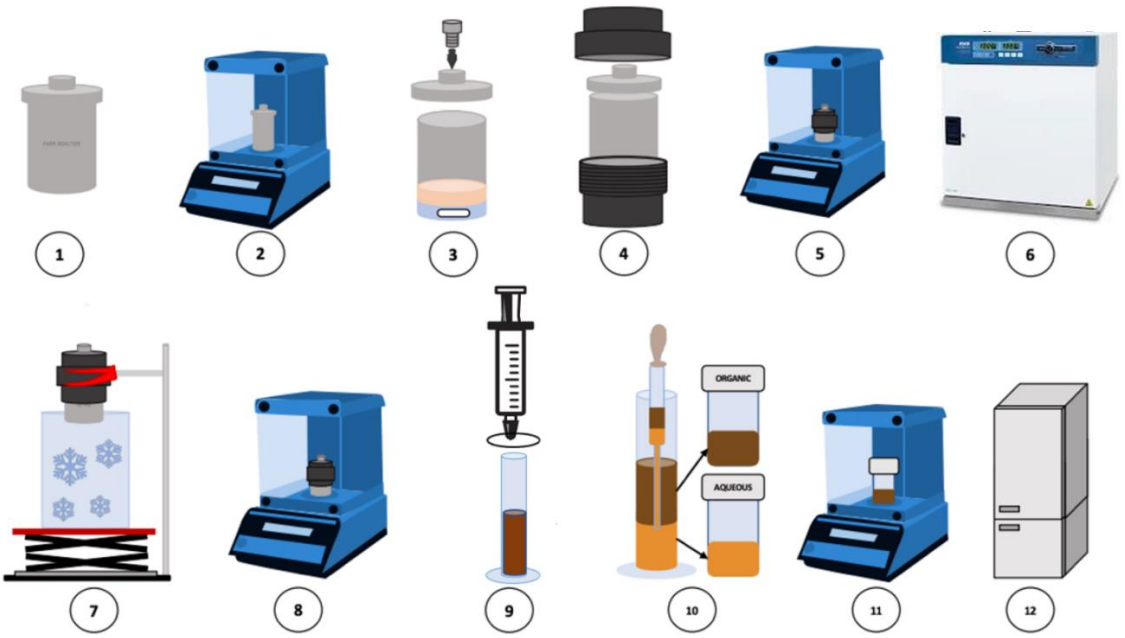

Figure 12: The procedural steps for the conversion reaction of fruit biomass to HMF. Adapted and parts redrawn from Molnes, 2021[72].

Prior to adding the pre-prepared fruit biomass, catalyst, solvents (water and MIBK), and a magnetic stirrer to the reactor, the empty reactor (1) was first weighed (2 & 3). The reactor was then properly closed (4) and weighed once more (5). It was then put into an oven (6) that was heated to a temperature between 150-210°C for 30 to 120 minutes. After the rection completed, the reactor was put into an ice bath to quench the reaction (7). Every time, the same-sized ice bath was utilized to guarantee a constant cooling rate. The reactor was dried and weighed once it had cooled down (8). This was carried out to look for any potential reactor leaks. The product solution was then put into a 20 mL syringe equipped with a 0.45µm filter that had been previously weighed (9). The solution was squeezed through the filter and collected with a labeled and pre-weighed graduated cylinder (9). To calculate the product loss, the reactor, syringe, and filter were weighed

again after being emptied. A disposable glass pipette measuring 230mm was used for phase-separation (10). The organic and aqueous phases were separated and put into 20mL sample vials that had already been weighed (10). After being emptied, the graduated cylinder was weighed once again to calculate the product loss. the sample vials containing the organic and aqueous phases were weighed to determine the mass recovery (11). Finally, both phase products were kept in refrigerator (12).

3.4.3. LC-ESI-MS/MS analysis of product fraction

In biphasic thermochemical conversion process, there are different product fractions in organic and aqueous phase (Figure 13).

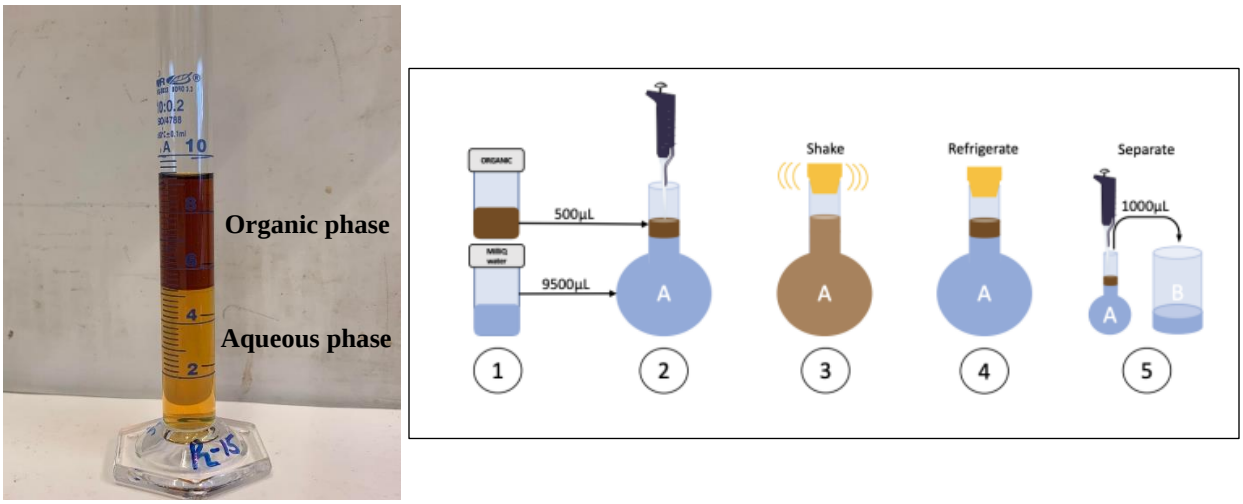

Figure 13: The procedural steps for LC-ESI-MS/MS sample preparation. Steps 1-4 shows the extraction with water for the organic phase.

The organic phase had to be extracted with water before sample preparation (steps 1-4). To perform the extraction with water, 500µL of the organic phase was transferred to a 10mL volumetric flask. Then, distilled water was added until the volume reached 10mL (2). Both the organic phase and water added were weighed so that an accurate dilution factor could be calculated. The mixture was shaken vigorously (3) before refrigeration for at least an hour to ensure adequate phase separation (4) . From this point the steps are the same for the aqueous phase and the extracted organic phase. Subsequently, 1000.0 µL of the aqueous phase/extracted organic phase and normal aqueous phase was further diluted 50 mL milliQ Water. Finally, 50 µL diluted filtrate of product fraction and 50 µL working internal standard solution was added and mixed in a HPLC Vial to make a prepared sample of 100.0 µL for LC-MS/MS measurement.

4. Results and Discussions

This section covers all experimental results that were generated during the laboratory work with appropriate interpretation in line with the primary objective of the thesis. According to our objectives listed in the introduction section, the results and discussion are split into two major sections. The experimental details related to LC-ESI-MS/MS method development for sugar analysis will first be presented and discussed. Next, the results from the optimization of the thermochemical conversion process will be presented. Finally, the thermochemical conversion process will be discussed along with the outcomes of the optimizing process.

4.1.The novel AQbD approach for the analysis of sugar in Plums using LC-MS/MS

The analytical method was developed according to the AQbD approach adapted from recommendations defined in ICHQ8(R2) (ICH 2009) guideline[74]. The workflow chart for AQbD approach is described in Appendix 1.The first step in AQbD based method development is to define the ATP for stepwise and scientific procedures. An analytical method which can quantitatively determine the specified nine sugar and 5-Hydroxymethylfurfural (HMF) in Plums and product fraction from thermochemical conversion is a target of this study. Various elements of ATP were summarized in Table 4 as the intended target criteria.

Table 4: Analytical Target Profile (ATP) for LC-MS/MS method development

ATP elements	Objective(s)	Explanation
Target sample	Plums	Analytical method development for the quantitatively detect of sugar in Plums
Analytical technique	HILIC	Polar stationary phase tends to provide improved retention of sugar molecules
Instrument requirement	LC-MS/MS	MS/MS provides higher sensitivity
Nature of sample	Liquid state	Analyte should be prepared in liquid state for ensuring absolute miscibility with mobile phase
Sample preparation	Hydrolysis	Preparation of sample is carried according to NREL guideline
Method application	Estimate of sugar	The method is applicable to detect sugars in fruit biomass

After ATP identification and set-up, the potential critical method attributes (CMAs) were considered based on preliminary studies and review of the literature. The general key CMA is the total peak area (TPA), peak resolution (PR) of critical peaks (5, 6,7, 8), and retention time of the last peak (RTLP) which may be a critical attribute to avoid peak overlap for selective identification with short analysis time in LC-ESI-MS/MS. In addition, to carry out design-based method development studies, several preliminary tests were performed in different columns (i.e., length, particle size, manufacturer), using various solvents (i.e., acetonitrile, methanol), and acidified water (i.e., non-acidified, 0.1% acetic acid, 0.1% formic acid) and different metal salt (NaCl, NaAc). Also, the modes of scanning and acquiring MS data were tested to acquire the best specific detection. The achieved results were organized in Table 5, and the final decision is to use XBridge Premier BEH Amide VanGuard FIT (2.1 x 100 mm i.d., 2.5 µm) column, acetonitrile and 0.1% formic acid water solvent system, NaAc metal salt modifier and selected ion monitoring (SIM), respectively.

Table 5: Preliminary screening results

Parameters	**Experimental strategy**	**Inference drawn**
Different columns	***XBridge Premier BEH Amide VanGuard FIT (2.1 × 100 mm i.d., 2.5 µm)**	Good sugar separation capacity because of the amide functional group attached to the stationary phase.
	Agilent ZORBAX SB-C18 RRHT threaded (2.1 × 50 mm i.d., 1.8 µm)	Poor sugar separation capacity
	A Rezex RFQ fast aid (100 x 7.8mm i.d., 1.7 µm)	Required strong acid that is not compatible for MS.
Various combination of solvents	Methanol and non-acidified water	Sugar molecules are not separated.
	Acetonitrile and non-acidified water	Poor peak resolution and intensity, most peaks were not fully separated from a neighboring.
	Acetonitrile and 0.1% acetic acid	Poor resolution of substances; Some peaks were not fully separated from a neighboring.
	***Acetonitrile and 0.1% formic acid**	Improved peak shape and resolution.
	Sodium chloride (NaCl)	Precipitate formation at MS entrance
	***Sodium acetate (NaAc)**	Free from precipitate formation
Scanning Mode	Multiple reaction monitoring (MRM)	Not effective
	***Selective ion monitoring (SIM)**	Very effective

*Selected conditions of each parameter

There have been different distinct methods for LC-MS quantitative analysis of sugar reported in literature. The first method relies on the post-column addition of chloroform to bind Cl^- to sugar. However, Cl^- attachment as a general single quadrupole technique has significant drawbacks[75-77]. The second approach is based on small cation attachment to sugar such as Na^+ and Li^+ . The analytical strategy based on Na^+ attachment is simpler to apply than chlorine attachment since it does not require post-column addition. In this method, "free" Na^+, a frequent glassware contaminant in aqueous mobile phases, is used. Contrary to chlorine attachment, the Na^+ attachment method only produces a single m/z peak because Na^+ is monoisotopic[78]. Therefore, in this study sodium adduct of sugar $[M+Na]^+$ was used for SIM based LC-ESI-MS/MS analysis. To obtain the main quantitative ions of each sugar, the fragmentor voltages were optimized by direct injection. According to One-Factor-At-a-time optimization approach , the optimum fragmentor voltages is 140 eV.

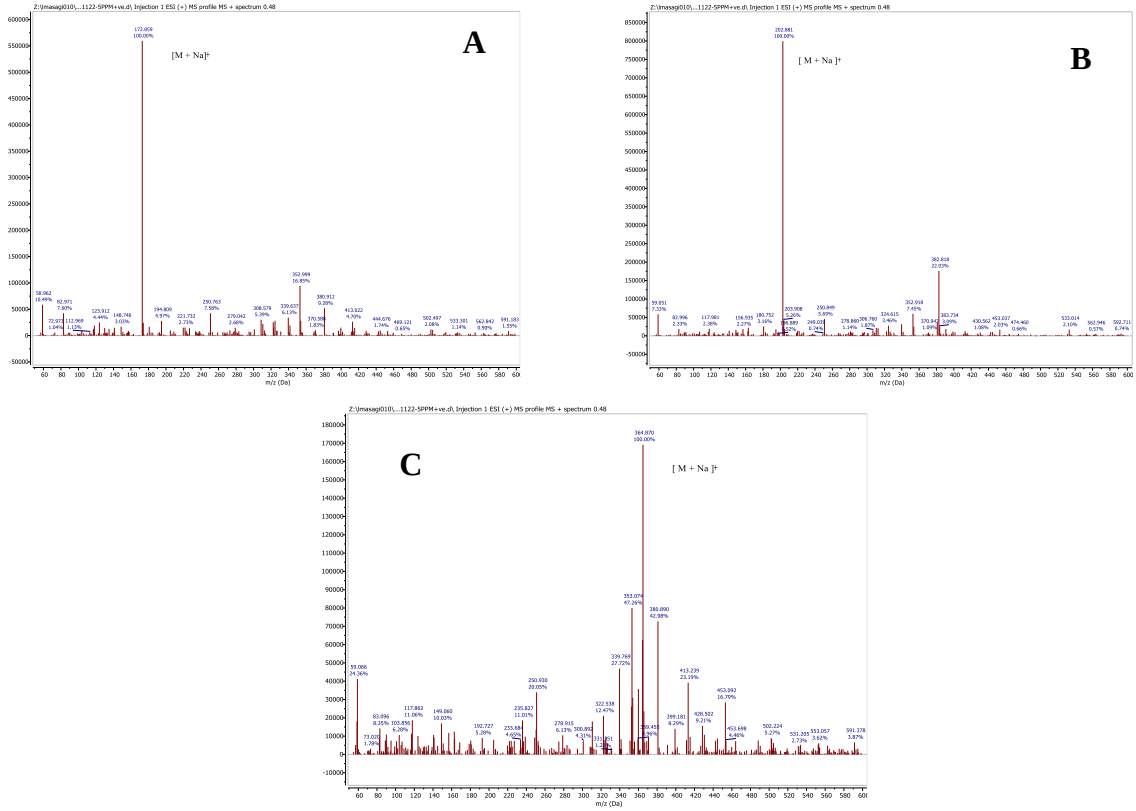

Figure 14: Full scan mass spectrum of (A) Xylose; (B) Glucose ; (C) Sucrose

Therefore, the main characteristic precursor ions at m/z 172.9, m/z 202.9 and m/z 364.9 were extracted for quantitative analysis of xylose, glucose, sucrose, respectively (Figure 14). Xylose represents low molecular sugar (ribose & arabinose), glucose represents medium molecular weight

sugar (fructose, galactose, & mannose), and sucrose represents high molecular weight sugar (maltose & lactose).

4.1.1. CMAs and CMPs identification

The analytical target profile (ATP) of this study was defined by the separation, identification, and quantification of sugars in the Plums sample through LC-ESI-MS/MS analytical method. Glucose, fructose, galactose, mannose, xylose, ribose, arabinose, sucrose, and maltose were selected in this study because these are the most abundant sugars in Plums. In addition, these sugars are also widely present in other fruits. The total peak area (TPA), peak resolution (PR), and retention time of the last peak (RTLP) of each sugar standard were chosen as the critical method attributes (CMAs) based on the chromatographic performance of the analytical method. The limits for CMAs values were established according to the minimal requirements for a satisfactory chromatography performance.

The scouting of chromatography performance was based on results from WATERS technology brief [79], where the analysis of fructose , glucose, sucrose, maltose, and lactose in several fruit juices was performed by LC-RI with an X-Bridge BEH Amide XP column and a binary mobile phase (15% H_2O with 0.05% TEA and 85% ACT) in isocratic gradient mode. The selection of critical method parameters (CMPs) was performed by quality risk analysis (QRA) through an Ishikawa fishbone cause-effect diagram constructed according to the results obtained on the method scouting step, being displayed in Figure 15.

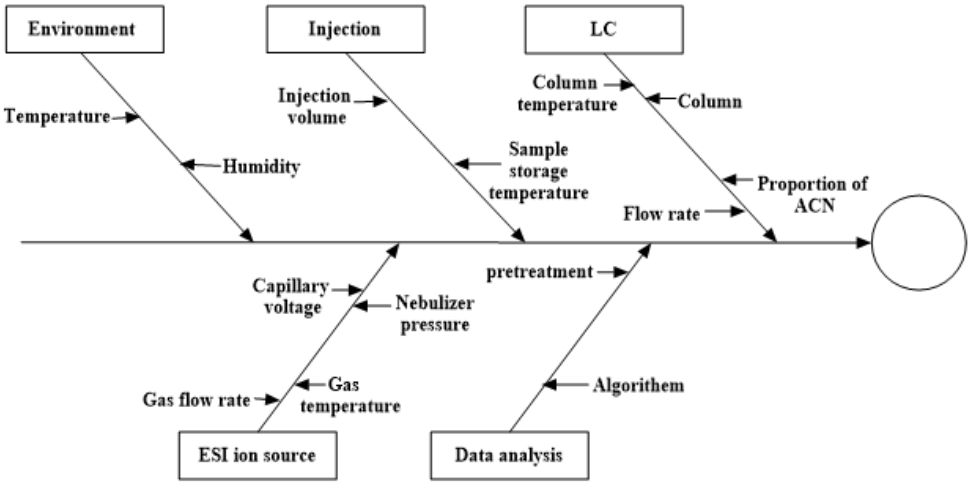

Figure 15: Ishikawa cause-and-effect fish-bone diagram for potential CMPs selection.

prospective causes of failure for liquid chromatography could be determined from the cause-and-effect diagram, and in the following step, the organized failure effects for each of the prospective causes were computed with a risk priority number (RPN) to separate out the high-risk causes. To assign risk to each failure mode, RPN numbers were generated using the formula "Severity Probability Detectability" in accordance with ICH Q1130. Table 6 presents an overview of the risk assessment and control method.

Table 6: Identifying high risk factors through the risk priority number (RPN)

Factor	Failure affect (s)	Risk mitigation	S	P	D	RPN
MP Flow rate	Changes in peak resolutions and elute time	Optimized by DoE & control	2	2	3	12
ACN Proportion	Change in peak symmetry and chromatograph	Fix ACN proportion at 90 %	2	2	2	8
Column Temp	Changes in peak resolutions, elute time, & S/N	Optimized by DoE & control	2	3	2	12
Gas flow rate	Change in peak resolutions, peak intensity & S/N	Optimized by DoE & control	2	2	3	12
Gas Temp	Change in peak resolutions, peak intensity & S/N	Optimized by DoE & control	2	2	3	12
Nebulizer Press	Change in peak resolutions, peak intensity & S/N	Optimized by DoE & control	3	4	2	24
Capillary voltage	Change in peak resolutions, peak intensity & S/N	Optimized by DoE & control	3	2	3	18
Injection volume	Change the peak resolutions and S/N	At least 3 different volume were tested	2	1	3	6
Conc. NaAc	Change in peak resolutions, peak intensity & S/N	Optimized by DoE & control	3	2	3	18
Storage Temp	May change the peak resolutions	Control autosampler temperature at 20℃	1	2	2	4
Column type	Lot variability may change	At least 3 columns were tested	2	2	2	8

RPN – risk priority number: < 5 (low risk factors), 6–10 (medium risk), > 11 (high risk)

According to the result, column temperature, MP flow rate , Conc. NaAc, gas flow rate, gas temperature, nebulizer pressure, and capillary voltage indicate highly influential factors, which are calculated as greater than 11 RPN. Thus, these seven parameters were thereby selected as CMPs for further factor screening studies. the parameters counted less than 10 RPN were controlled as the constant.

4.1.2. Knowledge Space (KS) and CMPs Screening

The WATERS technology application note provides an excellent source of valuable information for the definition of influencing CMPs ranges and screening of KS. DSD with a 21-run model was applied as the design of experiments for KS screening. The CMAs (TPA, PR and RTLP) results, CMPs and respective range values of the KS DSD model are summarized in Appendix 2. The seven factors screened through DSD (2(n+1) +1) showed a relation between the main effects. The results were analyzed using a Pareto chart as shown in Figure 16.

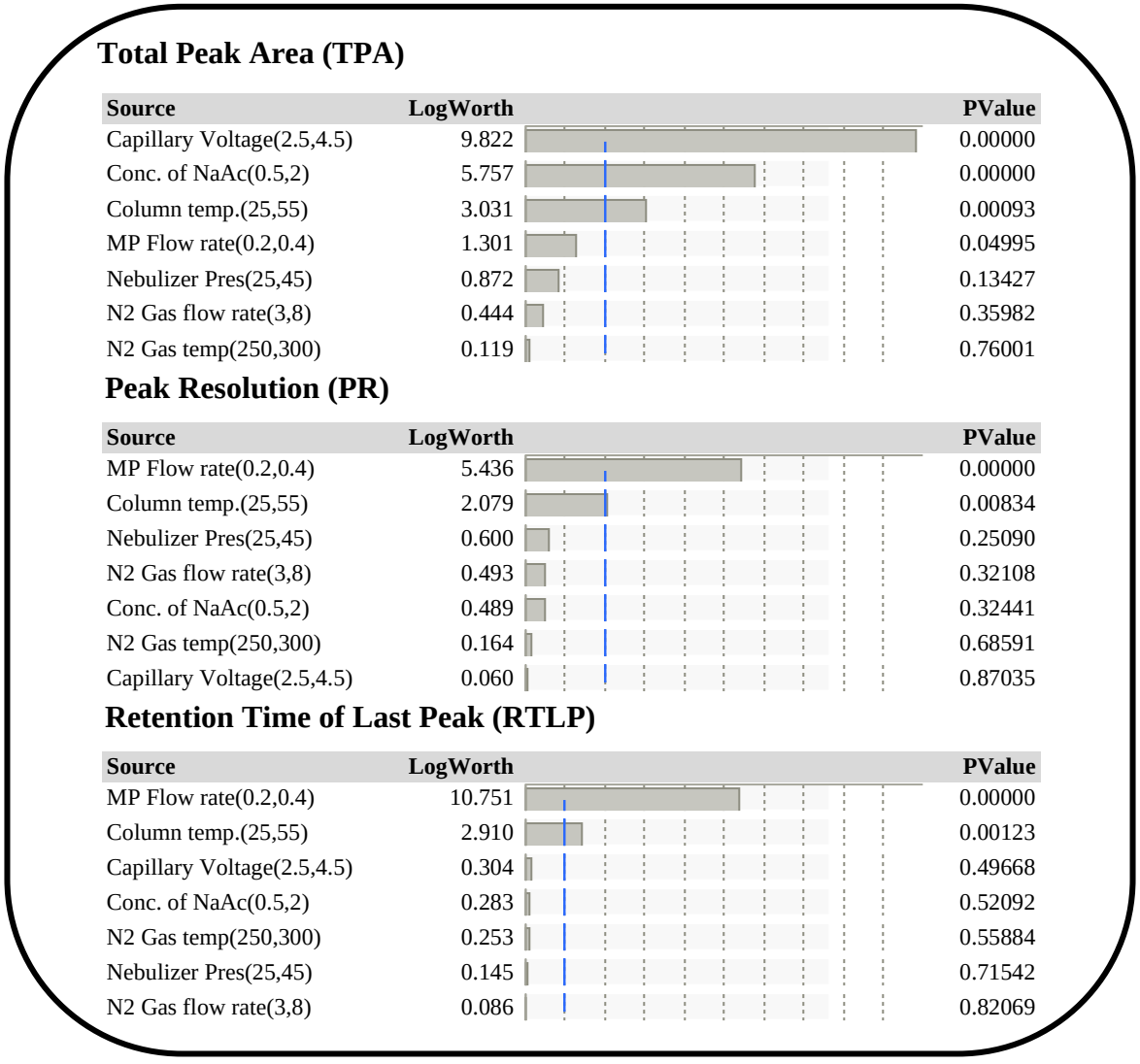

Figure 16: Pareto chart representing the significance of risk factors on chosen CMAs.

Screening of factors prior optimization helps reduce the experimental burden and errors. Pareto ranking analysis (PRA) shows that the MP flow rate and column temperature had a significant effect on PR and RTLP, while the capillary voltage, Conc. of NaAc and column temperature influenced TPA. Hence, optimization was carried out using these four factors.

4.1.3. Method Optimization and Method Operable Design Region (MODR)

The definition of MODR was based on LC-ESI-MS/MS analysis, wherein the CMA responses from the interactions of previously selected CMPs were evaluated through the DSD model defined previously in KS. To create a MODR where the analytical approach will achieve the intended ATP, the best CMA responses resulting from interactions between CMPs were thoroughly investigated using Pareto ranking analysis (PRA), response surface methods (RSM), and desirability analysis (DA). The MODR definition was achieved through the TPA, PR, and RTLP responses obtained from conc. of NaAc, MP flow rate, column temperature, capillary voltage, and from its interactions (Table 7).

Table 7: Pareto ranking analysis (PRA) result of CMPs

Source	LogWorth	PValue
MP Flow rate(0.2,0.4)	11.755	0.00000
Capillary Voltage(2.5,4.5)	10.714	0.00000
Column temp.(25,55)	6.698	0.00000
Conc. of NaAc(0.5,2)	6.319	0.00000
Conc. of NaAc*Capillary Voltage	1.464	0.03433
MP Flow rate*Column temp.	0.797	0.15952

P value < 0.0500 indicates that the terms of the model are significant. According to results, all CMPs demonstrated, individually, a significant influence on the TPA, PR, and RTLP response, being that its influence decreased in the following order: MP flow rate > capillary voltage > column temperature > conc. of NaAc. However, only the interaction between conc. of NaAc and MP flow rate presented a little significant influence on the TPA, PR, and RTLP response. For each CMAs, prediction models were built. Each main effect, interaction, and quadratic term is assigned a coefficient by the models, Figure 17. The coefficients determined the direction and magnitude of each influence on the related response, whilst the latter defined the non-linear (polynomial)

interactions. P-values were calculated using ANOVA statistical analysis to show the significance of each term at a significance level of 0.05.

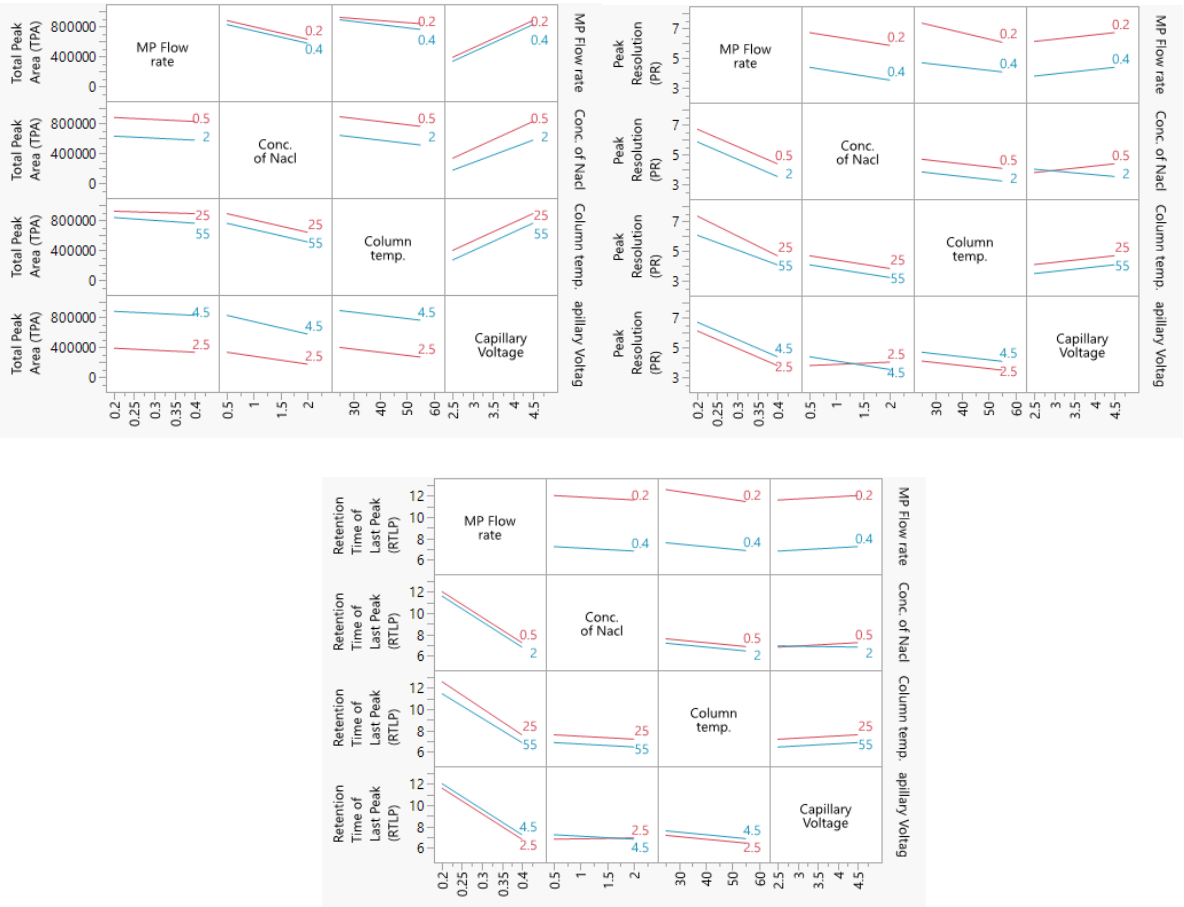

Figure 17: Interaction profiles plot showing effects of each CMP and their combined effects on the CMAs.

The actual predicted plot in Figure 18 revealed that the created model is used to forecast the responses . the estimated R^2 for the three responses reached 0.97, suggesting that the expected and experimental responses were perfectly fit. The prediction expression (equation) is available in Appendix 3. Furthermore, the modest difference between R^2 and R^2 adjusted supported the model's good fit. On the other hand, the calculated residuals presented in Appendix 4, looked to be approximately normally distributed (with a mean of zero) and independent of one another over time. As a result, residual analysis confirmed that the models adequately characterized the data. The predication equations for all CMAs, i.e., TPA, PR and RTLP.

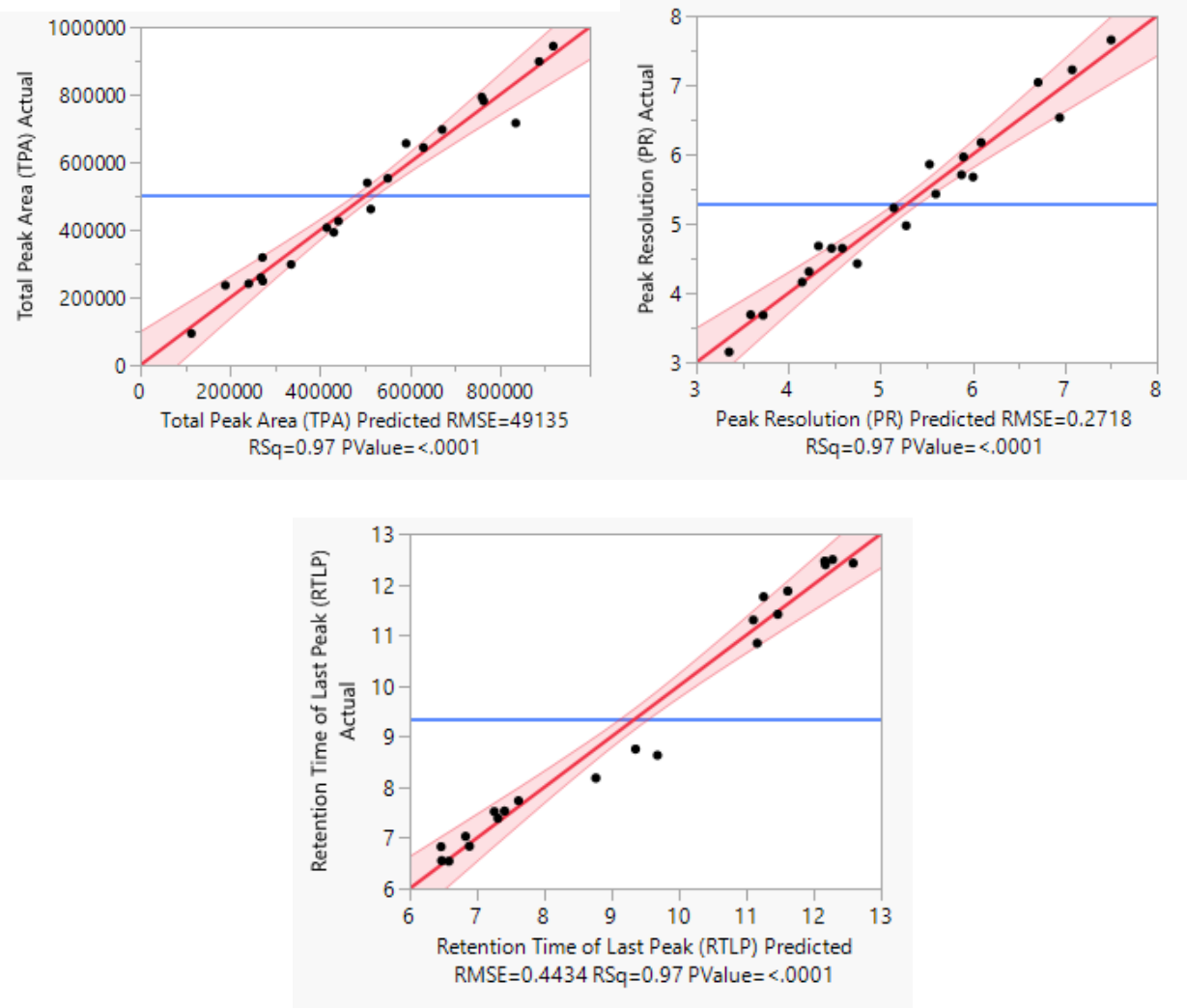

Figure 18: Prediction vs experimental plot for TPA, PR, and RTLP

The impacts of CMPs on each CMA were studied using graphical data interpretation using response surface methodology (RSM) like contour and surface plots (Appendix 5). When multiple responses are present, the desirability function technique provides a simple, quick, and accurate tool for optimizing them[80]. The desirability function is the recommended way for multi-response optimization because its less sophisticated, easy to understand and implement, and more flexible with respect to other existing approaches[81]. The predication profiler optimizer tool was used to establish the optimum parameters. Additionally, the "maximize desirability" option was chosen to maximize desirability. From Figure 19 we can see that the MP flow rate (0.4) , Conc. NaAc (0.5), column Temp (40), and Capillary voltage (4.5) gives us an overall maximum Desirability Index of 0.77.

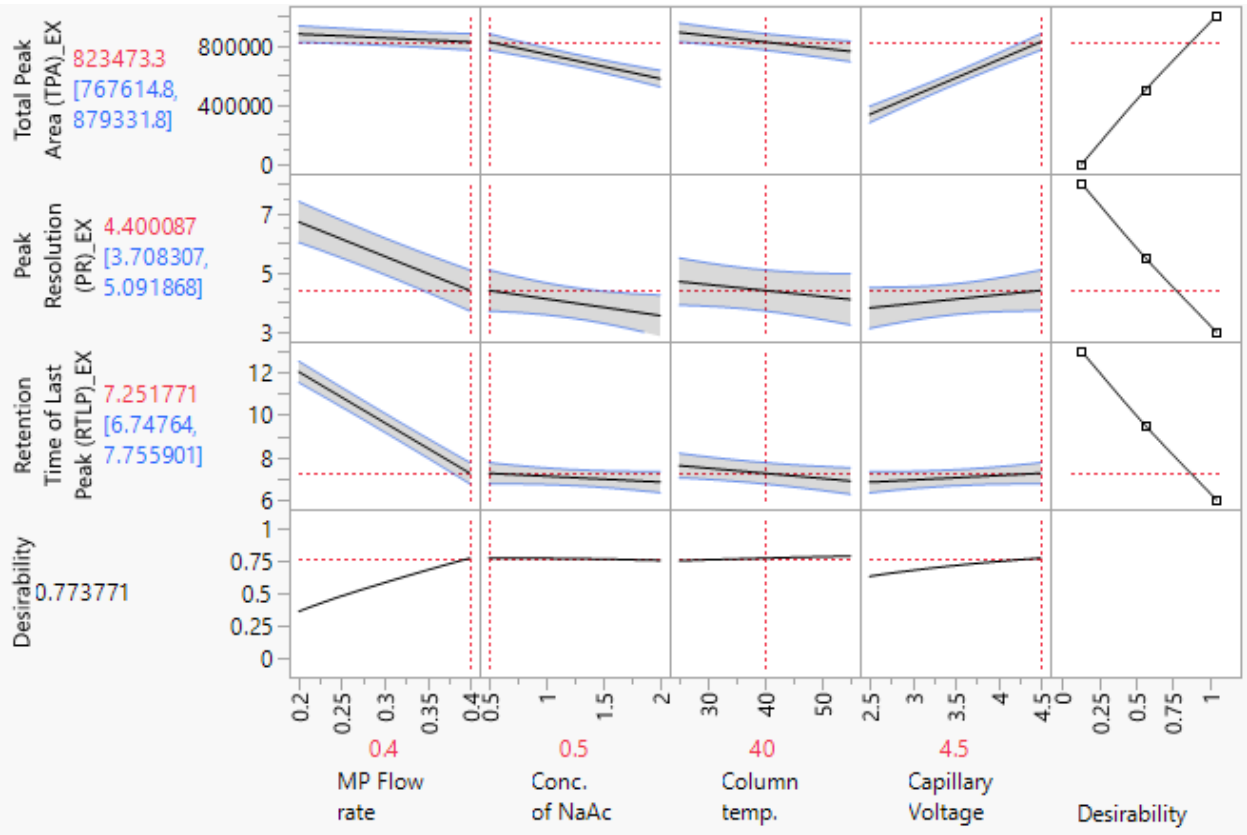

Figure 19: Prediction Profiler for TPA, PR and RTLP

The optimal LC-MS/MS condition was MP flow rate at 0.4 ml/hr , capillary voltage (4,5 kv) , column temperature (40 ^{0}C), conc. of NaAc (0.5 mM), Nebulizer Pres (35 Psi), N_2 Gas flow rate (8 L/hr) and N_2 Gas temp at 300 ^{0}C as acceptable TPA, PR, and RTLP were obtained, Figure 20.

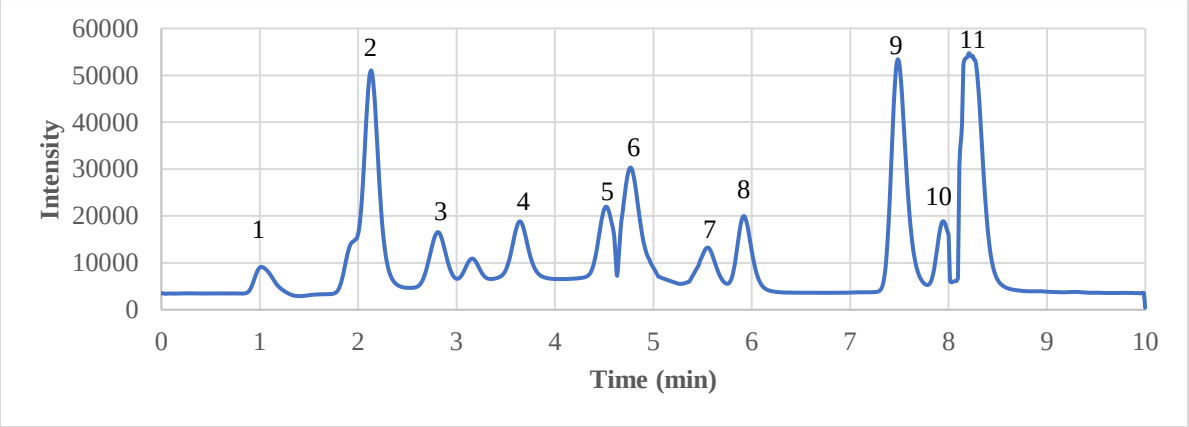

Figure 20: LC-MS/MS chromatogram of sugars. 1-5-HMF (0.978 min); 2-Ribose (2.853 min); 3 -Xylose (2.16 min); 4-Arabinose (3.695 min); 5 – D-(−)-fructose (4.578 min); 6 – D-(+)-mannose (4.823 min); 7-D-glucose (5.597 min); 8-D-(+)-galactose (5.964 min); 9 -sucrose (7.499 min); 10- maltose (7.947 min); 11- lactose (8.501 min)

A method operable design region (MODR) is the establishment of a multidimensional space using the results of DOE's statistical computation. A method's performance may be improved within the MODR, resulting in ATP compliance. The center point technique for the design space will typically be finished and validated; in addition, modifications made within the existing design space are not regarded as changes, therefore revalidation regarding those modifications is not required.

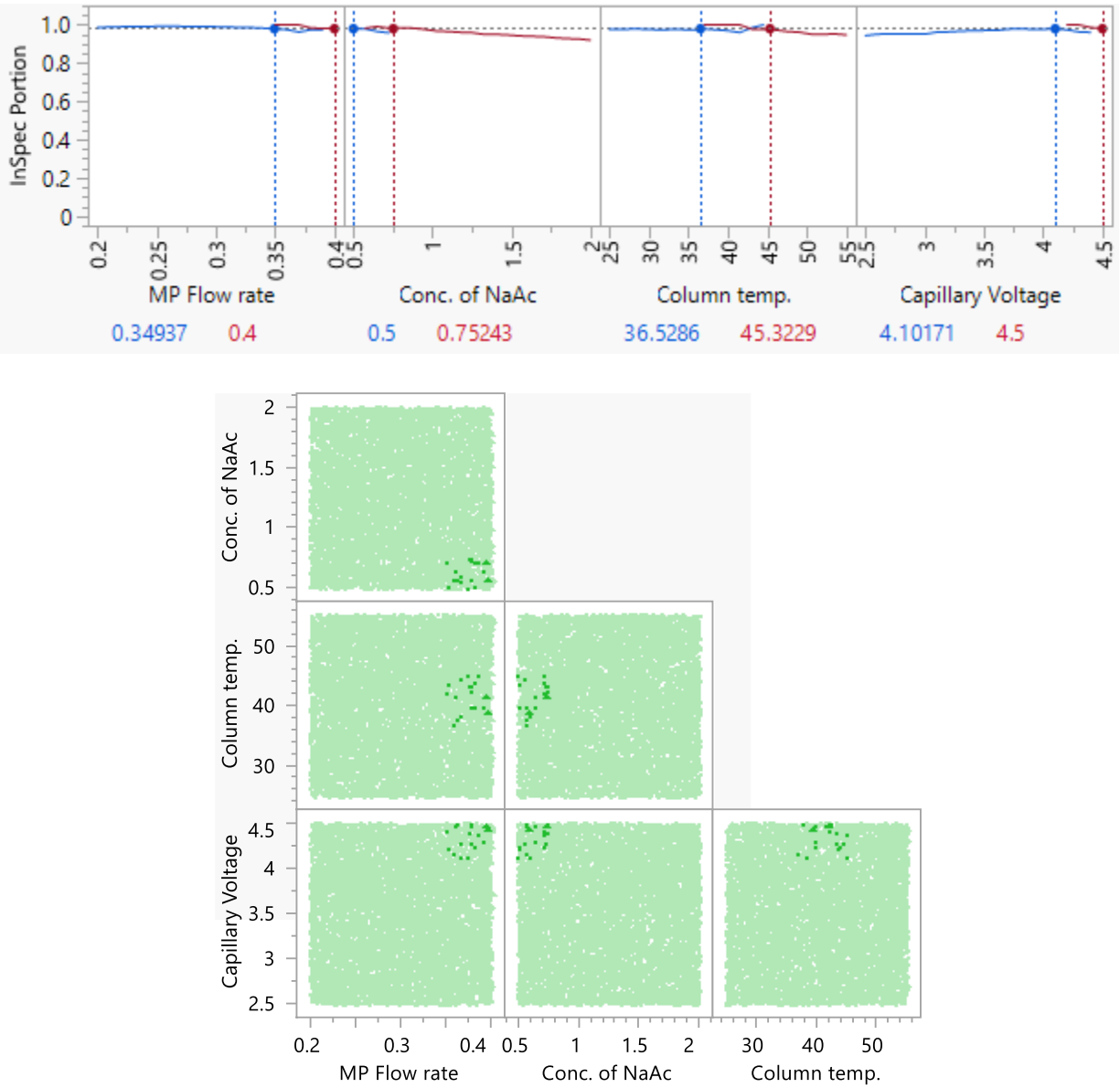

Figure 21: Design space profiler with inspection portion and volume for CMPs

Table 8: Design space and setpoint parameters

Parameters	Study range	Design space	Robust setpoint
MP Flow rate (mL/min)	0.2 - 0.4	0.35 - 0.4	0.4
Conc. of NaAc (mM)	0.5 - 2	0.5 - 0.75	0.5
Column Temperature (^{0}C)	25 - 55	36.5 - 45.3	40
Capillary Voltage (kV)	2.5 – 4.5	4.1 - 4.5	4.5

The design space with a low probability of deviating outside the specification limits was determined using the design space profiler tools in JMP Pro 17. As seen in Figure 21, the design space obtained had a regular form. The deep green regions are part of the design space and have very little chance of deviating from the permitted range. Table 8 displays the experimental and expected results. These findings suggest that even at the edge point, the target specification can be met under certain design space conditions.

4.1.4. Robustness and Method Control

The evaluation of robustness serves as the foundation for a control strategy for an analytical method's performance during routine applications. This is often accomplished by intentionally introducing slight changes to the optimum conditions to see if the analytical performance was unaffected. The method control was based on establishment of system suitability limits by generating large amount of data (10000 run) through the Monte Carlo bootstrapping simulation (Figure 22) at CMP optimal point into MODR, followed by application of capability analysis for estimation of residual errors from CMAs responses. The capability analysis for TPA, PR and PA are presented in Appendix 6.

The process capability index (Cpk) for TPA, PR, and RTLP was 1.3281, 1.756, and 1.921 respectively. The reference value of Cpk is 1.33, being the minimum value for a method to be considered robust[79]. Thus, our newly method was found to have remarkable robustness and prediction ability based on the findings of robustness and method control analysis at the optimal point into MODR.

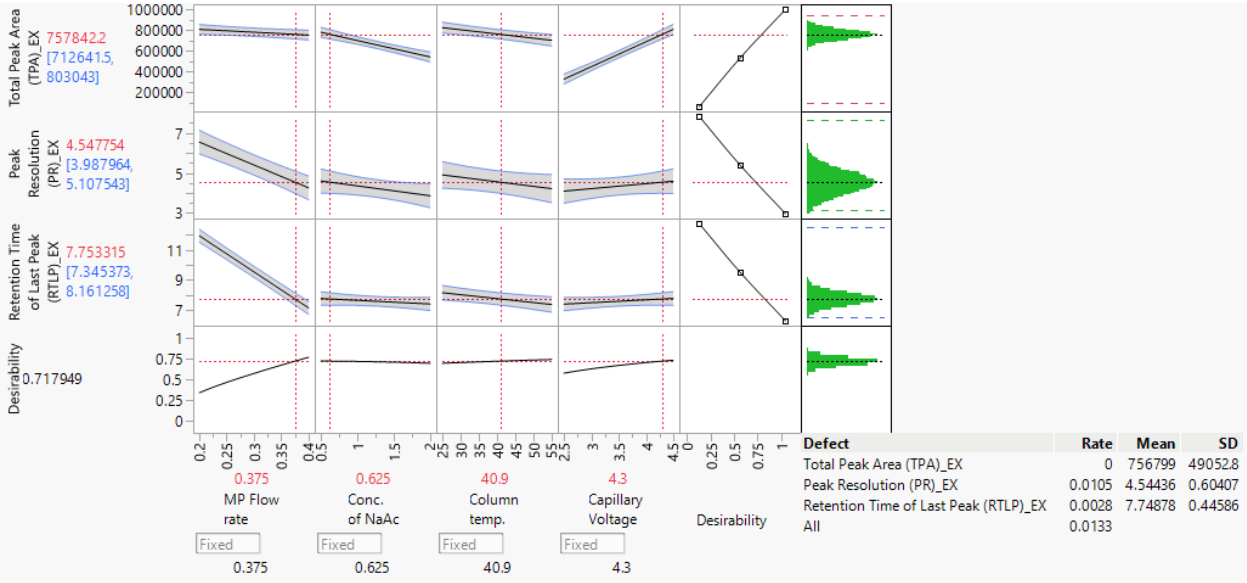

Figure 22: Monte Carlo bootstrapping simulation for LC-ESI-MS/MS development.

4.1.5. Validation of the Analytical Method

Validation studies are considered essential to demonstrate the reliability of an analytical method, prior to its application. The analytical method was validated for the following parameters: selectivity, calibration function (Appendix 7), linearity, accuracy, precision, LOD, and LOQ, being performed according to guidelines from IUPAC. The validation parameter is summarized in Table 9. The specificity of the method was proven by analyzing the blank, which confirms that there was no coelution as shown in figure 23.

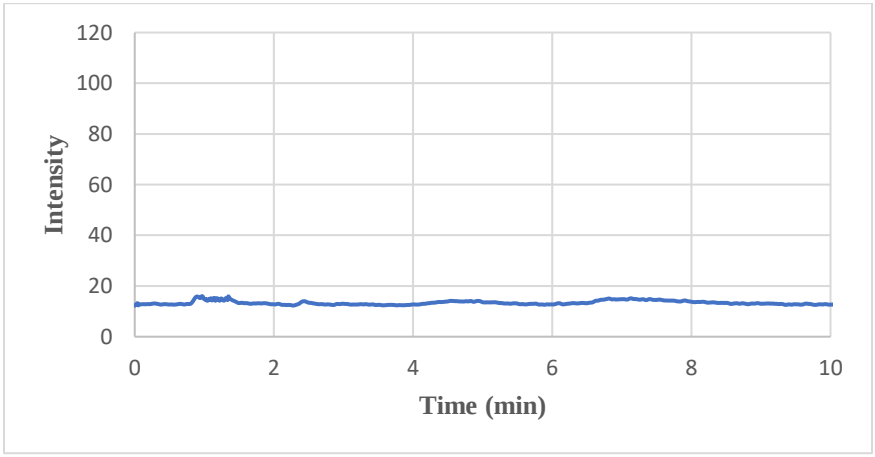

Figure 23: Chromatograms obtained from blank injection

The peak purity was also confirmed with the mass spectra. Seven calibration standard mixtures were used to construct the calibration curves. A 1/x weighted least-square model was fit to all the calibration curves. The standard calibration curve indicated a linear relationship with a high degree of correlation ($R^2 > 0.999$). The residual plot in the inset signified the lack of any outliers, thus ruling out the plausibility of any chance correlation(s).

Method accuracy and repeatability were evaluated using spike recovery results. Accuracy implies the degree of conformity between the theoretical and experimental outcomes. The recovered concentration of sugar ranged between 90 and 103%, with low magnitude of % RSD (i.e., < 2%). The results obtained, therefore, construed superior accuracy of the developed analytical method.

Method precision was evaluated by calculating the coefficient of variation of the sets of measurements over a period of certain day. The values of inter and intra-day precision for various spike control samples of sugar were found to be ranging between 98.32 and 100.26%, quite well within the acceptable limits (± 2%), thereby verifying good degree of precision of the developed method. The method sensitivity determined in terms of LOD (0.11-1.72 $\mu g \cdot mL^{-1}$) and LOQ (0.33-5.16 $\mu g \cdot mL^{-1}$) indicated quite high sensitivity of the analytical method developed for the quantitative estimation of sugar. Overall, the analytical method was validated to be reproducible, sensitive, accurate, precise, and reliable

Table 9: Summary of validation parameters for LC-MS/MS method of sugar analysis

Compound	LOD (µg/mL)	LOQ (µg/mL)	Linearity (R^2)	Range (µg/mL)	Precision (CV%)	Recovery
Ribose	0.8	2.4	0.9958	1-500	2.0	91
Xylose	1.72	5.16	0.9913	1-250	1.4	99
Arabinose	0.38	1.14	0.9923	1-500	1.7	95
Mannose	0.42	1.26	0.9977	1-500	1.6	93
Fructose	0.11	0.33	0.9952	0.25-500	1.8	90
Glucose	0.29	0.87	0.9996	0.5-500	1.8	97
Galactose	0.33	0.99	0.9924	0.5-500	1.5	90
Sucrose	0.11	0.33	0.9998	0.25-128	1.5	101
Maltose	0.22	0.66	0.9999	0.5-128	1.8	103
HMF	0.37	1.11	0.9996	1-128	1.2	98

4.1.6. Method Application

The applicability of the developed LC-ESI-MS/MS analytical method was verified through the analysis of sugar in Plum samples obtained from a Norwegian vendor. The results for the method applicability are summarized in Table 10.

Table 10: LC-MS/MS analysis of sugar in Norwegian Plums

	Total Sugar		Free Sugar	
	Mean (g/Kg)	SD	Mean (g/Kg)	SD
Arabinose	40.4725	0.00827	12.7307	0.003
Fructose	120.632	0.00601	69.7186	0.002
Galactose	66.017	0.00342	36.9849	0.001
Glucose	327.69	0.60573	140.598	0.073
Sucrose	43.437	0.00021	0	0
Maltose	31.7459	0.00353	12.1001	0.005

Based on the obtained results, it was possible to confirm the applicability of the developed analytical method on real samples. Moreover, the results also demonstrated its high repeatability when applied in real Plums samples, where the highest RSD value was less than 1 %, being that all concentrations values were obviously above the LODs and LOQs from the validation procedure. Our results in agreement with recently reported by Fotirc´*et al*., 2023[82].

4.2. Thermochemical conversion of Plums biomass to HMF

The main process for producing HMF is the acid-catalyzed dehydration of monosaccharides like glucose and fructose. Furfural, levulinic acid, formic acid, lactic acid, and glycolaldehyde are just a few other chemicals that can be created from sugars in an acidic aqueous medium[83]. Different parameters of thermochemical process affect conversion rate, HMF selectivity and yield. Therefore, a systematic approach using design of experiment (DoE) was used to optimize thermochemical conversion process.

4.2.1. Optimization of HMF yield and pathway

As a first step, the HMF yield, selectivity and sugar conversion is optimized, using a DSD requiring 17 experimental runs. The experimental domain of the main factors was selected based on a

reported value in previous work in our group (Molnes, 2021 & Mayhew, 2022) and in the literature. The complete experimental set-up of the independent variables is revealed in the experimental section (Table 2). The results from the DSD model are presented in Table 11.

HMF yield, selectivity and sugar conversion was calculated using the following equation :

$$HMF\ Yield = \frac{HMF\ produced\ (g)}{initial\ biomass\ weight\ (g)} x100$$

$$HMF\ Selectivity = \frac{HMF\ produced\ (g)}{intial\ mass\ of\ sugars\ in\ the\ biomass\ (g)}\ x\ 100$$

$$Sugar\ Conversion = \frac{initial\ mass\ of\ sugar\ (g) - final\ mass\ of\ sugar\ (g)}{initial\ mass\ of\ sugar\ (g)}\ x\ 100$$

Here , we define yield related to the amount of HMF produced related to the initial biomass weight, but the selectivity calculated only related to sugar fraction of the initial biomass.

Table 11 : The calculated mass percent (m%) yield of HMF, Selectivity (%), and conversion rate (%) for the DSD model, quantified with LC-MS/MS.

Run	HMF_Aqu (g/g)	HMF_Org (g/g)	HMF (%)	Selectivity (%)	Sugar Conversion (%)
1	0.00200	0.05755	14.85	23.57	92.82
2	0.00365	0.01550	7.57	12.01	98.66
3	0.00155	0.02227	9.51	15.09	62.98
4	0.00491	0.01054	3.86	6.12	83.82
5	0.00144	0.02732	28.44	45.15	22.49
6	0.00345	0.02066	9.59	15.22	73.14
7	0.00225	0.00385	6.04	9.58	24.22
8	0.00164	0.04579	11.85	18.81	99.68
9	0.00267	0.01759	5.05	8.02	70.57
10	0.00430	0.00981	3.51	5.56	80.6
11	0.00002	0.00482	1.21	1.92	71.06
12	0.00328	0.00509	8.36	13.26	29.04
13	0.00195	0.02534	26.65	42.30	56.6
14	0.00101	0.03344	8.58	13.63	84.07
15	0.00312	0.01745	20.55	32.61	78.21
16	0.00160	0.03193	33.49	53.16	96.27
17	0.00404	0.00847	12.32	19.56	86.14

The statistical analysis was performed in four steps: significance test of the factors, graphical analysis of the residuals, ANOVA, and application of F test to subsequently trace the response

surface. The magnitude of the effects of the factor's temperature, time and catalyst concentration on the response variables is shown in the diagrams of Figure 24.which presents Pareto charts for HMF selectivity (a), Sugar conversion (b) and HMF yield (c). For the conversion, the temperature was the most influential factor, which is consistent with the natural tendency of sugar (specifically fructose and glucose) to be converted with increasing temperature, and all the other factors except sulfamic acid concentration and water content were significant. On the other hand, the major influence on the HMF yield and selectivity was the water content, substrate load, temperature, and its interaction. Since the HMF yield and selectivity are the main parameters of the study, all subsequent analysis will be directed to evaluate the optimization of this factor.

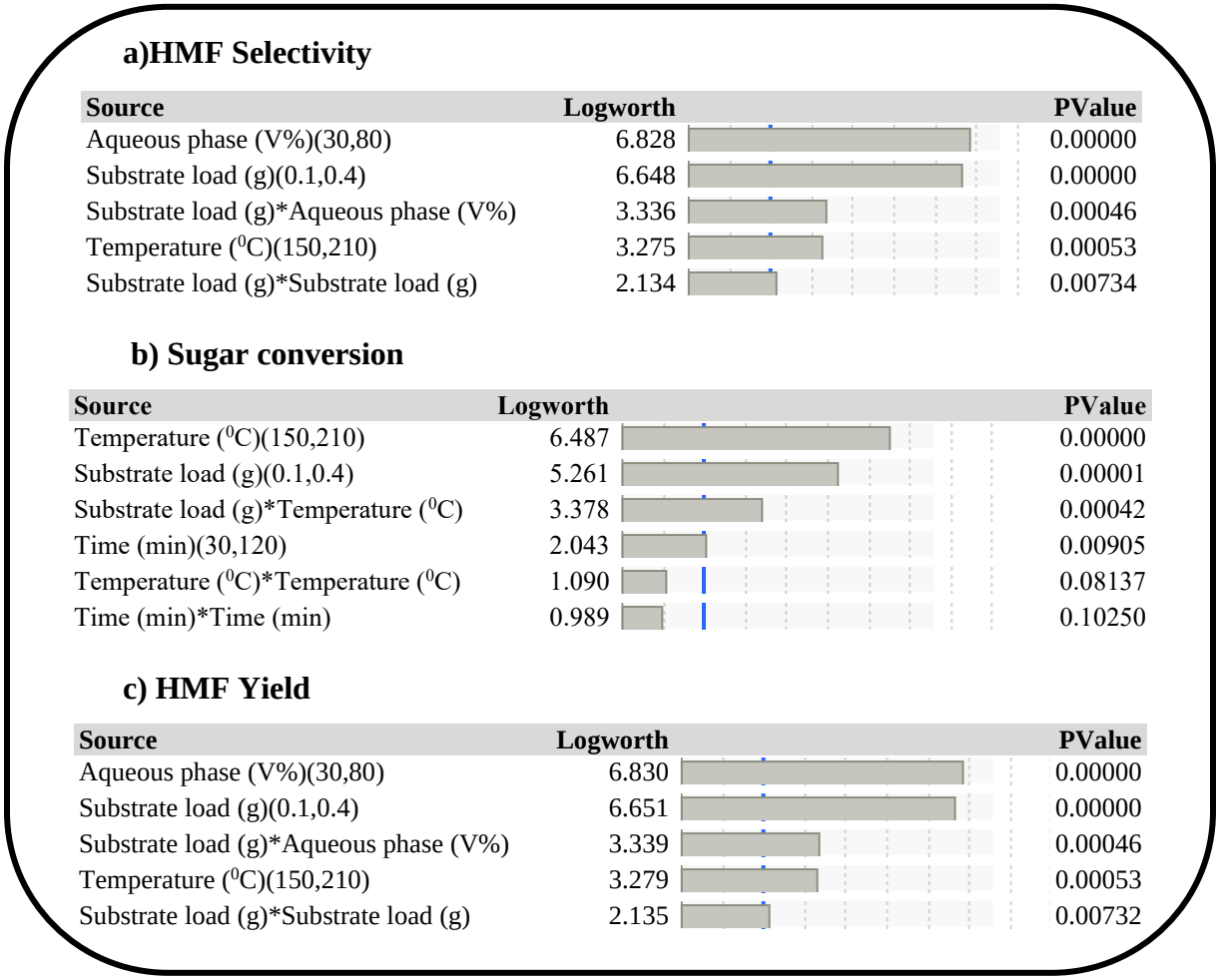

Figure 24: Pareto charts of DSD. HMF Selectivity (a), Conversion rate (b) and HMF yield (c).

Central composite design (CCD) was used for optimizing substrate load, water content, and temperature. Pareto ranking analysis of the CCD model (Table 12) showed that all main factors

influence sugar conversion, HMF yield, and selectivity. in addition to the main effect, the interaction between water content and substrate load has also a significant effect on the response factor.

Table 12: Pareto ranking analysis for CCD.

Source	Logworth	PValue
Temperature (0C)(150,210)	7.420	0.00000
Substrate load (g)(0.1,0.4)	6.414	0.00000
Substrate load (g)*Temperature (0C)	5.786	0.00000
Aqueous phase (V%)(30,80)	4.557	0.00003
Substrate load (g)*Substrate load (g)	3.167	0.00068
Aqueous phase (V%)*Aqueous phase (V%)	2.767	0.00171
Substrate load (g)*Aqueous phase (V%)	2.150	0.00707
Temperature (0C)*Aqueous phase (V%)	1.199	0.06319
Temperature (0C)*Temperature (0C)	0.158	0.69531

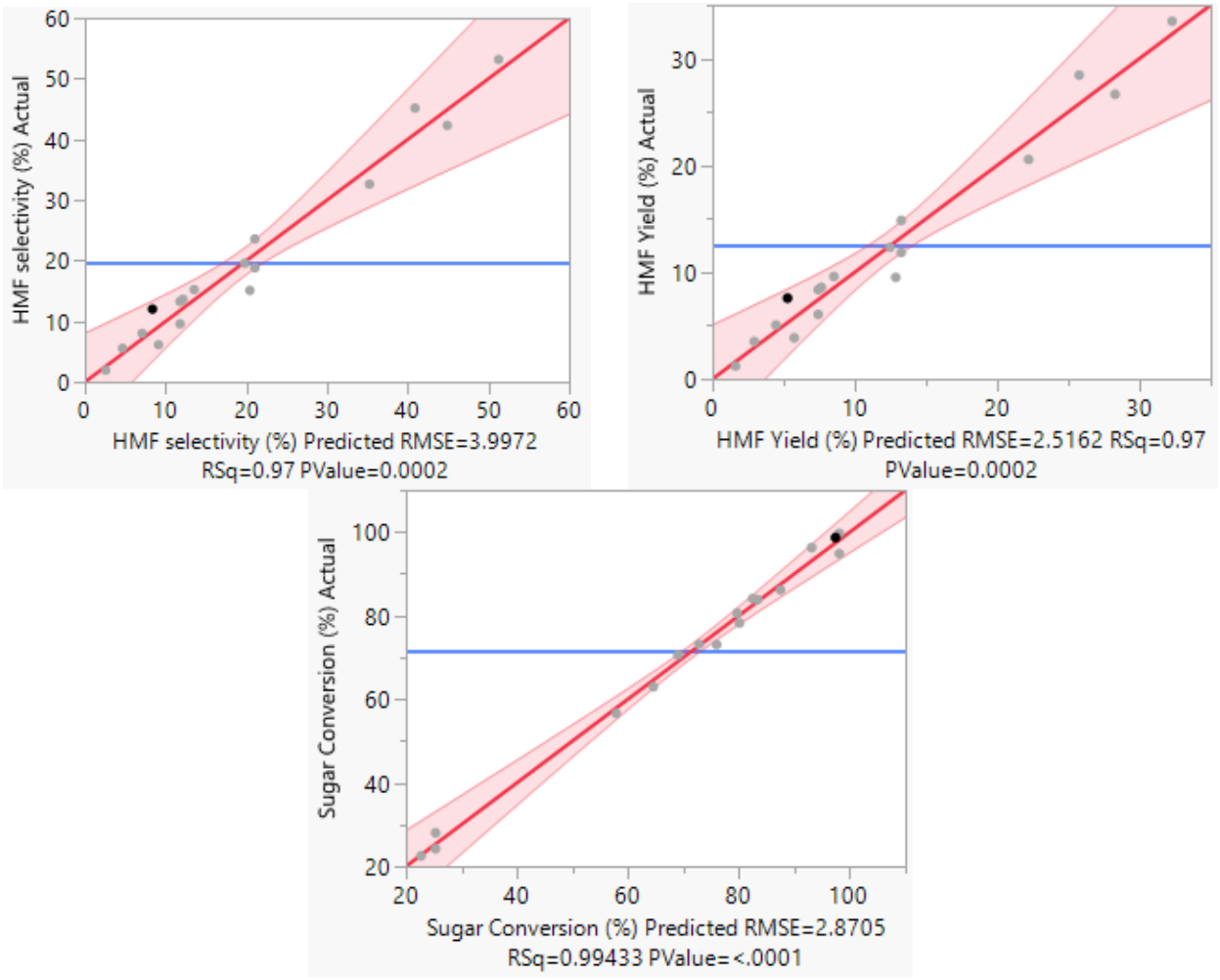

Figure 25: Prediction vs experimental plot of CCD for HMF yield, selectivity & conversion rate.

The graphical analysis of the residuals was used to assess the normality of the data, which is indicated in Appendix 8. The expected behavior for a normal sample is observed in the graph, for which the points approximate a straight line. Once the normality of the data is verified, other tests can be performed to assess the statistical model generated by the JMP Pro 17. One important analysis is shown above in Figure 25, comparing the values predicted versus values observed, in which the deviation from the straight line through the origin is acceptable ($R^2 = 0.97$) and the graph shows a linear trend, confirming that model is fit for purpose.

Table 13 summarizes the regression analysis for HMF yield, selectivity, and sugar conversion. Analysis of variance (ANOVA) was applied to test the mathematical modeling with $\alpha = 0.05$ (level of significance) and is presented in a simplified form.

Table 13: ANOVA of HMF yield and selectivity.

Model	Sum of squares	DF	Mean square	F_{value}	F_{table}	R^2
HMF yield						
Lack of fit	37.127744	5	7.42555	2.0652	0.3576	0.9949
Pure Error	7.191200	2	3.59560			
Total Error	44.318944	7				
HMF Selectivity						
Lack of fit	93.74336	5	18.7487	2.0717	0.3568	0.9949
Pure Error	18.10000	2	9.0500			
Total Error	111.84336	7				
Sugar Conversion						
Lack of fit	38.571191	5	7.71424	0.8075	0.6343	0.9981
Pure Error	19.106	2	9.553			
Total Error	57.677191	7				

The F test was used to determine whether there was a significant relationship between the change in the independent variable and the variation of the dependent variable; in that case, the calculated value of F (F_{calc}) would be higher than the tabulated F (F_{table}). This hypothesis was verified. for the three response variables, indicating that the model generated adequately described the phenomenon. The F test was used to verify that the change of the independent variable had a significant influence on the variation of the dependent variable; since F_{calc} = 2.06 and 2.07 is greater than F_{value} = 0.36, this hypothesis was verified, indicating that the model generated describes adequately fit for purpose. The model Equation (Appendix 9) was obtained for the HMF yield and selectivity. The quadratic fit of the model should satisfy R^2 greater than 0.95 featuring an acceptable degree of agreement between the predicted and the observed values.

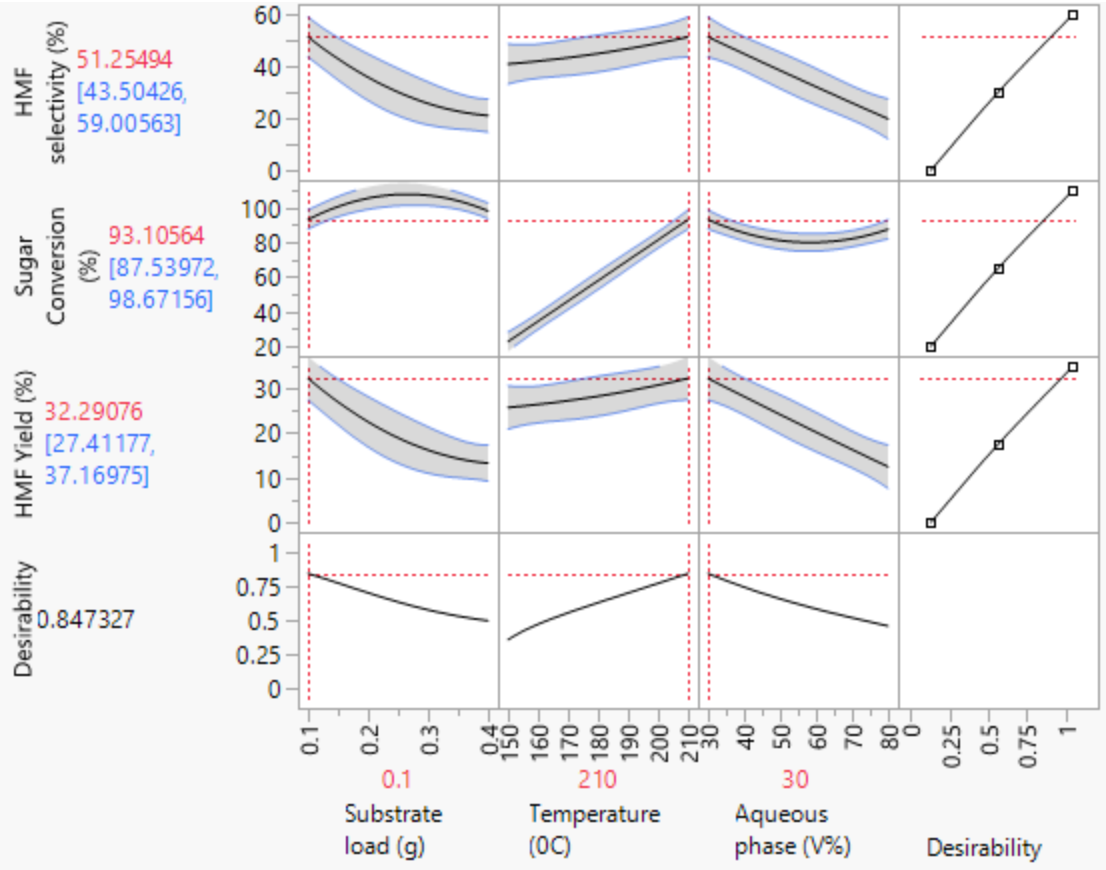

Figure 26: CCD Prediction Profiler for sugar conversion, HMF Yield, & selectivity

The desirability function is the recommended way for multi-response optimization of thermochemical process. The predication profiler optimizer tool in JMP Pro 17 was used to establish the best thermochemical process parameters, Figure 26. Also, the "maximize desirability" option was chosen to maximize desirability. From Figure 26 we can see that the substrate load (0.1 g), temperature (210 ^{0}C), and water content (30 %V) gives us an overall maximum Desirability Index of 0.847.

Furthermore, the model generates the response surface (Appendix 10), in which the relation between the HMF yield and selectivity with substrate load , temperature and water content, is shown graphically. Despite the borderline fit of the model, it is possible to verify the advantage of modeling the data showing clearly that the HMF yield is optimized for the system studied. In general, at optimum condition (temperature (210 ^{0}C), water content (30 %V), time (75 min), Sulfamic acid load (0.025 g) , and substrate load (0.1 g)) the maximum HMF yield, selectivity, and conversion rate is 32.29 %, 51.25% and 93.11% respectively.

To verify the model's prediction ability, the conversion of Plum biomass was performed at the optimal reaction conditions suggested by the prediction profile. Table 14 shows the model-predicted and experimental results for a specific solution. The outcomes revealed that the experimental HMF selectivity, conversion rate, and yield values were extremely close to the model's predicted value. For the HMF selectivity and production yield, the relative error between predicted and experimental values was less than 2%. It can be concluded that within the experimental domain, the established model for HMF selectivity and production yield displayed excellent predictability with sufficient precision.

Table 14: Comparison between the experimental and model-predicted values at the optimum condition

Response	Experimental value (%)	Predicted value (%)	Error (%)
HMF selectivity	53.16	51.25	1.91
Sugar conversion	96.27	93.11	3.16
HMF yield	33.49	32.29	1.2

Optimized condition: 210 ^{0}C, 120-minute, 0.1 g plum biomass, 0.01 g Sulfamic acid, 7 mL MIBK solvent, and distilled water = 3 mL

4.2.2. Effect of Thermochemical conversion parameters on HMF selectivity

With all the reactant and products profiles, an overall trend can be analyzed to gain quantitative information on the effects of the process conditions on the selectivity of the reaction. For this purpose, it is convenient to use selectivity, which is defined as the ratio of the amount of desired product (HMF) and the amount of sugar fraction initially present in the feedstock. The influence of reaction temperature, substrate load , aqueous phase volume and its interaction on HMF selectivity was analyzed. The major products (HMF) and unconverted sugars were identified and quantified by HPLC, as shown in Figure 27.

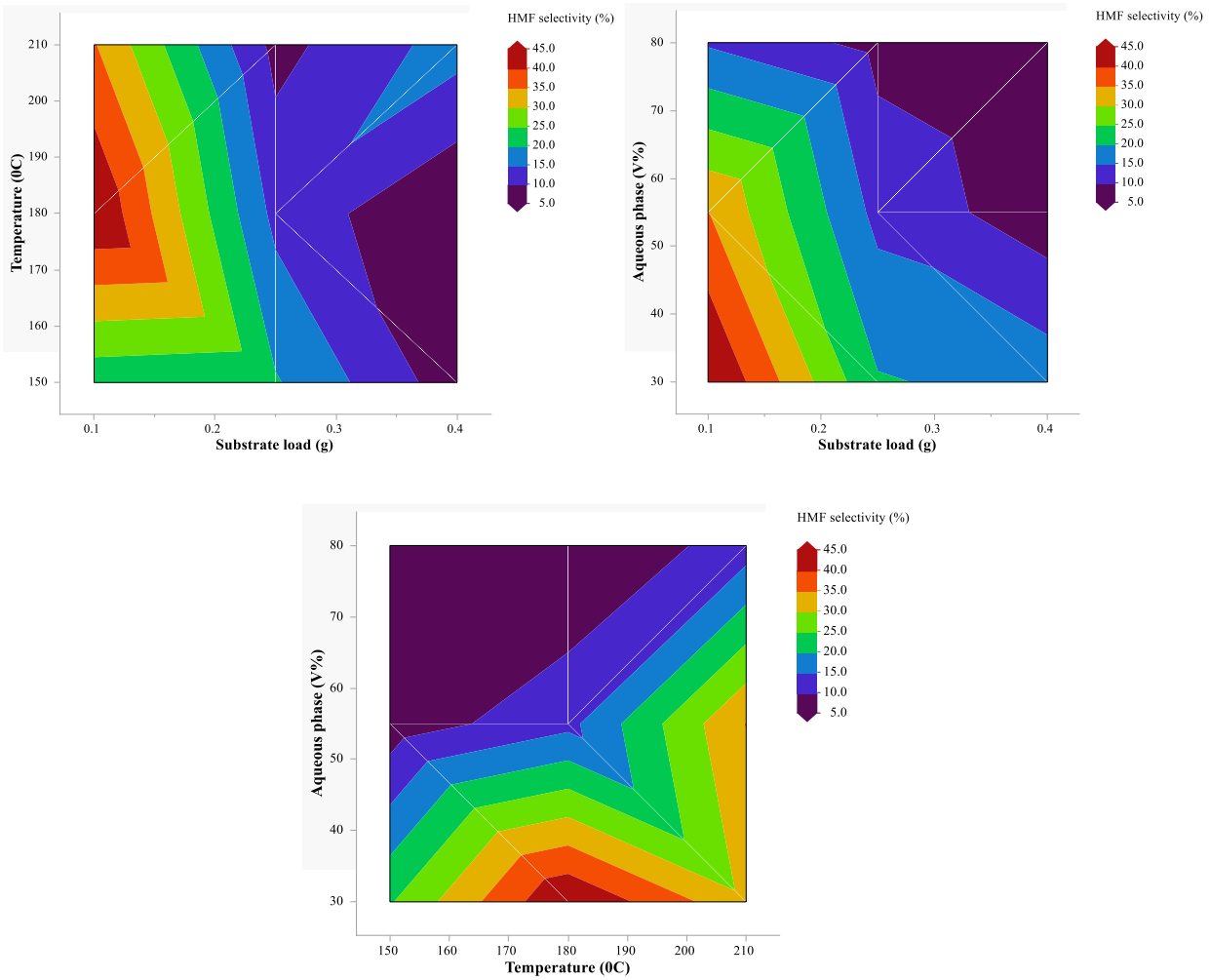

Figure 27: Contour plots represent the temperature-substrate load, aqueous phase-substrate load, and aqueous phase-temperature interaction effect on 5-HMF selectivity.

It was observed that selectivity to HMF increased as the temperature increased from 150°C to 210°C. unlike the effect of increasing substrate loading and aqueous phase volume, which did not change HMF selectivity. Increasing water content and substrate load were observed to also hinder the conversion process. Therefore, increasing aqueous volume and substrate load influences both HMF selectivity and yields. The selectivity to HMF increased with temperature, suggesting that HMF selectivity is thermodynamically controlled. The conversion and the HMF selectivity were affected by different initial loads of substrate. The sugar conversion increased but the HMF selectivity decreased with the increase of feedstock's load. As shown in Figure 28, the highest HMF selectivity was reached in low initial substrate load (experiment 5,13 and 16). In some case low selectivity obtained at low initial substrate load (experiment 7 and 12), the loss of selectivity

for low substrate load was attributed to the more catalytic sites compared to the high substrate load, resulting in more by-products. Compared to low substrate load, the 38.07% reduction of selectivity for medium substrate load might be attributed to the higher sugar concentration leading to higher rates of condensation reactions. This result agreed with literature reports[84].

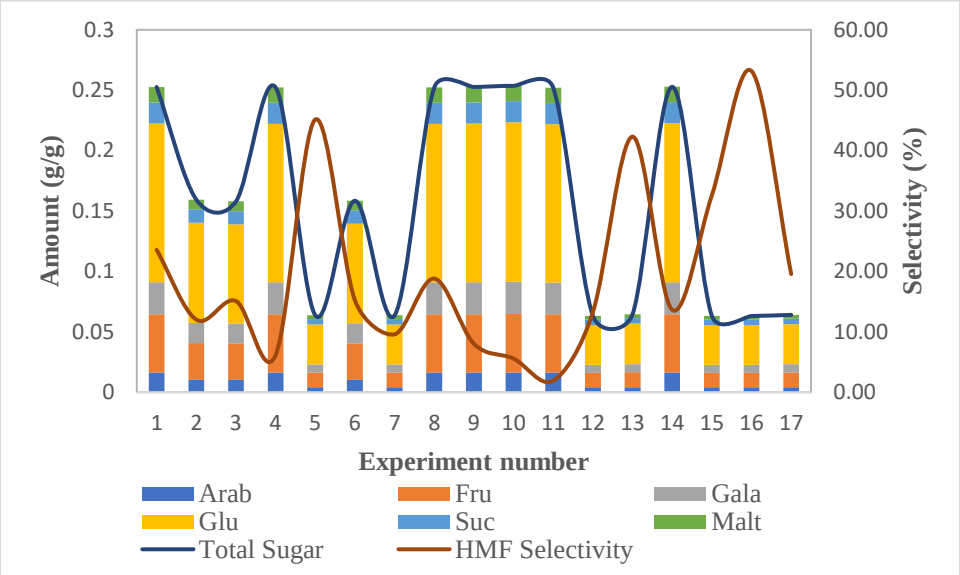

Figure 28: Results of the HMF selectivity for sugar dehydration reaction with different initial substrate load**.**

Fructose and glucose are dominant sugars presented in Plums, therefore the HMF selectivity of the thermochemical conversion process depends on this two dominant sugars. As we can see from Figure 29 , in all experiments the amount of fructose that remains unconverted is less than that of glucose. The conversion pathway of glucose to HMF mainly comprises two steps; firstly, glucose is isomerized to fructose ; after that, HMF can be obtained in fructose dehydration (Figure 30). Several researchers have found evidence that isomerization is required in glucose conversion to HMF. This could mean that the rate-determining step is the isomerization of glucose to fructose[85].

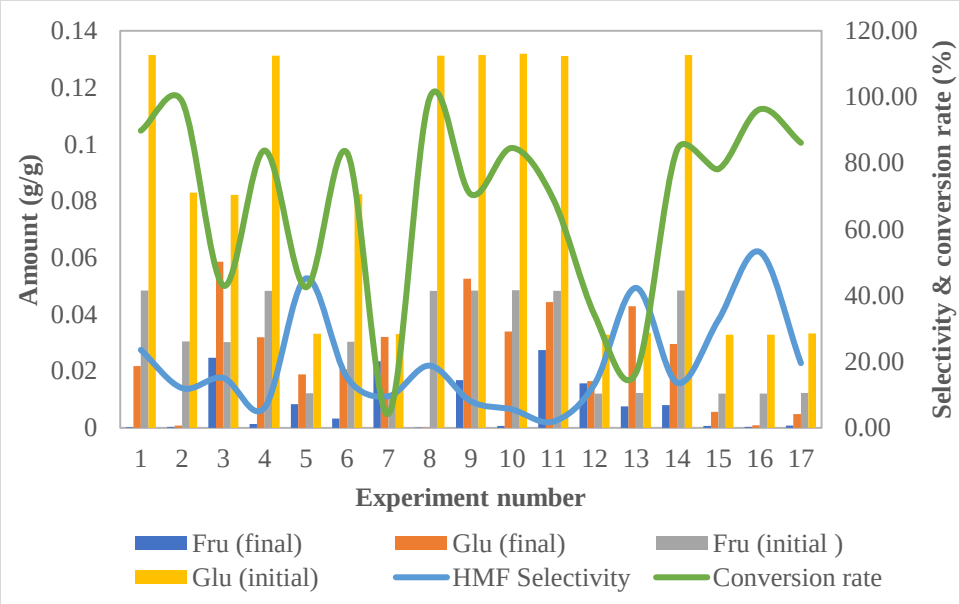

Figure 29 : Results of the HMF selectivity for sugar dehydration reaction with respect to glucose and fructose.

HMF may only be formed directly from fructose and reacts consecutively to produce levulinic and formic acids as side products. In addition, polymerization occurs. Both glucose and fructose react via aldol splitting (retro aldol condensation) to more minor compounds[86]. In the case of glucose, erythrose and glycolaldehyde molecules are formed. In the case of fructose, two molecules with three carbon atoms are formed, which are isomers and can transform to each other by keto-enol isomerization. These are dihydroxyacetone and glyceraldehyde .

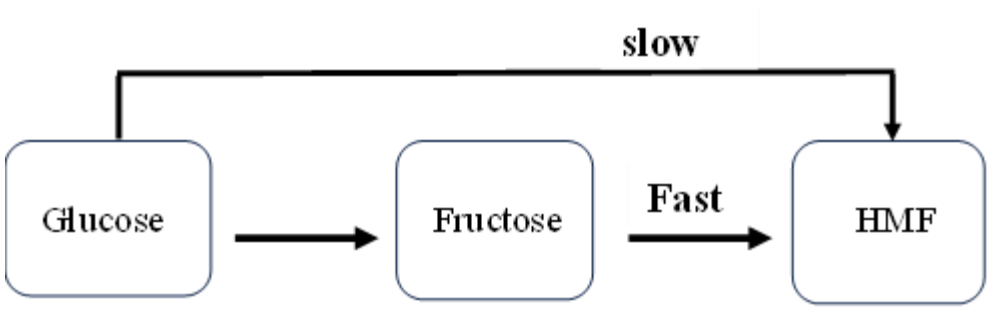

Figure 30 : Conversion of glucose and fructose to HMF

As HMF is formed from fructose, not from glucose, the yields are higher with fructose. Fructose can be formed from glucose by keto-enol tautomerization (Lobry de Bruyn van Ekenstein transformation), catalyzed typically by acids[87].

If glucose is the starting material, the transformation to fructose competes with the aldol splitting. Therefore, the overall yield and the selectivity to HMF decrease compared to fructose as the initial material. Noteworthy that sugars have a higher dissolution capacity in water than organic solvents. However, the sugar catalysis towards HMF synthesis in water can undertake the side reactions, yielding levulinic acid, and formic acid and humin byproducts under the prevailing conditions. Therefore, the trend of supplementation of organic co-solvent as a reaction medium is popular to shield the HMF from further degradation and to develop a solvation shell around the carbohydrate molecule to enable a selective transformation.

According to the previous work in our group and published literature[73], MIBK is a good solvent that could suppress unwanted side reactions for sugar dehydration in water using acid catalysts and could extract more HMF into organic phase with good partitioning of HMF compared to other solvents. The influence of amount of MIBK on conversion and selectivity was given in Figure 31. The HMF selectivity was low in higher aqueous phase due to the side products. The selectivity increased significantly using MIBK. As the amount of MIBK in biphasic system increased, the conversion and HMF selectivity increased. The biomass conversion, HMF yield and HMF selectivity reached maximum values of 96.3% , 33.5 and 53.2%, respectively, at volume ratio of 1:2.33 of water to MIBK.

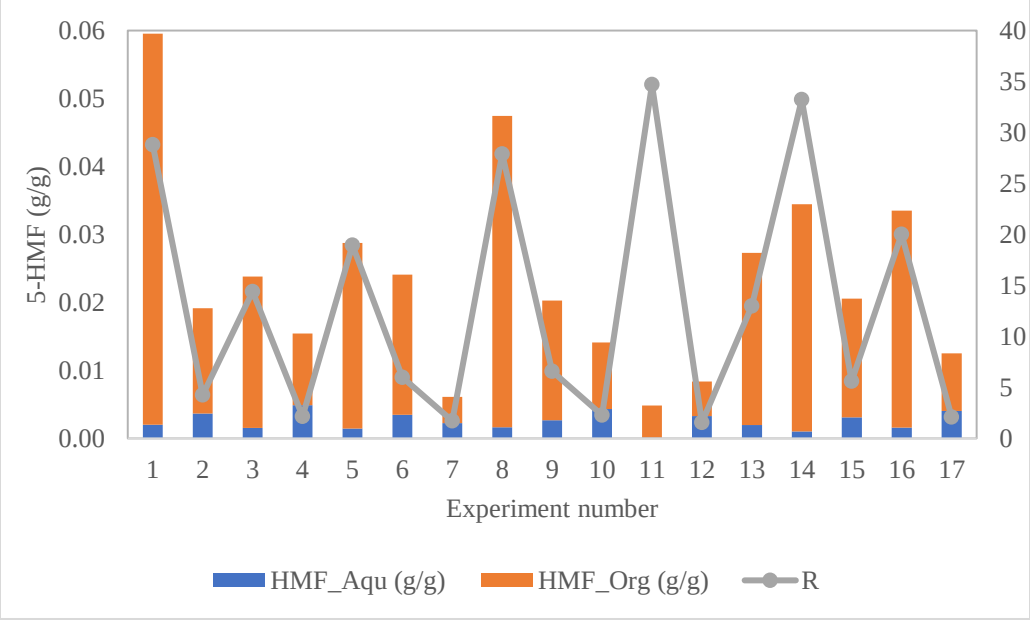

Figure 31: Distribution of HMF between the organic and aqueous phases

For biphasic systems, the partition coefficient (R) is defined in equation (1)

$$R = \frac{HMF\ Concentration\ in\ organic\ phase}{HMF\ Concentration\ in\ aqueous\ phase} \quad (1)$$

Figure 30 shows the distribution of HMF between the organic and aqueous phases, and values of the partition coefficient R for the sugar dehydration reaction with MIBK and the aqueous phase. Without changing the total mass of the two solvents, increasing the mass ratio of MIBK to aqueous solution in the biphasic system would be beneficial to improve the extraction efficiency of HMF from aqueous phase to organic phase, which may favor increasing the final HMF yield and selectivity. As expected, with the increase of the mass ratio of aqueous to MIBK from 4:1 to 1:2.33, the yield and selectivity of furfural increased gradually.

In summary, the evaluation of thermochemical reaction conditions using the biphasic (water/MIBK) system revealed that the HMF selectivity decreased with increasing substrate load due to the higher contribution of condensation reactions. The HMF selectivity increased with temperature (in the range of 150-210 °C) and showed a maximum value with low catalyst load. Using an organic system, the HMF selectivity was significantly higher than in aqueous medium alone. The best result was obtained with the 1:2.33 water: MIBK system, i.e., an 53.2 % of HMF selectivity with a partition coefficient of 20, which is very promising compared to other studies in the literature as shown in table 14.

Table 15: Comparison of results obtained with previously reported literature

Substrate type	Catalyst	Solvent	Temp.	5-HMF yield	5-HMF selectivity	Ref.
30 wt.% Fructose	HCl	MIBK	180 ^{0}C	30.6%	47%	[88]
Fructose	Nb_2O_5	Water	180 ^{0}C	5%	28%	[89]
Chicory	H_2SO_4	Water	140 ^{0}C	16.2%	35%	[90]
Glucose	$(TfO)_3Yb$	Water	140 ^{0}C	13.7%	25.2%	[91]
Strach	KH_2PO_4	MIBK	180 ^{0}C	27.1%	42.5%	[92]
Starch-rich food waste	Sulfonated biochar	DMSO	180 ^{0}C	22%	-	[93]
Food waste	zirconium phosphate	Water	180 ^{0}C	4.3%	-	[94]
Waste Plums	Sulfamic acid	MIBK	210 ^{0}C	33.5%	53.2%	in this study

4.2.3. Quantification of product fraction

To begin with plum biomass characterization, the moisture content of plum biomass was determined using NREL Laboratory Analytical Procedures "Preparation of sample for compositional analysis". The measurement was done three times and the average was taken to increase the accuracy. The results were in general agreement with other results reported elsewhere. The plum biomass having higher moisture content (78 ± 4%) needs more heat for moisture vaporization. Having low moisture content is suggested for the catalytic conversion process since high moisture content may increase water content in the reaction, which hinders the catalytic activity of the catalyst by interacting with hydrogen bond of the cellulose component of the biomass with the water molecule rather than with the catalyst. The amount of accessible mono and disaccharide is main critical for identifying the potential feedstock for HMF production. Therefore, the sugar profile of Plum biomass was identified and quantified using acid hydrolysis with subsequent LC-ESI-MS/MS analysis. In figure 32 below shows the sugar composition with respect to the total dry weight of plum biomass.

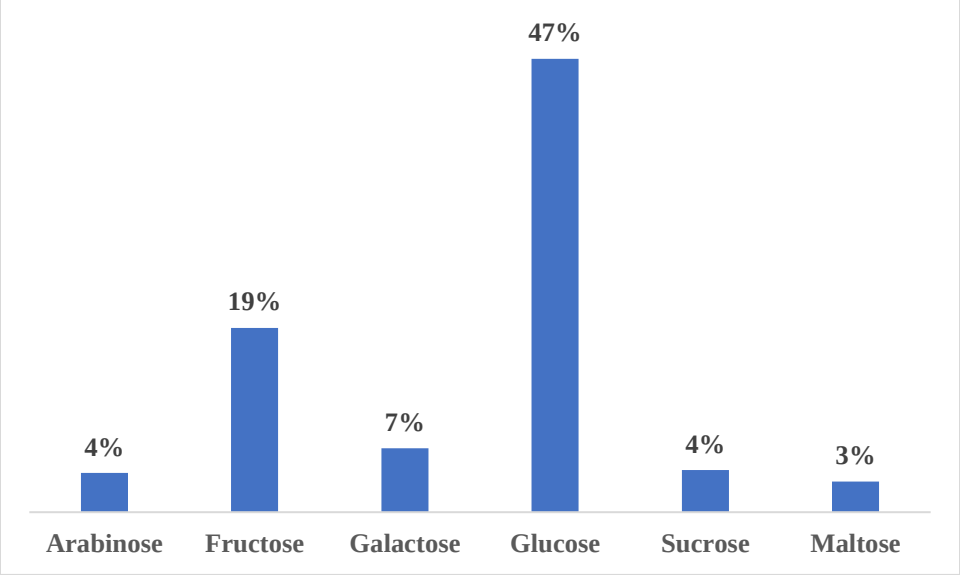

Figure 32: Sugar composition with respect to the total dry weight of plums biomass

According to the result , the sugar content of plum accounts 84% of its total dry weight. Glucose and fructose are the two dominate monosaccharide which is 66% of the total dry weight of plum biomass. Therefore, it is potential feedstock to be used to produce 5-HMF. The main product fraction in the thermochemical catalytic conversion of plum biomass in to 5-HMF via biphasic

system consisting of water and MIBK, with Sulfamic acid as catalyst under different experimental conditions are shown in figure 33. High yield of 5-HMF was obtained in the organic phase (31.9%) compared to the aqueous phase (1.6%) under optimized condition.

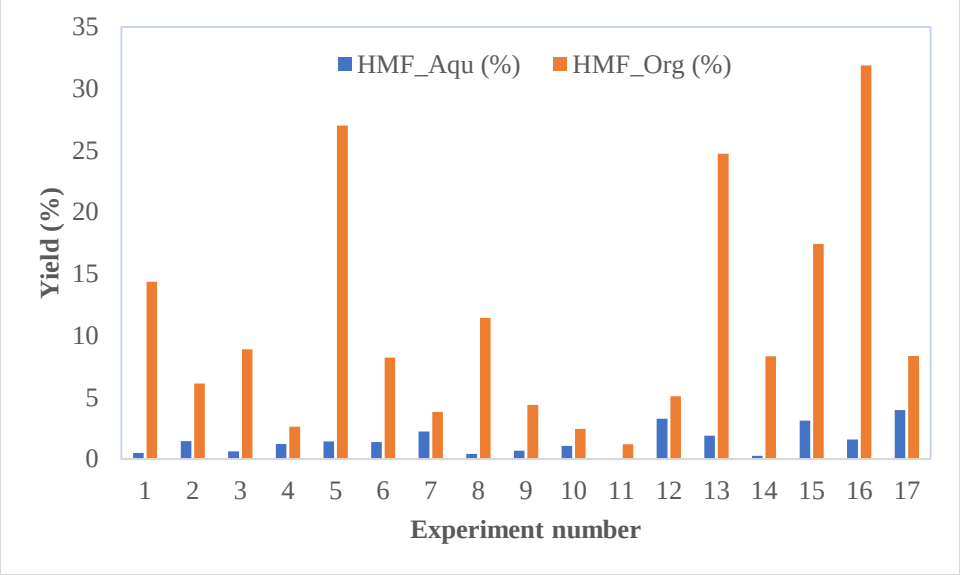

Figure 33: HMF yield in organic and aqueous phase

To further understand the mechanism in catalytical conversion of plum biomass, the distribution of unconverted sugar in aqueous phase was analyzed by LC-ESI-MS/MS and the results are shown in Figure 34 & 35.

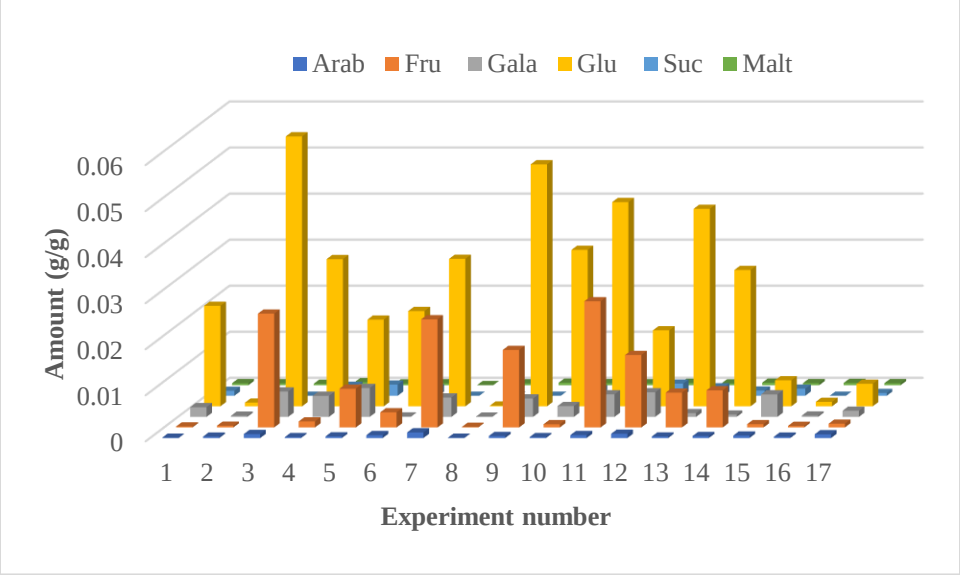

Figure 34: unconverted sugar left in aqueous phase

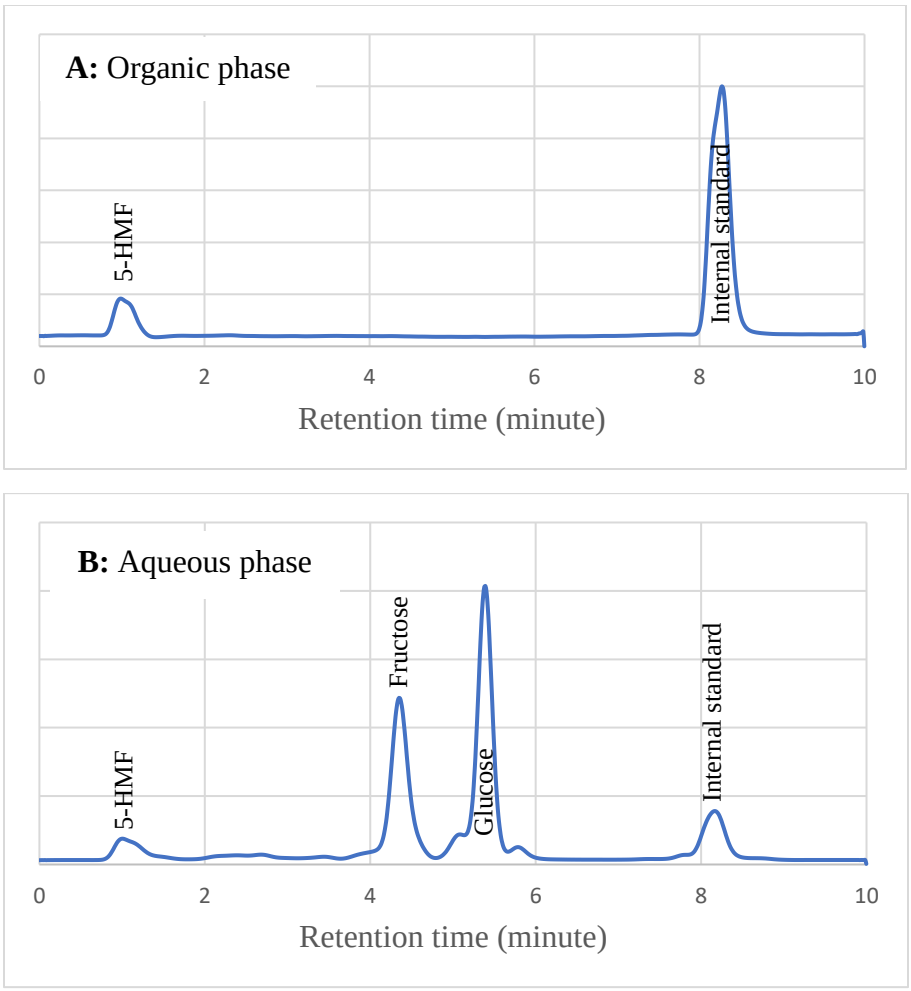

Figure 35: LC-MS/MS analysis of the composition of product fraction. Upper (A); organic phase (B); aqueous phase

On the basis of the above analysis of the liquid-phase product, a thermochemical catalytical conversion pathways of the six saccharides could be proposed, as shown in Figure 36. Disaccharides were first hydrolyzed into monosaccharides, including fructose, glucose, and galactose, according to their structural compositions. Most of the monosaccharides were dehydrated in to HMF. The selectivity of different monosaccharides toward 5-HMF were different, which was reflected as the differences in product distribution of each mono and disaccharide. In addition, humins, which mainly contained furan oligomers, were formed by the condensation reaction between furan products during the dehydration of all the saccharides.

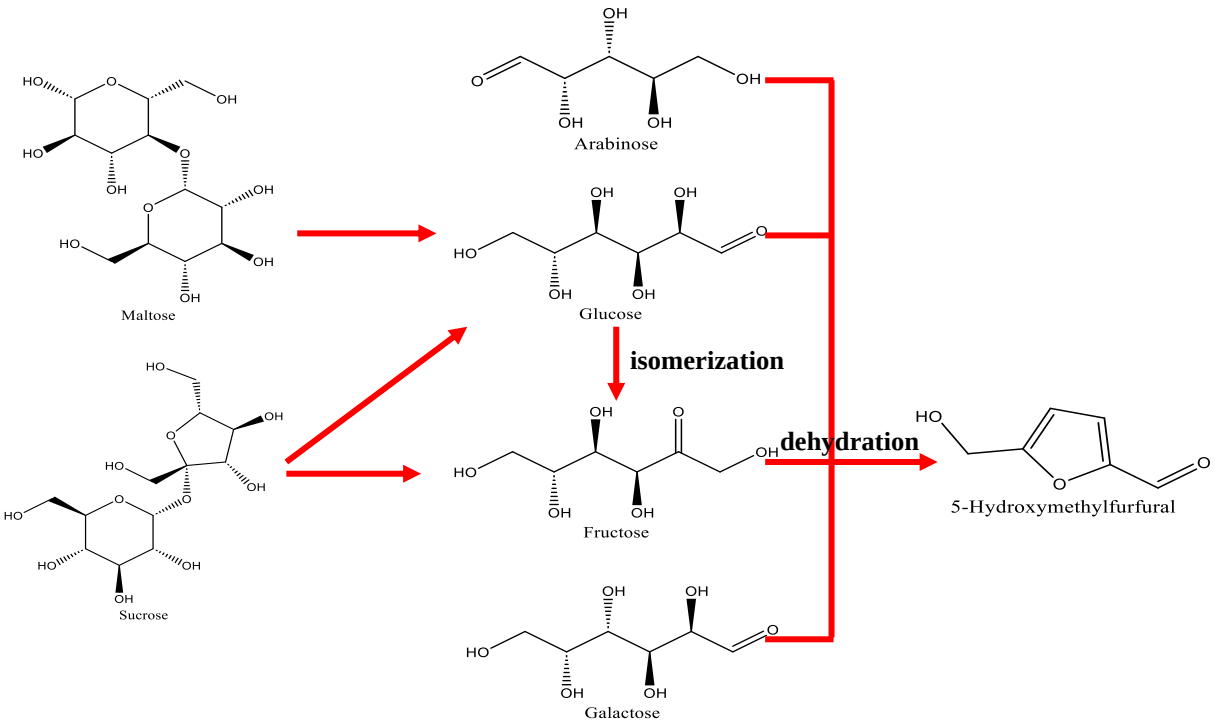

Figure 36: Thermochemical conversion pathways of disaccharide and monosaccharide

5. Conclusions

In this research, a new LC-ESI-MS/MS method based on AQbD approach was developed and applied to characterize the plums biomass. In addition, plum biomass was converted into HMF using a one-step catalytical process or through thermochemical sugar dehydration. Sulfamic acid was utilized as catalyst in MIBK based biphasic reaction system. The overall objective of the thesis was to study the selectivity of thermochemical conversion process to maximize the biomass conversion and HMF yield. The following conclusions can be drawn based on the research outcome of the thesis:

- A rapid and robust selective ion monitoring (SIM) based LC-ESI-MS/MS method using hydrophilic interaction chromatography (HILIC) column was developed for the simultaneous analysis of sugars and HMF. The developed method has been successfully applied to quantify the level of ribose, xylose, arabinose, mannose, glucose, fructose, galactose, maltose, sucrose, and HMF in Plum biomass before and after the thermochemical catalytic conversion process. The distinctive novelty of the studies encompassed the appropriate utilization of Analytical quality by design (AQbD) approaches to improve analytical performance. The developed method is robust and reliable for analysis over method operable design region (MODR). Risk assessment was applied in this work, definitive screening design experiment was implemented for selecting the CMPs. On the basis of MODR, the analytical control strategy was established demanding strict controls on the CMPs. The method showed good linearity and selectivity, in addition to excellent recovery, precision, and limit of quantitation. Hence, it permitted a concurrent quantification of sugar and HMF in row biomass and liquid products of thermochemical biomass conversion with a short chromatographic analysis time.
- Nature and types of raw biomass is an extremely important factor for HMF production from biomass via thermochemical conversion process. Our data show that plum biomass has higher moisture content (78 ± 4%) , and 84% of its dry weight is covered by sugar. Glucose and fructose are the dominant monosaccharide which accounts 47% and 19% of its dry weight respectively. therefore, plums biomass could be a potential feedstock to produce HMF.

- A simple, fast, and efficient process for HMF production from Plums samples was developed, Sulfamic acid and MIBK were used as a catalyst and solvent under conventional oven heating. The critical reaction parameters, including substrate load, temperature, and aqueous phase percentage were optimized using DSD followed by CCD. The empirical model equations for all the responses were developed by JMP software, and the models were found to be statistically well fitted with an R2 value of 0.97 for the major reaction products. At the optimum reaction condition (temperature (210 ^{0}C), aqueous phase (30 %V), time (120 min), Sulfamic acid load (0.01 g) , and substrate load (0.1 g)) suggested by prediction profiler, a higher yield (~32%) of HMF, selectivity (~51%) and sugar conversion (~93%) was achieved. The relative error between the experimental and predicted response for HMF selectivity and product (HMF) yield was found to be in the acceptable range (< 2%). However, a little higher relative error (~3%) was obtained conversion rate.
- The product analysis suggested that the HMF yield was closely related to the type of monosaccharide unit in carbohydrates. Almost all unconverted sugar is distributed only in the aqueous phase. At optimum condition resulting the V_{org}/V_{aque} of the reaction system reached as high as 20/1 with high yield of HMF was obtained in organic phase (31.9%) compared to aqueous phase (1.6%).

Finally, the low-cost catalyst and solvent system, the effective and environmentally friendly reaction conditions, and the simple procedure provided in the present study for the formation of HMF seem like a promising strategy to produce HMF as a crucial precursor in the formation of alternative fuel and other value-added chemicals from Plum biomass.

6. Outlook on further research

In this study significant findings are reported related to HMF production from Plum biomass, however there are still certain challenges to overcome and things to be developed further. Even though a biphasic system was used, selectivity to HMF never approached 100%, which is consistent with previous observations in our group and in literature as well. This indicates that regardless of the extraction of HMF, there are reaction routes to degradation products that do not include HMF that can consume carbohydrates in the aqueous phase and reduce major product selectivity. Controlling the aqueous phase's Brønsted acidity can prevent these reactions, but it can be challenging when utilizing hydrolysable catalysts, as was the case in this study. The addition of metal halides to aqueous solutions has been reported in literature to improve the thermodynamics of solute extraction from aqueous phases into organic phases. Therefore, for future work it is important to select an appropriate type of metal halide and its concentration to improve the partitioning efficacy of a biphasic system by reducing water activity and increasing the activity coefficients of HMF in water without interfering in the dehydration chemistry.

On the other hands further in-situ ^{13}C NMR spectroscopy investigations are required to propose detailed mechanistic pathways and to identify the selectivity controlling factors in the biphasic catalytical biomass conversion process. Additionally, the HMF selectivity and yield might be improved by exploring and developing efficient catalysts, both heterogeneous catalysts and homogeneous catalysts, since the catalyst is critical for HMF production. Similarly, exploring alternative deep eutectic solvents with appropriate design of separation strategies might be of interest for future works.

Finally, apart from the major product fraction (HMF) quantifying other side products with approperte analytical method is one of the potential research question. Also, the isolation and purification of the produced HMF from the reaction solutions are essential in the future.

REFERENCES

1. Khemthong, P.; Yimsukanan, C.; Narkkun, T.; Srifa, A.; Witoon, T.; Pongchaiphol, S.; Kiatphuengporn, S.; Faungnawakij, K., Advances in catalytic production of value-added biochemicals and biofuels via furfural platform derived lignocellulosic biomass. *Biomass and Bioenergy* **2021,** *148*, 106033.
2. Zhang, Z.-H.; Sun, Z.; Yuan, T.-Q., Recent advances in the catalytic upgrading of biomass platform chemicals via hydrotalcite-derived metal catalysts. *Transactions of Tianjin University* **2022**, 1-23.
3. Liu, S.; Cheng, X.; Sun, S.; Chen, Y.; Bian, B.; Liu, Y.; Tong, L.; Yu, H.; Ni, Y.; Yu, S., High-Yield and High-Efficiency Conversion of HMF to Levulinic Acid in a Green and Facile Catalytic Process by a Dual-Function Brønsted-Lewis Acid HScCl4 Catalyst. *ACS omega* **2021,** *6* (24), 15940-15947.
4. Li, X.; Yang, J.; Xu, R.; Lu, L.; Kong, F.; Liang, M.; Jiang, L.; Nie, S.; Si, C., Kinetic study of furfural production from Eucalyptus sawdust using H-SAPO-34 as solid Brønsted acid and Lewis acid catalysts in biomass-derived solvents. *Industrial Crops and Products* **2019,** *135*, 196-205.
5. Wang, A.; Berton, P.; Zhao, H.; Bryant, S. L.; Kibria, M. G.; Hu, J., Plasmon-enhanced 5-hydroxymethylfurfural Production from the Photothermal Conversion of Cellulose in a Biphasic Medium. *ACS Sustainable Chemistry & Engineering* **2021,** *9* (48), 16115-16122.
6. Kar, S.; Zhou, Q.-Q.; Ben-David, Y.; Milstein, D., Catalytic Furfural/5-Hydroxymethyl Furfural Oxidation to Furoic Acid/Furan-2, 5-dicarboxylic Acid with H2 Production Using Alkaline Water as the Formal Oxidant. *Journal of the American Chemical Society* **2022,** *144* (3), 1288-1295.
7. Svenningsen, G. S.; Kumar, R.; Wyman, C. E.; Christopher, P., Unifying mechanistic analysis of factors controlling selectivity in fructose dehydration to 5-hydroxymethylfurfural by homogeneous acid catalysts in aprotic solvents. *ACS Catalysis* **2018,** *8* (6), 5591-5600.
8. Fulignati, S.; Licursi, D.; Di Fidio, N.; Antonetti, C.; Raspolli Galletti, A. M., Novel Challenges on the Catalytic Synthesis of 5-Hydroxymethylfurfural (HMF) from Real Feedstocks. *Catalysts* **2022,** *12* (12), 1664.
9. Hou, Q.; Qi, X.; Zhen, M.; Qian, H.; Nie, Y.; Bai, C.; Zhang, S.; Bai, X.; Ju, M., Biorefinery roadmap based on catalytic production and upgrading 5-hydroxymethylfurfural. *Green Chemistry* **2021,** *23* (1), 119-231.
10. Kunnikuruvan, S.; Nair, N. N., Mechanistic insights into the Brønsted acid-catalyzed dehydration of β-D-glucose to 5-hydroxymethylfurfural under ambient and subcritical conditions. *ACS Catalysis* **2019,** *9* (8), 7250-7263.
11. Antonetti, C.; Licursi, D.; Fulignati, S.; Valentini, G.; Raspolli Galletti, A. M., New frontiers in the catalytic synthesis of levulinic acid: from sugars to raw and waste biomass as starting feedstock. *Catalysts* **2016,** *6* (12), 196.
12. Sajid, M.; Bai, Y.; Liu, D.; Zhao, X., Organic acid catalyzed production of platform chemical 5-hydroxymethylfurfural from fructose: Process comparison and evaluation based on kinetic modeling. *Arabian Journal of Chemistry* **2020,** *13* (10), 7430-7444.
13. Sailer-Kronlachner, W.; Thoma, C.; Böhmdorfer, S.; Bacher, M.; Konnerth, J.; Rosenau, T.; Potthast, A.; Solt, P.; van Herwijnen, H. W., Sulfuric Acid-Catalyzed Dehydratization of Carbohydrates for the Production of Adhesive Precursors. *ACS omega* **2021,** *6* (25), 16641-16648.

14. Garcés, D.; Díaz, E.; Ordóñez, S., Aqueous phase conversion of hexoses into 5-hydroxymethylfurfural and levulinic acid in the presence of hydrochloric acid: mechanism and kinetics. *Industrial & Engineering Chemistry Research* **2017,** *56* (18), 5221-5230.
15. Ginés-Molina, M. J.; Cecilia, J. A.; García-Sancho, C.; Moreno-Tost, R.; Maireles-Torres, P., Use of Ion-Exchange Resins in Dehydration Reactions. *Applications of Ion Exchange Materials in Chemical and Food Industries* **2019**, 1-18.
16. Kislitsa, O. V.; Manaenkov, O. V.; Ratkevich, E. A.; Sulman, M. G.; Kosivtsov, Y. Y., The Use of WO3-ZSM-5 Zeolites in the Dehydration of Monosaccharides. *Chemical Engineering Transactions* **2021,** *88*, 295-300.
17. Kammoun, M.; Istasse, T.; Ayeb, H.; Rassaa, N.; Bettaieb, T.; Richel, A., Hydrothermal dehydration of monosaccharides promoted by seawater: fundamentals on the catalytic role of inorganic salts. *Frontiers in chemistry* **2019,** *7*, 132.
18. B Nasirudeen, M.; C Hailes, H.; RG Evans, J., Preparation of 5-hydroxymethylfurfural from glucose and fructose in ionic liquids by reactive vacuum distillation over a solid catalyst. *Current Organic Synthesis* **2017,** *14* (4), 596-603.
19. Gilcher, E. B.; Chang, H.; Huber, G. W.; Dumesic, J. A., Controlled hydrogenation of a biomass-derived platform chemical formed by aldol-condensation of 5-hydroxymethyl furfural (HMF) and acetone over Ru, Pd, and Cu catalysts. *Green Chemistry* **2022,** *24* (5), 2146-2159.
20. Rosenfeld, C.; Konnerth, J.; Sailer-Kronlachner, W.; Solt, P.; Rosenau, T.; van Herwijnen, H. W., Current situation of the challenging scale-up development of hydroxymethylfurfural production. *ChemSusChem* **2020,** *13* (14), 3544-3564.
21. Pal, P.; Saravanamurugan, S., Recent advances in the development of 5-hydroxymethylfurfural oxidation with base (nonprecious)-metal-containing catalysts. *ChemSusChem* **2019,** *12* (1), 145-163.
22. Asghari, F. S.; Yoshida, H., Dehydration of fructose to 5-hydroxymethylfurfural in sub-critical water over heterogeneous zirconium phosphate catalysts. *Carbohydrate research* **2006,** *341* (14), 2379-2387.
23. Yadav, V. G.; Yadav, G. D.; Patankar, S. C., The production of fuels and chemicals in the new world: critical analysis of the choice between crude oil and biomass vis-à-vis sustainability and the environment. *Clean technologies and environmental policy* **2020,** *22* (9), 1757-1774.
24. Davidson, M. G.; Elgie, S.; Parsons, S.; Young, T. J., Production of HMF, FDCA and their derived products: A review of life cycle assessment (LCA) and techno-economic analysis (TEA) studies. *Green Chemistry* **2021,** *23* (9), 3154-3171.
25. Zhao, Q.; Wang, L.; Zhao, S.; Wang, X.; Wang, S., High selective production of 5-hydroymethylfurfural from fructose by a solid heteropolyacid catalyst. *Fuel* **2011,** *90* (6), 2289-2293.
26. Moreau, C.; Belgacem, M. N.; Gandini, A., Recent catalytic advances in the chemistry of substituted furans from carbohydrates and in the ensuing polymers. *Topics in Catalysis* **2004,** *27*, 11-30.
27. Teong, S. P.; Yi, G.; Zhang, Y., Hydroxymethylfurfural production from bioresources: past, present and future. *Green Chemistry* **2014,** *16* (4), 2015-2026.
28. Moreau, C.; Finiels, A.; Vanoye, L., Dehydration of fructose and sucrose into 5-hydroxymethylfurfural in the presence of 1-H-3-methyl imidazolium chloride acting both as solvent and catalyst. *Journal of Molecular Catalysis A: Chemical* **2006,** *253* (1-2), 165-169.

29. Long, J.; Guo, B.; Teng, J.; Yu, Y.; Wang, L.; Li, X., SO3H-functionalized ionic liquid: Efficient catalyst for bagasse liquefaction. *Bioresource technology* **2011,** *102* (21), 10114-10123.
30. Swatloski, R. P.; Spear, S. K.; Holbrey, J. D.; Rogers, R. D., Dissolution of cellose with ionic liquids. *Journal of the American chemical society* **2002,** *124* (18), 4974-4975.
31. Fort, D. A.; Remsing, R. C.; Swatloski, R. P.; Moyna, P.; Moyna, G.; Rogers, R. D., Can ionic liquids dissolve wood? Processing and analysis of lignocellulosic materials with 1-n-butyl-3-methylimidazolium chloride. *Green chemistry* **2007,** *9* (1), 63-69.
32. Wang, H.; Gurau, G.; Rogers, R. D., Ionic liquid processing of cellulose. *Chemical Society Reviews* **2012,** *41* (4), 1519-1537.
33. Chan, J. Y. G.; Zhang, Y., Selective conversion of fructose to 5-hydroxymethylfurfural catalyzed by tungsten salts at low temperatures. *ChemSusChem: Chemistry & Sustainability Energy & Materials* **2009,** *2* (8), 731-734.
34. Saha, B.; Abu-Omar, M. M., Advances in 5-hydroxymethylfurfural production from biomass in biphasic solvents. *Green Chemistry* **2014,** *16* (1), 24-38.
35. Wang, T.; Nolte, M. W.; Shanks, B. H., Catalytic dehydration of C 6 carbohydrates for the production of hydroxymethylfurfural (HMF) as a versatile platform chemical. *Green Chemistry* **2014,** *16* (2), 548-572.
36. Tarabanko, V.; Chernyak, M. Y.; Aralova, S.; Kuznetsov, B., Kinetics of levulinic acid formation from carbohydrates at moderate temperatures. *Reaction kinetics and catalysis letters* **2002,** *75* (1), 117-126.
37. Nie, Y.; Hou, Q.; Bai, C.; Qian, H.; Bai, X.; Ju, M., Transformation of carbohydrates to 5-hydroxymethylfurfural with high efficiency by tandem catalysis. *Journal of Cleaner Production* **2020,** *274*, 123023.
38. Buttersack, C.; Hofmann, J.; Gläser, R., Hydrolysis of Sucrose over Sulfonic Acid Resins. *ChemCatChem* **2021,** *13* (15), 3443-3460.
39. Akien, G. R.; Qi, L.; Horváth, I. T., Molecular mapping of the acid catalysed dehydration of fructose. *Chemical Communications* **2012,** *48* (47), 5850-5852.
40. Barclay, T.; Ginic-Markovic, M.; Cooper, P.; Petrovsky, N., The chemistry and sources of fructose and their effect on its utility and health implications. *Journal of Excipients and Food Chemicals* **2012,** *3* (2), 67-82.
41. Huang, Y.; Chao, P.-Y.; Cheng, T.-Y.; Ho, Y.; Lin, C.-T.; Hsu, H.-Y.; Wong, J.-J.; Tsai, T.-C., Design of sulfonated mesoporous silica catalyst for fructose dehydration guided by difructose anhydride intermediate incorporated reaction network. *Chemical Engineering Journal* **2016,** *283*, 778-788.
42. Antal Jr, M. J.; Mok, W. S.; Richards, G. N., Mechanism of formation of 5-(hydroxymethyl)-2-furaldehyde from D-fructose and sucrose. *Carbohydrate research* **1990,** *199* (1), 91-109.
43. Guo, W.; Zhang, Z.; Hacking, J.; Heeres, H. J.; Yue, J., Selective fructose dehydration to 5-hydroxymethylfurfural from a fructose-glucose mixture over a sulfuric acid catalyst in a biphasic system: Experimental study and kinetic modelling. *Chemical Engineering Journal* **2021,** *409*, 128182.
44. Telford, J. K., A brief introduction to design of experiments. *Johns Hopkins apl technical digest* **2007,** *27* (3), 224-232.
45. Weissman, S. A.; Anderson, N. G., Design of experiments (DoE) and process optimization. A review of recent publications. *Organic Process Research & Development* **2015,** *19* (11), 1605-1633.

46. Durakovic, B., Design of experiments application, concepts, examples: State of the art. *Periodicals of Engineering and Natural Sciences (PEN)* **2017,** *5* (3).
47. Guo, H.; Mettas, A. In *Design of experiments and data analysis*, 2012 Annual Reliability and Maintainability Symposium, 2010.
48. Tai, M.; Ly, A.; Leung, I.; Nayar, G., Efficient high-throughput biological process characterization: Definitive screening design with the Ambr250 bioreactor system. *Biotechnology progress* **2015,** *31* (5), 1388-1395.
49. Elsayed, M. S.; Eldadamony, N. M.; Alrdahe, S. S.; Saber, W. I., Definitive screening design and artificial neural network for modeling a rapid biodegradation of date palm fronds by a new Trichoderma sp. PWN6 into citric acid. *Molecules* **2021,** *26* (16), 5048.
50. Jones, B.; Nachtsheim, C. J., A class of three-level designs for definitive screening in the presence of second-order effects. *Journal of Quality Technology* **2011,** *43* (1), 1-15.
51. Jones, B.; Nachtsheim, C. J., Blocking schemes for definitive screening designs. *Technometrics* **2016,** *58* (1), 74-83.
52. Jones, B.; Nachtsheim, C. J., Definitive screening designs with added two-level categorical factors. *Journal of Quality Technology* **2013,** *45* (2), 121-129.
53. Vaz, S., The Use of Analytical Chemistry to Understand Biomass. In *Analytical Techniques and Methods for Biomass*, Springer: 2016; pp 1-13.
54. Le Brech, Y.; Delmotte, L.; Raya, J.; Brosse, N.; Gadiou, R.; Dufour, A., High resolution solid state 2D NMR analysis of biomass and biochar. *Analytical Chemistry* **2015,** *87* (2), 843-847.
55. Løhre, C.; Underhaug, J.; Brusletto, R.; Barth, T., A workup protocol combined with direct application of quantitative nuclear magnetic resonance spectroscopy of aqueous samples from large-scale steam explosion of biomass. *ACS omega* **2021,** *6* (10), 6714-6721.
56. Pratima, N. A.; Gadikar, R., Liquid chromatography-mass spectrometry and its applications: a brief review. *Arch. Org. Inorg. Chem. Sci* **2018,** *1*, 26-34.
57. Kumar, K. J.; Vijayan, V., An overview of liquid chromatography-mass spectroscopy instrumentation. **2014**.
58. Kang, J.-S., Principles and applications of LC-MS/MS for the quantitative bioanalysis of analytes in various biological samples. *Tandem Mass Spectrometry–Applications and Principles* **2012**, 441-492.
59. Niessen, W. M., *Liquid chromatography-mass spectrometry*. CRC press: 2006.
60. Ichiro, H. *Shimadzu's Fundamental Guide to LCMS*; 2019.
61. Shah, Z.; Patel, H.; More, J.; Dalwadi, M.; Shah, C.; Upadhayay, U., A REVIEW ON LC-MS TECHNIQUE AND IT'S APPLICATION. **2021**.
62. Izat, N.; Yerlikaya, F.; Capan, Y., A glance on the history of pharmaceutical quality by design. *OA Drug Design and Delivery* **2014,** *2* (1), 1-8.
63. Holm, P.; Allesø, M.; Bryder, M. C.; Holm, R., Q8 (R2) Pharmaceutical Development. *ICH quality guidelines: an implementation guide* **2017**, 535-577.
64. Nethercote, P.; Borman, P.; Chatfield, M.; Thompson, D.; Truman, K., The application of Quality by design to analytical methods. *Pharma Tech* **2007**, 1-10.
65. Schweitzer, M.; Pohl, M.; Hanna-Brown, M.; Nethercote, P.; Borman, P.; Hansen, G.; Smith, K.; Larew, J., Implications and opportunities of applying QbD principles to analytical measurements. *Pharmaceutical Technology* **2010,** *34* (2), 52-59.

66. Freed, A.; Colgan, S.; Kochling, J.; Alasandro, M., AAPS workshop: accelerating pharmaceutical development through predictive stability approaches, April 4–5, 2016. SpringerOpen: 2017.
67. Sandhu, P. S.; Beg, S.; Katare, O.; Singh, B., QbD-driven development and validation of a HPLC method for estimation of tamoxifen citrate with improved performance. *Journal of chromatographic science* **2016,** *54* (8), 1373-1384.
68. Sharma, G.; Thakur, K.; Raza, K.; Katare, O., Stability kinetics of fusidic acid: Development and validation of stability indicating analytical method by employing Analytical Quality by Design approach in medicinal product (s). *Journal of Chromatography B* **2019,** *1120*, 113-124.
69. Mitrović, M.; Protić, A.; Malenović, A.; Otašević, B.; Zečević, M., Analytical quality by design development of an ecologically acceptable enantioselective HPLC method for timolol maleate enantiomeric purity testing on ovomucoid chiral stationary phase. *Journal of Pharmaceutical and Biomedical Analysis* **2020,** *180*, 113034.
70. Hames, B.; Ruiz, R.; Scarlata, C.; Sluiter, A.; Sluiter, J.; Templeton, D., Preparation of samples for compositional analysis. *Laboratory Analytical Procedure (LAP)* **2008,** *1617*, 65-71.
71. Sluiter, A.; Hames, B.; Ruiz, R.; Scarlata, C.; Sluiter, J.; Templeton, D.; Crocker, D., Determination of structural carbohydrates and lignin in biomass. *Laboratory analytical procedure* **2008,** *1617* (1), 1-16.
72. MOLNES, J. L. Furfural Synthesis from Xylose, Plums and Cherries in a Biphasic Reaction System for Renewable Fuel and Chemicals Production. University of Bergen 2021.
73. Mayhew, H. M. H. Thermochemical conversion of waste biomass (cherry rejects) to renewable platform chemicals: FUR and HMF. The University of Bergen, 2022.
74. Guideline, I. H. T.; HH, T., Q8 (R2) Pharmaceutical Development. *Step 4 Version* **2009**.
75. Kato, Y.; Numajiri, Y., Chloride attachment negative-ion mass spectra of sugars by combined liquid chromatography and atmospheric pressure chemical ionization mass spectrometry. *Journal of Chromatography B: Biomedical Sciences and Applications* **1991,** *562* (1-2), 81-97.
76. Tannenbaum, H. P.; Roberts, J. D.; Dougherty, R. C., Negative chemical ionization mass spectrometry. Chloride attachment spectra. *Analytical Chemistry* **1975,** *47* (1), 49-54.
77. Rogatsky, E.; Jayatillake, H.; Goswami, G.; Tomuta, V.; Stein, D., Sensitive LC MS quantitative analysis of carbohydrates by Cs+ attachment. *Journal of the American Society for Mass Spectrometry* **2005,** *16* (11), 1805-1811.
78. McIntosh, T.; Davis, H.; Matthews, D., A liquid chromatography–mass spectrometry method to measure stable isotopic tracer enrichments of glycerol and glucose in human serum. *Analytical biochemistry* **2002,** *300* (2), 163-169.
79. Silva, P.; Silva, C. L.; Perestrelo, R.; Nunes, F. M.; Câmara, J. S., Application of quality-by-design approach in the analytical method development for quantification of sugars in sugarcane honey by reversed-phase liquid chromatography. *Food Analytical Methods* **2020,** *13* (8), 1634-1649.
80. Fares, M. Y.; Hegazy, M. A.; El-Sayed, G. M.; Abdelrahman, M. M.; Abdelwahab, N. S., Quality by design approach for green HPLC method development for simultaneous analysis of two thalassemia drugs in biological fluid with pharmacokinetic study. *RSC advances* **2022,** *12* (22), 13896-13916.
81. Aksezer, S. Ç., On the sensitivity of desirability functions for multiresponse optimization. **2008**.

82. Fotirić Akšić, M.; Tešić, Ž.; Kalaba, M.; Ćirić, I.; Pezo, L.; Lončar, B.; Gašić, U.; Dojčinović, B.; Tosti, T.; Meland, M., Breakthrough Analysis of Chemical Composition and Applied Chemometrics of European Plum Cultivars Grown in Norway. *Horticulturae* **2023,** *9* (4), 477.
83. Shao, Y.; Long, Y.; Zhou, Y.; Jin, Z.; Zhou, D.; Shen, D., 5-Hydroxymethylfurfural production from watermelon peel by microwave hydrothermal liquefaction. *Energy* **2019,** *174*, 198-205.
84. Iris, K.; Ong, K. L.; Tsang, D. C.; Haque, M. A.; Kwan, T. H.; Chen, S. S.; Uisan, K.; Kulkarni, S.; Lin, C. S. K., Chemical transformation of food and beverage waste-derived fructose to hydroxymethylfurfural as a value-added product. *Catalysis Today* **2018,** *314*, 70-77.
85. Zhao, Y.; Lu, K.; Xu, H.; Qu, Y.; Zhu, L.; Wang, S., Comparative study on the dehydration of biomass-derived disaccharides and polysaccharides to 5-hydroxymethylfurfural. *Energy & fuels* **2019,** *33* (10), 9985-9995.
86. Zhang, R.; Eronen, A.; Du, X.; Ma, E.; Guo, M.; Moslova, K.; Repo, T., A catalytic approach via retro-aldol condensation of glucose to furanic compounds. *Green Chemistry* **2021,** *23* (15), 5481-5486.
87. Steinbach, D.; Klier, A.; Kruse, A.; Sauer, J.; Wild, S.; Zanker, M., Isomerization of glucose to fructose in hydrolysates from lignocellulosic biomass using hydrotalcite. *Processes* **2020,** *8* (6), 644.
88. Román-Leshkov, Y.; Chheda, J. N.; Dumesic, J. A., Phase modifiers promote efficient production of hydroxymethylfurfural from fructose. *Science* **2006,** *312* (5782), 1933-1937.
89. García-López, E. I.; Pomilla, F. R.; Megna, B.; Testa, M. L.; Liotta, L. F.; Marcì, G., Catalytic dehydration of fructose to 5-hydroxymethylfurfural in aqueous medium over Nb2O5-based catalysts. *Nanomaterials* **2021,** *11* (7), 1821.
90. Świątek, K.; Olszewski, M. P.; Kruse, A., Continuous synthesis of 5-hydroxymethylfurfural from biomass in on-farm biorefinery. *GCB Bioenergy* **2022,** *14* (6), 681-693.
91. Zhang, Y.; Wang, J.; Li, X.; Liu, X.; Xia, Y.; Hu, B.; Lu, G.; Wang, Y., Direct conversion of biomass-derived carbohydrates to 5-hydroxymethylfurural over water-tolerant niobium-based catalysts. *Fuel* **2015,** *139*, 301-307.
92. Teng, J.; Ma, H.; Wang, F.; Wang, L.; Li, X., A facile and eco-effective catalytic system for synthesis of 5-hydroxymethylfurfural from glucose. *BioResources* **2016,** *11* (1), 2152-2165.
93. Cao, L.; Iris, K.; Chen, S. S.; Tsang, D. C.; Wang, L.; Xiong, X.; Zhang, S.; Ok, Y. S.; Kwon, E. E.; Song, H., Production of 5-hydroxymethylfurfural from starch-rich food waste catalyzed by sulfonated biochar. *Bioresource technology* **2018,** *252*, 76-82.
94. Parshetti, G. K.; Suryadharma, M. S.; Pham, T. P. T.; Mahmood, R.; Balasubramanian, R., Heterogeneous catalyst-assisted thermochemical conversion of food waste biomass into 5-hydroxymethylfurfural. *Bioresource technology* **2015,** *178*, 19-27.

APPENDIXES

Appendix-1 :Workflow chart for Quality-by-Design approach-based analytical method development

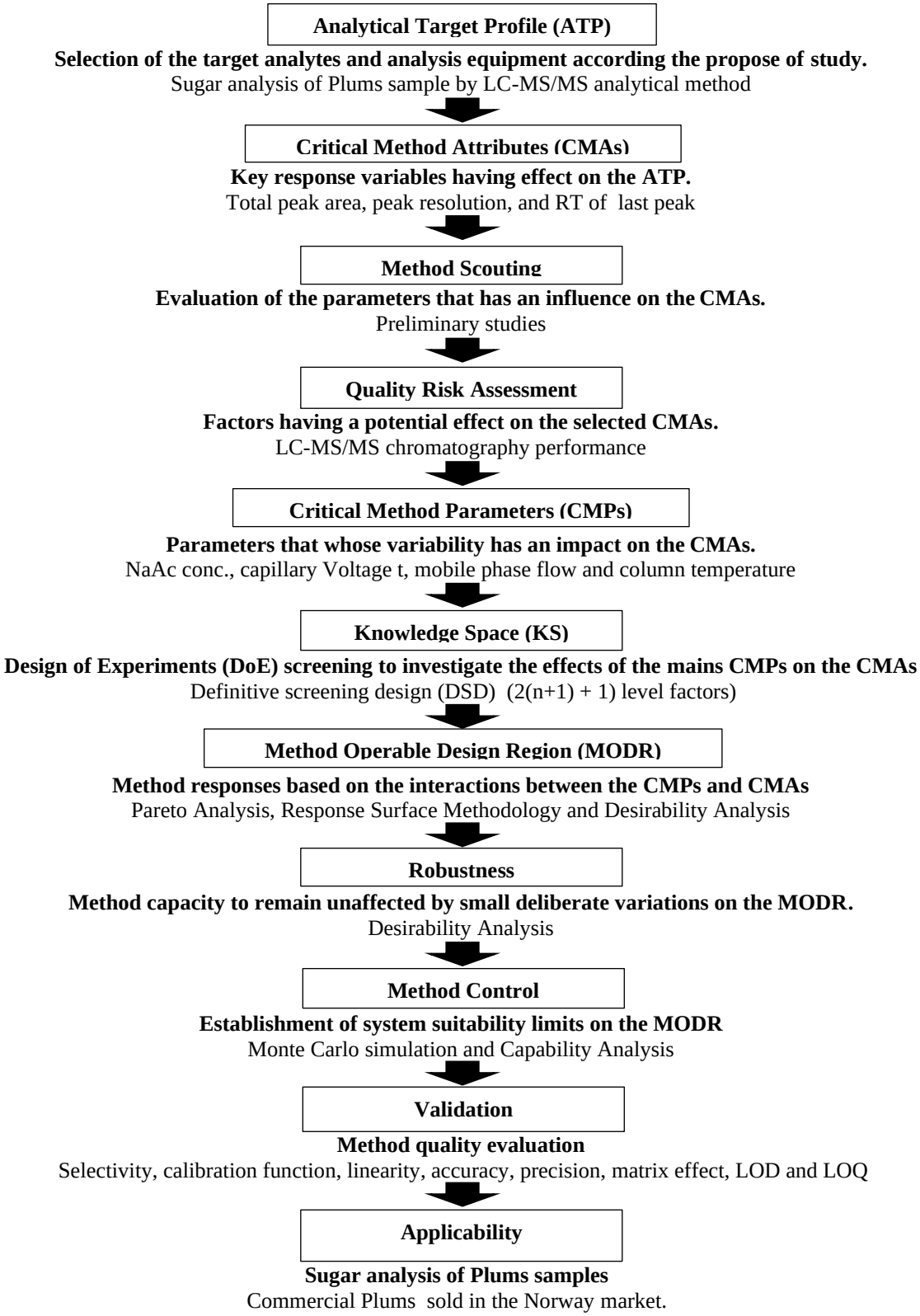

Appendix-2 : TPA, PR, and RTLPT results for all runs (21) of the DSD model.

MP flow rate (mL/min)	Conc. NaAc (Mm)	Column Temp (^{0}C)	N_2 gas flow rate (Lpm)	N_2 gas Temp (^{0}C)	Nebulizer press (psi)	Capillary voltage (KV)	TPA	PR	RTLP
0.4	0.5	55	8	275	25	2.5	318518.2	3.679	6.826
0.2	2	25	3	300	35	2.5	248524.4	6.53	12.491
0.3	0.5	25	3	250	25	2.5	406424.6	3.964	8.63
0.2	0.5	55	3	250	45	4.5	716006.4	6.173	11.411
0.2	0.5	25	8	250	45	2.5	392721	7.222	12.46
0.4	0.5	55	8	250	35	4.5	792858.4	4.157	6.836
0.4	0.5	40	3	300	45	2.5	298032.9	4.309	7.03
0.4	0.5	25	5.5	300	45	4.5	898256.5	4.228	7.733
0.4	1.25	25	3	250	25	4.5	781620.2	4.424	7.529
0.4	2	55	3	250	45	2.5	93768.02	3.688	6.541
0.2	0.5	25	8	300	25	4.5	943802.2	7.652	12.42
0.4	2	25	8	250	45	3.5	425793.7	4.645	7.519
0.2	0.5	55	3	300	25	3.5	655869.4	5.705	11.757
0.2	2	40	8	250	25	4.5	643778.3	5.674	11.869
0.4	2	25	8	300	25	2.5	241073.5	4.646	7.387
0.3	1.25	40	5.5	275	35	3.5	539459	4.972	8.752
0.4	2	55	3	300	25	4.5	461524.5	3.149	6.551
0.3	2	55	8	300	45	4.5	552435.4	3.679	8.181
0.2	1.25	55	8	300	45	2.5	259112.8	6.429	11.299
0.2	2	25	3	275	45	4.5	696861.4	7.04	12.389
0.2	2	55	5.5	250	25	2.5	236161.6	5.257	10.84

Appendix-3: Prediction equation for LC-MS/MS

Total Peak Area (TPA)

$$
\begin{aligned}
&504885.82952 \\
&+ -26743.98278 \cdot \left(\frac{\left(\text{MP Flow rate} - 0.3 \right)}{0.1} \right) \\
&+ -101253.8272 \cdot \left(\frac{\left(\text{Conc. of NaAc} - 1.25 \right)}{0.75} \right) \\
&+ -52712.38278 \cdot \left(\frac{\left(\text{Column temp.} - 40 \right)}{15} \right) \\
&+ 221822.57111 \cdot \left(\text{Capillary Voltage} - 3.5 \right) \\
&+ \left(\frac{\left(\text{MP Flow rate} - 0.3 \right)}{0.1} \right) \cdot \left(\left(\frac{\left(\text{Column temp.} - 40 \right)}{15} \right) \cdot -11018.47383 \right) \\
&+ \left(\frac{\left(\text{Conc. of NaAc} - 1.25 \right)}{0.75} \right) \cdot \left(\left(\text{Capillary Voltage} - 3.5 \right) \cdot -22255.05467 \right)
\end{aligned}
$$

Peak Resolution (PR)

$$
\begin{aligned}
&5.1058095238 \\
&+ -1.153166667 \cdot \left(\frac{\left(\text{MP Flow rate} - 0.3 \right)}{0.1} \right) \\
&+ -0.1545 \cdot \left(\frac{\left(\text{Conc. of NaAc} - 1.25 \right)}{0.75} \right) \\
&+ -0.468611111 \cdot \left(\frac{\left(\text{Column temp.} - 40 \right)}{15} \right) \\
&+ 0.0251111111 \cdot \left(\text{Capillary Voltage} - 3.5 \right) \\
&+ \left(\frac{\left(\text{MP Flow rate} - 0.3 \right)}{0.1} \right) \cdot \left(\left(\frac{\left(\text{Column temp.} - 40 \right)}{15} \right) \cdot 0.1675833333 \right) \\
&+ \left(\frac{\left(\text{Conc. of NaAc} - 1.25 \right)}{0.75} \right) \cdot \left(\left(\text{Capillary Voltage} - 3.5 \right) \cdot -0.267833333 \right)
\end{aligned}
$$

Retention time of last peak (RTLP)

$$9.3548095238$$

$$+ -2.388 \cdot \left(\frac{\left(\text{MP Flow rate} - 0.3 \right)}{0.1} \right)$$

$$+ -0.074166667 \cdot \left(\frac{\left(\text{Conc. of NaAc} - 1.25 \right)}{0.75} \right)$$

$$+ -0.462 \cdot \left(\frac{\left(\text{Column temp.} - 40 \right)}{15} \right)$$

$$+ 0.0786111111 \cdot \left(\text{Capillary Voltage} - 3.5 \right)$$

$$+ \left(\frac{\left(\text{MP Flow rate} - 0.3 \right)}{0.1} \right) \cdot \left(\left(\frac{\left(\text{Column temp.} - 40 \right)}{15} \right) \cdot 0.0979833333 \right)$$

$$+ \left(\frac{\left(\text{Conc. of NaAc} - 1.25 \right)}{0.75} \right) \cdot \left(\left(\text{Capillary Voltage} - 3.5 \right) \cdot -0.132183333 \right)$$

Appendix-4 : Residual by Predicted Plot

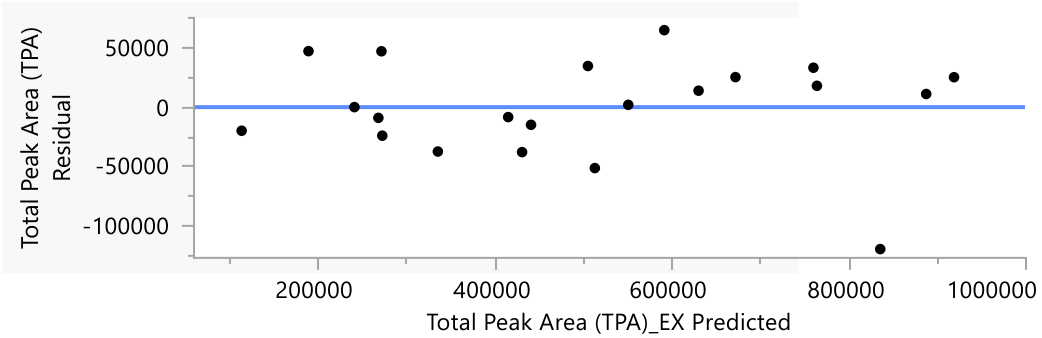

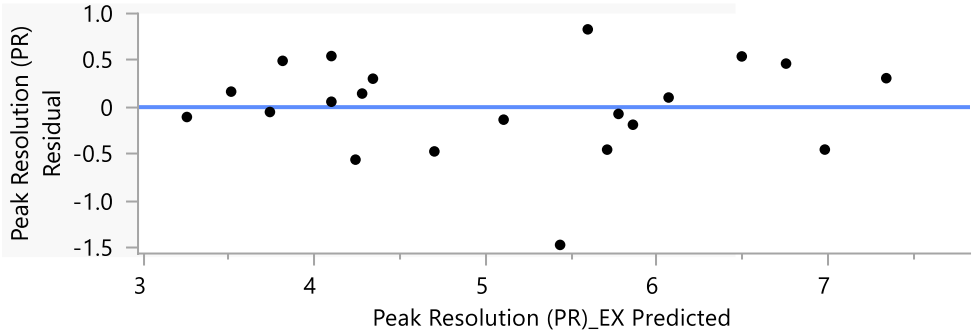

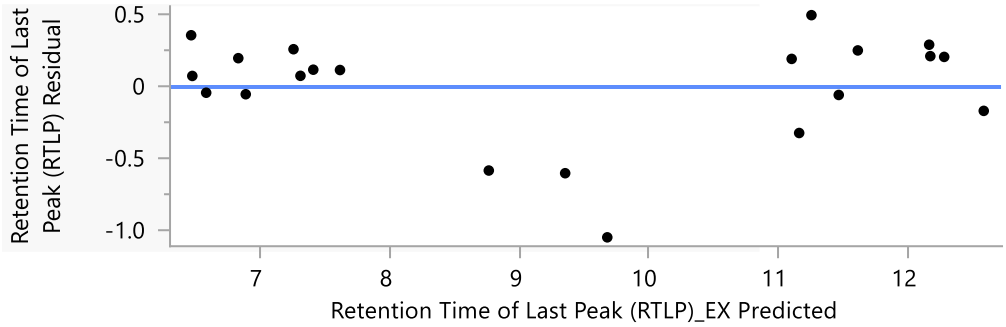

Appendix-5 : 3D surface profile Plot for LC-MS/MS

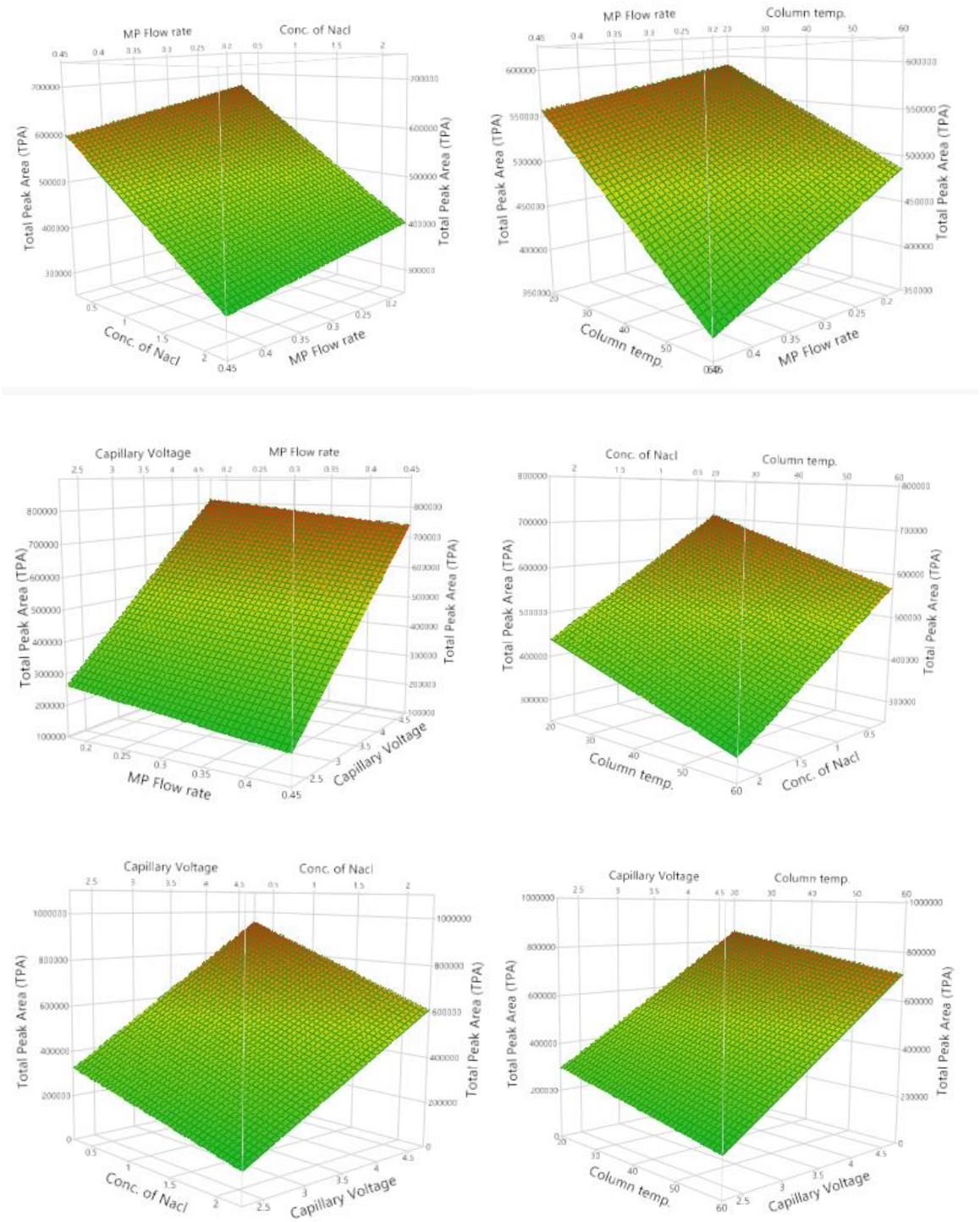

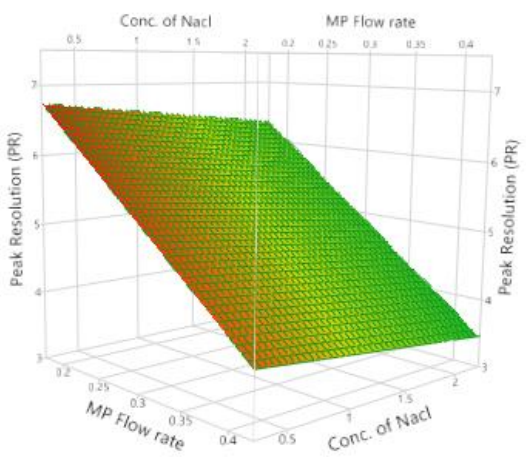
Conc. of Nacl
MP Flow rate
Peak Resolution (PR)
MP Flow rate
Conc. of Nacl

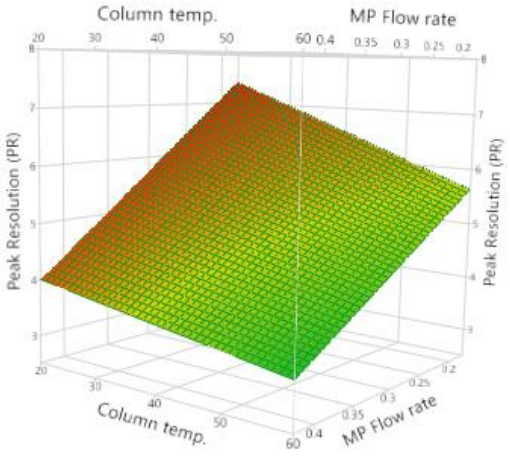
Column temp.
MP Flow rate
Peak Resolution (PR)
Column temp.
MP Flow rate

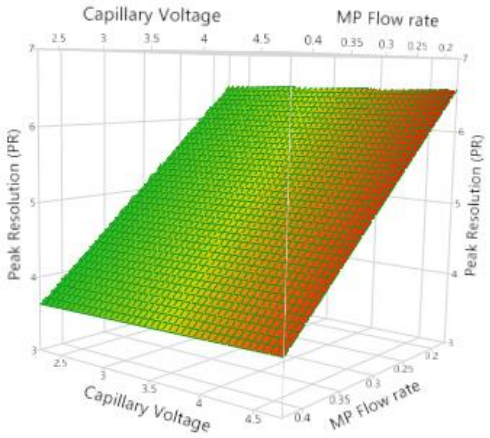
Capillary Voltage
MP Flow rate
Peak Resolution (PR)
Capillary Voltage
MP Flow rate

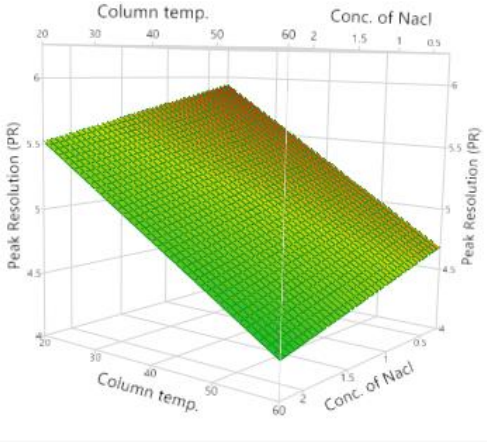
Column temp.
Conc. of Nacl
Peak Resolution (PR)
Column temp.
Conc. of Nacl

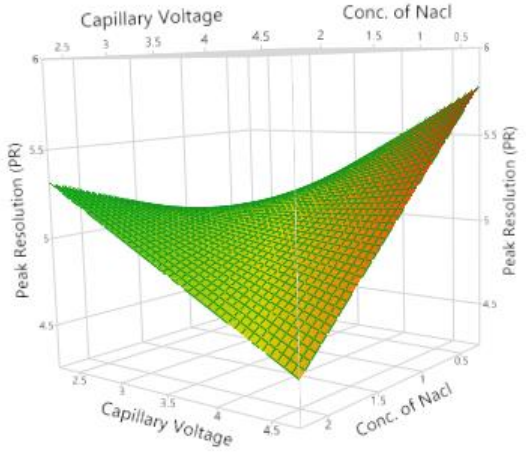
Capillary Voltage
Conc. of Nacl
Peak Resolution (PR)
Capillary Voltage
Conc. of Nacl

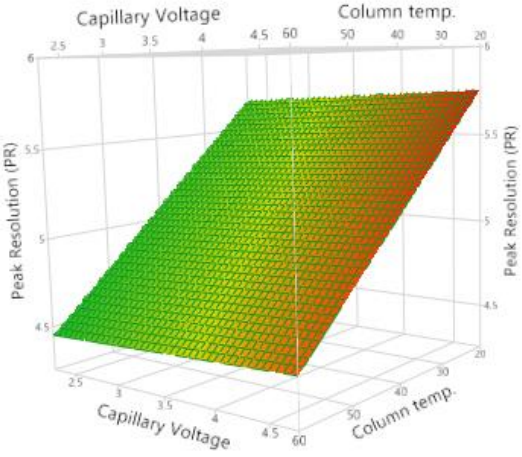
Capillary Voltage
Column temp.
Peak Resolution (PR)
Capillary Voltage
Column temp.

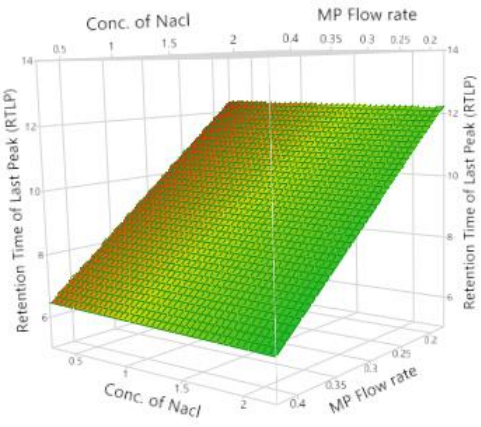
Conc. of Nacl
MP Flow rate
Retention Time of Last Peak (RTLP)
Conc. of Nacl
MP Flow rate

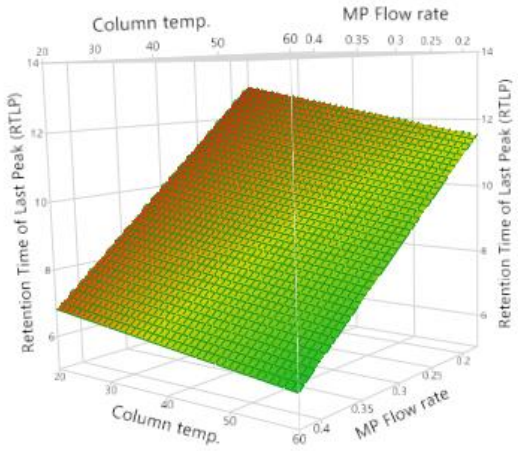
Column temp.
MP Flow rate
Retention Time of Last Peak (RTLP)
Column temp.
MP Flow rate

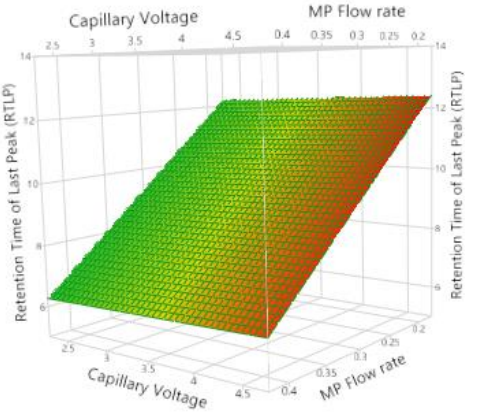
Capillary Voltage
MP Flow rate
Retention Time of Last Peak (RTLP)
Capillary Voltage
MP Flow rate

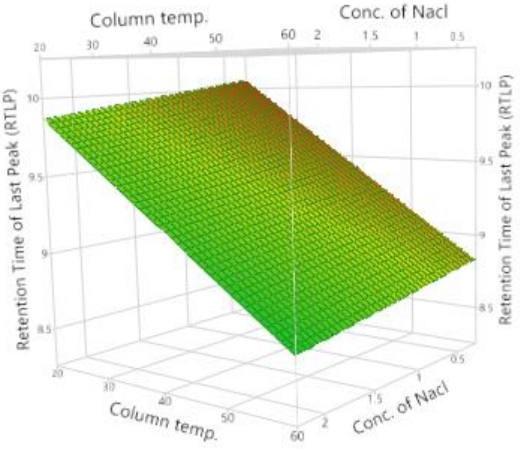
Column temp.
Conc. of Nacl
Retention Time of Last Peak (RTLP)
Column temp.
Conc. of Nacl

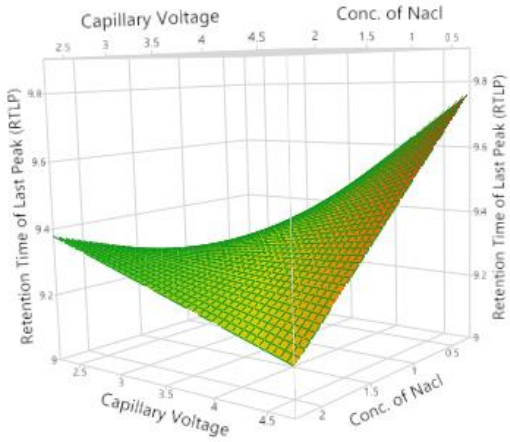
Capillary Voltage
Conc. of Nacl
Retention Time of Last Peak (RTLP)
Capillary Voltage
Conc. of Nacl

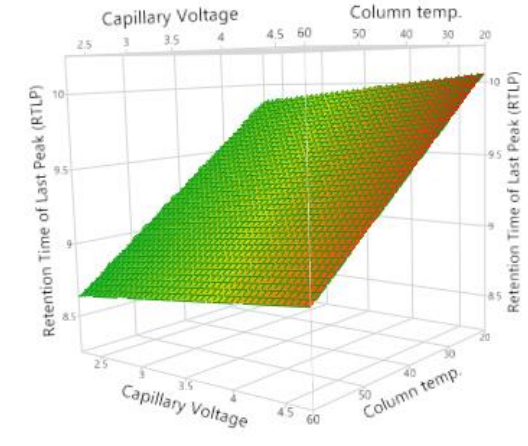
Capillary Voltage
Column temp.
Retention Time of Last Peak (RTLP)
Capillary Voltage
Column temp.

Appendix-6 : method capability results of Monte Carlo bootstrapping simulation

Process Capability
Total Peak Area (TPA) Capability
Histogram

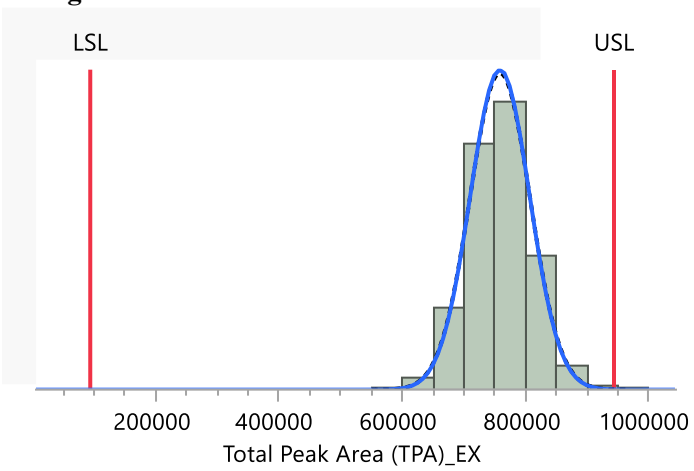

Process Summary

LSL	93768
USL	943802
N	10000
Sample Mean	758642.3
Within Sigma	48176.06
Overall Sigma	48715.15
Stability Index	1.01119

Within sigma estimated by average moving range.

Within Sigma Capability

Index	Estimate	Lower 95%	Upper 95%
Cpk	1.381	1.358	1.305
Cpl	4.600	4.519	4.681
Cpu	1.281	1.258	1.305
Cp	2.941	2.889	2.992

Overall Sigma Capability

Index	Estimate	Lower 95%	Upper 95%
Ppk	1.267	1.248	1.286
Ppl	4.549	4.486	4.613
Ppu	1.267	1.248	1.286
Pp	2.908	2.868	2.948

Nonconformance

Portion	Observed %	Expected Within %	Expected Overall %
Below LSL	0.0000	0.0000	0.0000
Above USL	0.0100	0.0061	0.0072
Total Outside	0.0100	0.0061	0.0072

Process Capability
Peak Resolution (PR) Capability
Histogram

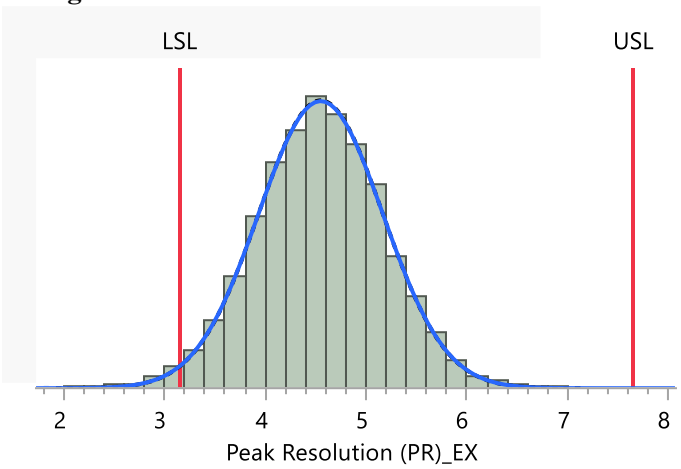

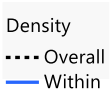

Process Summary

LSL	3.149
USL	7.652
N	10000
Sample Mean	4.549581
Within Sigma	0.617497
Overall Sigma	0.616021
Stability Index	0.99761

Within sigma estimated by average moving range.

Within Sigma Capability

Index	Estimate	Lower 95%	Upper 95%
Cpk	1.756	1.741	1.771
Cpl	1.756	1.741	1.771
Cpu	1.675	1.644	1.705
Cp	1.215	1.194	1.237

Overall Sigma Capability

Index	Estimate	Lower 95%	Upper 95%
Ppk	0.758	0.745	0.770
Ppl	0.758	0.745	0.770
Ppu	1.679	1.655	1.703
Pp	1.218	1.201	1.235

Nonconformance

Portion	Observed %	Expected Within %	Expected Overall %
Below LSL	1.1100	1.1660	1.1495
Above USL	0.0000	0.0000	0.0000
Total Outside	1.1100	1.1660	1.1496

Process Capability
Retention Time of Last Peak (RTLP) Capability
Histogram

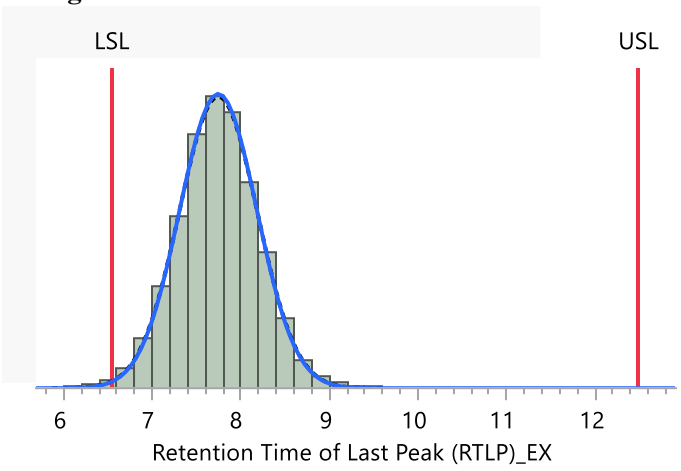

Process Summary

LSL	6.541
USL	12.491
N	10000
Sample Mean	7.744301
Within Sigma	0.435734
Overall Sigma	0.439822
Stability Index	1.009381

Within sigma estimated by average moving range.

Within Sigma Capability

Index	Estimate	Lower 95%	Upper 95%
Cpk	1.921	1.903	1.938
Cpl	1.921	1.903	1.938
Cpu	3.631	3.567	3.695
Cp	2.276	2.236	2.316

Overall Sigma Capability

Index	Estimate	Lower 95%	Upper 95%
Ppk	0.912	0.898	0.926
Ppl	0.912	0.898	0.926
Ppu	3.597	3.547	3.648
Pp	2.255	2.223	2.286

Nonconformance

Portion	Observed %	Expected Within %	Expected Overall %
Below LSL	0.3400	0.2876	0.3111
Above USL	0.0000	0.0000	0.0000
Total Outside	0.3400	0.2876	0.3111

Appendix 7 : Calibration curve and its function

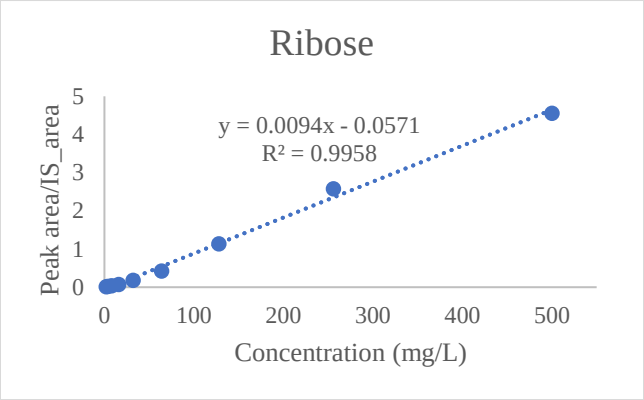

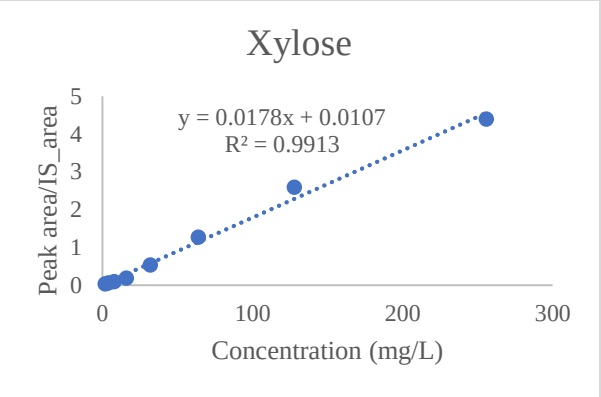

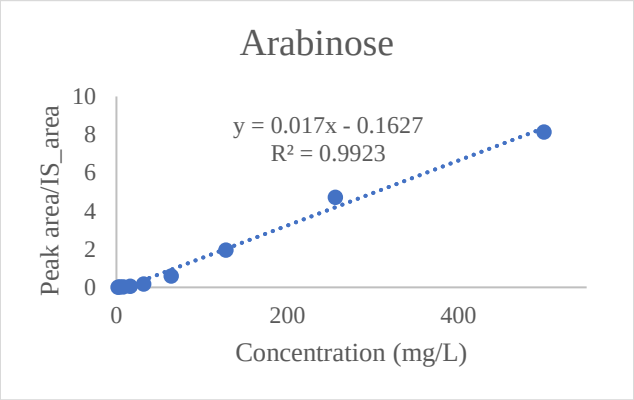

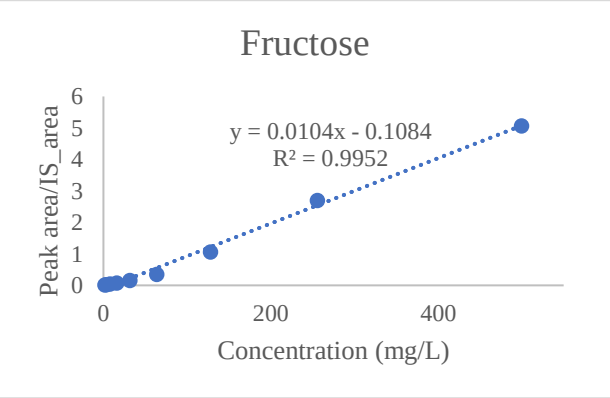

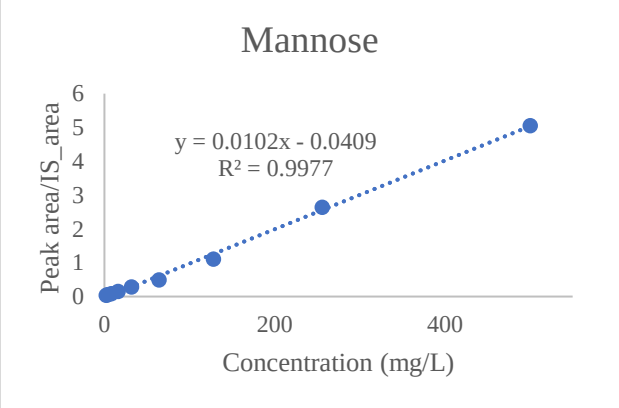

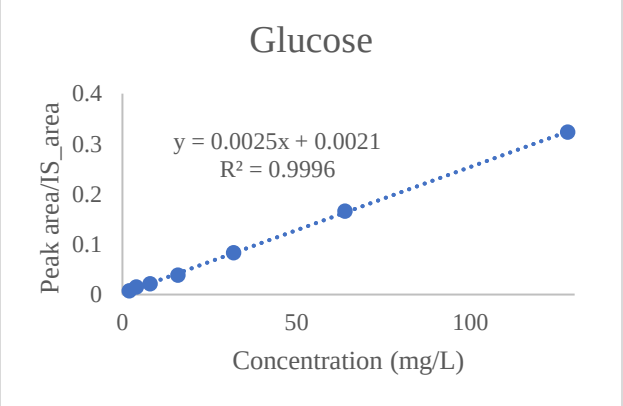

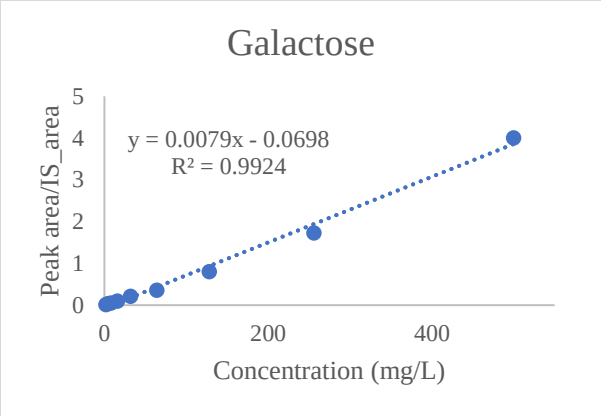
Galactose
y = 0.0079x - 0.0698
R² = 0.9924
Peak area/IS_area
Concentration (mg/L)
0
1
2
3
4
5
0
200
400

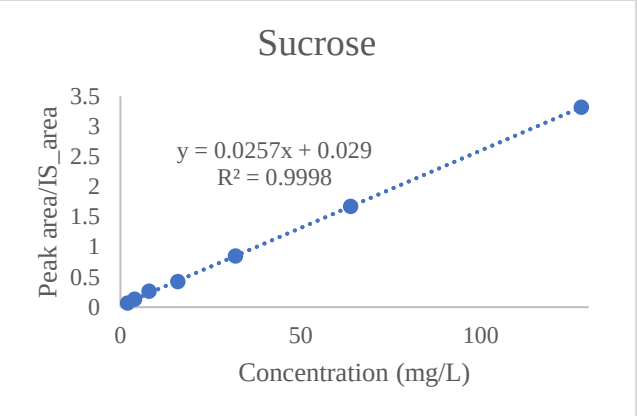
Sucrose
y = 0.0257x + 0.029
R² = 0.9998
Peak area/IS_area
Concentration (mg/L)
0
0.5
1
1.5
2
2.5
3
3.5
0
50
100

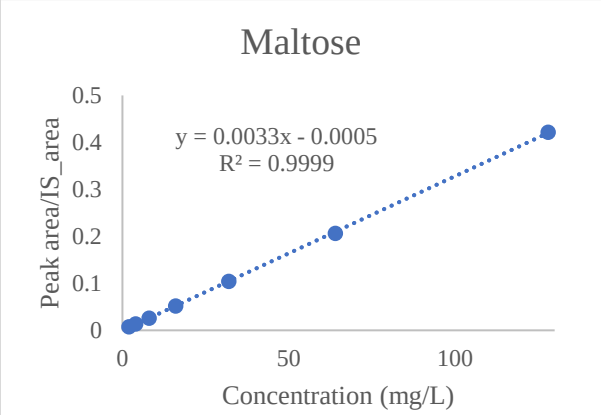
Maltose
y = 0.0033x - 0.0005
R² = 0.9999
Peak area/IS_area
Concentration (mg/L)
0
0.1
0.2
0.3
0.4
0.5
0
50
100

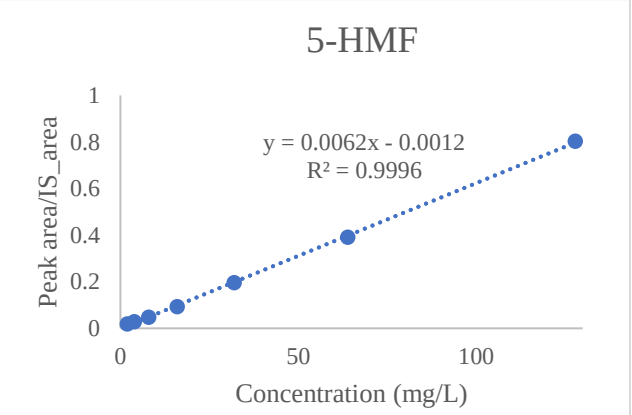
5-HMF
y = 0.0062x - 0.0012
R² = 0.9996
Peak area/IS_area
Concentration (mg/L)
0
0.2
0.4
0.6
0.8
1
0
50
100

Appendix 8: Residual by predicted plot for conversion rate, HMF yield, and selectivity.

HMF Selectivity

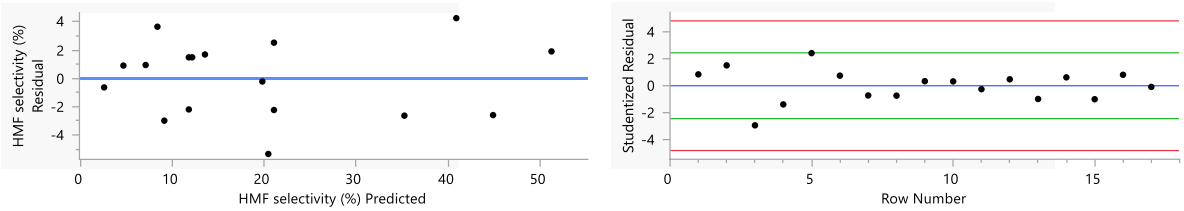

HMF yield

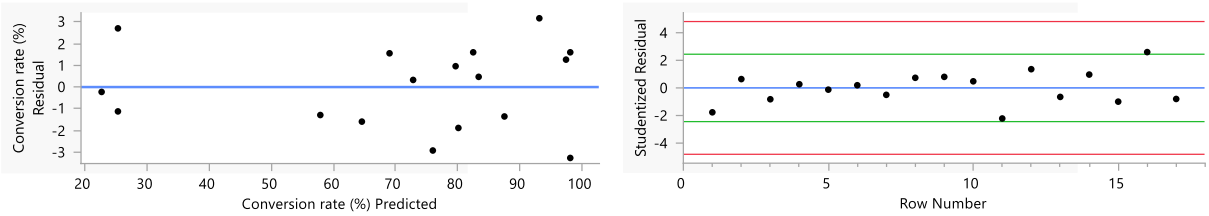

Sugar Conversion

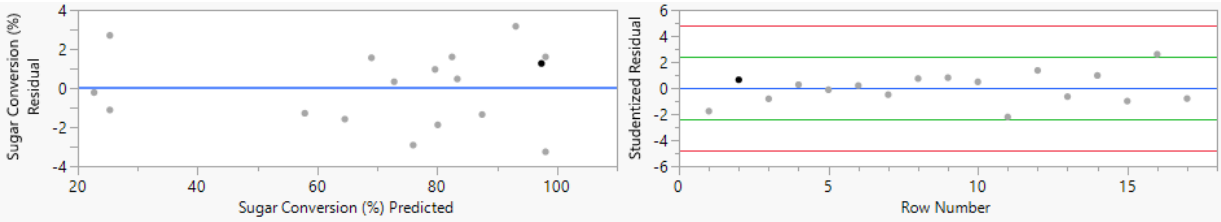

Appendix 9: Predication expression for conversion rate, HMF yield and selectivity.

HMF Selectivity

$$
\begin{aligned}
&13.530325581 \\
&+ -9.856428571 \cdot \left(\frac{\left(\text{Substrate load (g)} - 0.25 \right)}{0.15} \right) \\
&+ 4.2278571429 \cdot \left(\frac{\left(\text{Temperature (0C)} - 180 \right)}{30} \right) \\
&+ -10.26428571 \cdot \left(\frac{\left(\text{Aqueous phase (V\%)} - 55 \right)}{25} \right) \\
&+ \left(\frac{\left(\text{Substrate load (g)} - 0.25 \right)}{0.15} \right) \cdot \left(\left(\frac{\left(\text{Substrate load (g)} - 0.25 \right)}{0.15} \right) \cdot 6.0865348837 \right) \\
&+ \left(\frac{\left(\text{Substrate load (g)} - 0.25 \right)}{0.15} \right) \cdot \left(\left(\frac{\left(\text{Temperature (0C)} - 180 \right)}{30} \right) \cdot -0.36394186 \right) \\
&+ \left(\frac{\left(\text{Temperature (0C)} - 180 \right)}{30} \right) \cdot \left(\left(\frac{\left(\text{Temperature (0C)} - 180 \right)}{30} \right) \cdot 1.1790348837 \right) \\
&+ \left(\frac{\left(\text{Substrate load (g)} - 0.25 \right)}{0.15} \right) \cdot \left(\left(\frac{\left(\text{Aqueous phase (V\%)} - 55 \right)}{25} \right) \cdot 4.8839418605 \right) \\
&+ \left(\frac{\left(\text{Temperature (0C)} - 180 \right)}{30} \right) \cdot \left(\left(\frac{\left(\text{Aqueous phase (V\%)} - 55 \right)}{25} \right) \cdot -0.58855814 \right) \\
&+ \left(\frac{\left(\text{Aqueous phase (V\%)} - 55 \right)}{25} \right) \cdot \left(\left(\frac{\left(\text{Aqueous phase (V\%)} - 55 \right)}{25} \right) \cdot 0.2740348837 \right)
\end{aligned}
$$

HMF Yield

$$
\begin{aligned}
&8.5291627907 \\
&+ -6.21 \cdot \left(\frac{\left(\text{Substrate load (g)} - 0.25 \right)}{0.15} \right) \\
&+ 2.6642857143 \cdot \left(\frac{\left(\text{Temperature (0C)} - 180 \right)}{30} \right) \\
&+ -6.464285714 \cdot \left(\frac{\left(\text{Aqueous phase (V\%)} - 55 \right)}{25} \right) \\
&+ \left(\frac{\left(\text{Substrate load (g)} - 0.25 \right)}{0.15} \right) \cdot \left(\left(\frac{\left(\text{Substrate load (g)} - 0.25 \right)}{0.15} \right) \cdot 3.8317674419 \right) \\
&+ \left(\frac{\left(\text{Substrate load (g)} - 0.25 \right)}{0.15} \right) \cdot \left(\left(\frac{\left(\text{Temperature (0C)} - 180 \right)}{30} \right) \cdot -0.22772093 \right) \\
&+ \left(\frac{\left(\text{Temperature (0C)} - 180 \right)}{30} \right) \cdot \left(\left(\frac{\left(\text{Temperature (0C)} - 180 \right)}{30} \right) \cdot 0.7417674419 \right) \\
&+ \left(\frac{\left(\text{Substrate load (g)} - 0.25 \right)}{0.15} \right) \cdot \left(\left(\frac{\left(\text{Aqueous phase (V\%)} - 55 \right)}{25} \right) \cdot 3.0777209302 \right) \\
&+ \left(\frac{\left(\text{Temperature (0C)} - 180 \right)}{30} \right) \cdot \left(\left(\frac{\left(\text{Aqueous phase (V\%)} - 55 \right)}{25} \right) \cdot -0.37227907 \right) \\
&+ \left(\frac{\left(\text{Aqueous phase (V\%)} - 55 \right)}{25} \right) \cdot \left(\left(\frac{\left(\text{Aqueous phase (V\%)} - 55 \right)}{25} \right) \cdot 0.1717674419 \right)
\end{aligned}
$$

Conversion rate

$$
\begin{aligned}
&72.812186047 \\
&+ 13.903571429 \cdot \left(\frac{\left(\text{Substrate load (g)} - 0.25 \right)}{0.15} \right) \\
&+ 19.440714286 \cdot \left(\frac{\left(\text{Temperature (0C)} - 180 \right)}{30} \right) \\
&+ -3.026428571 \cdot \left(\frac{\left(\text{Aqueous phase (V\%)} - 55 \right)}{25} \right) \\
&+ \left(\frac{\left(\text{Substrate load (g)} - 0.25 \right)}{0.15} \right) \cdot \left(\left(\frac{\left(\text{Substrate load (g)} - 0.25 \right)}{0.15} \right) \cdot -11.97683721 \right) \\
&+ \left(\frac{\left(\text{Substrate load (g)} - 0.25 \right)}{0.15} \right) \cdot \left(\left(\frac{\left(\text{Temperature (0C)} - 180 \right)}{30} \right) \cdot -13.69539535 \right) \\
&+ \left(\frac{\left(\text{Temperature (0C)} - 180 \right)}{30} \right) \cdot \left(\left(\frac{\left(\text{Temperature (0C)} - 180 \right)}{30} \right) \cdot 0.0231627907 \right) \\
&+ \left(\frac{\left(\text{Substrate load (g)} - 0.25 \right)}{0.15} \right) \cdot \left(\left(\frac{\left(\text{Aqueous phase (V\%)} - 55 \right)}{25} \right) \cdot -2.279604651 \right) \\
&+ \left(\frac{\left(\text{Temperature (0C)} - 180 \right)}{30} \right) \cdot \left(\left(\frac{\left(\text{Aqueous phase (V\%)} - 55 \right)}{25} \right) \cdot -2.059604651 \right) \\
&+ \left(\frac{\left(\text{Aqueous phase (V\%)} - 55 \right)}{25} \right) \cdot \left(\left(\frac{\left(\text{Aqueous phase (V\%)} - 55 \right)}{25} \right) \cdot 10.208162791 \right)
\end{aligned}
$$

Appendix 10 : 3D surface profile Plot for Thermochemical process

HMF Selectivity

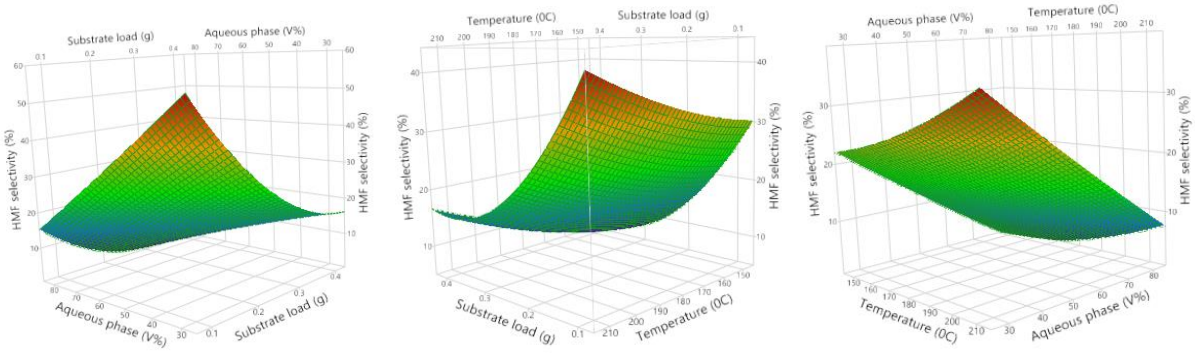

Conversion rate

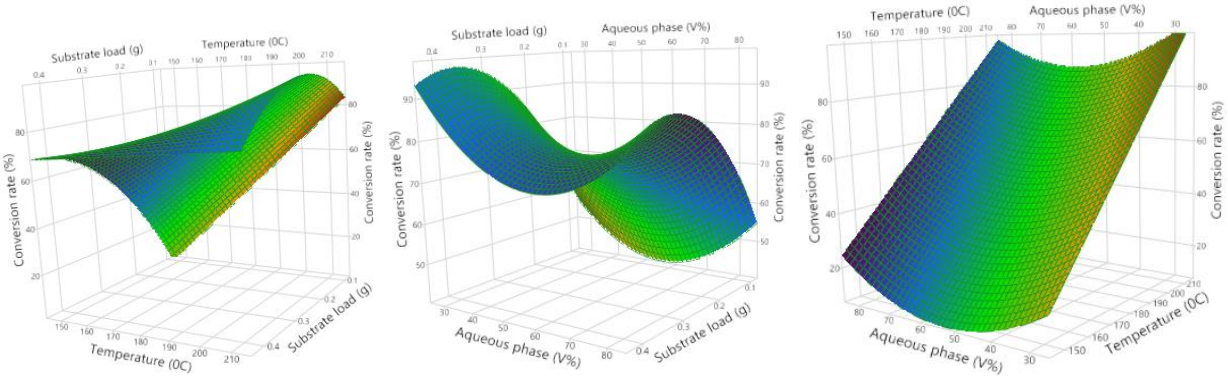

HMF Yield